CHARACTERISATION OF ACIDIC/BASIC PROPERTIES OF ALUMINA SUPPORTS

BY

RIKI FERREIRA

B.SC. HONS. (UPE)

A thesis submitted to the University of Cape Town
in partial fulfilment of the requirements for the degree of
Master of Applied Science

2002

ACKNOWLEDGEMENTS

I would like to express my gratitude to my supervisors: A/Prof. Jack Fletcher, Kobus Visagie and Walter Böhringer, for their help and support throughout this project.

I am also grateful to everyone from the Catalysis Research Unit, in particular Eric van Steen, Helen Divey, Suzana Vasic, Susan Fick and Noko Phala.

A special word of thanks to Walter, who was assigned at the end of the project to help sort out the huge pile of results (and other nonsense) in order to create a sensible thesis. I am glad that amidst the bad case of chicken pox, you were still ready and willing to help!

Also to my employer, Sasol Ltd., for their financial support and to my manager, Arno de Klerk, for allowing me the opportunity to complete my thesis in Cape Town and his motivation throughout.

Thank you to the Catalyst Characterisation Group (Beatrice, Monica and Michael), SCI laboratories (Gunter and Petro) and the guys from BCR laboratory 2 (Francois, Jeanette and especially Kobus) for all their help.

To my parents, Nico and Jeanette, without whose love and support I would not have survived throughout this trying time. A word of gratitude also to other members of my family: Imo, Nicole, Elmo and Hennelene.

'Ek is tot alles in staat deur Christus wat my krag gee.'

Filippense 4:13

SYNOPSIS

Previous experience with the preparation and testing of Co/alumina catalysts for Fischer-Tropsch synthesis has revealed that, while commercial available aluminas result in materials of significantly different catalytic performance, no correlation between the physical properties of the aluminas and the resulting catalytic performance was evident. Consequently, it was proposed that differences in the chemical (acid/base) nature of the alumina surfaces might be responsible for the observed differences in catalytic behaviour. In this study, isopropanol conversion was evaluated as a possible test reaction for characterisation of the acid/base nature of commercial aluminas – literature indicates acetone to result from isopropanol reaction on basic sites, and DIPE and propene products to result from isopropanol conversion over acid sites of varying strength.

Alumina samples included materials from three commercial manufacturers, Condea (γ-alumina), Procatalyse (γ-alumina) and La Roche (boehmite), as well as samples calcined at temperatures in the range 750-950°C. Physical characterisation included loss on ignition, surface area, pore volume, pore size distribution, ammonia temperature programmed desorption, x-ray diffraction and surface charge (Zeta potential). Other than for the boehmite starting material, all samples after calcination exhibited similar and stable physical properties in the calcination range applied, typical for γ-aluminas.

Isopropanol conversion tests were conducted in a fixed bed reactor in the vapour phase. Upon calcination at 750°C, activity decreased as Condea > Procatalyse > La Roche. Increasing calcination temperatures resulted in generally increasing activity for isopropanol conversion over the La Roche materials, while decreasing activity resulted for Procatalyse and Condea alumina. Although conversion levels varied significantly with increasing calcination temperatures, product selectivity was essentially unchanged. Consequently, it is concluded that calcination at increasing temperatures

results in a change in the number of active sites but without any significant change in the nature of the active sites present.

Experimental difficulties, in particular the presence of small amounts of acetone in the isopropanol feed, precluded any definitive conclusions in respect of acetone formation and, consequently, the presence of basic sites on the aluminas considered. It is likely, however, that the alumina samples included in this study exhibited either no or negligible basic sites, at least in terms of the ability of the test reaction to reveal such sites. No correlation was evident in respect of the presence of alumina impurities and catalytic performance.

Should any future study be considered in respect of the application of the isopropanol test reaction for the purpose of characterising the surface chemical nature of typical γ-aluminas, it is recommended that adequate steps be taken to prevent feed contamination with acetone.

TABLE OF CONTENTS

LIST OF FIGURES

LIST OF TABLES

CHAPTER 1: INTRODUCTION

Routine catalyst testing experiments revealed that different γ-aluminas, used for the preparation of cobalt-alumina catalysts, resulted in significantly different Fischer-Tropsch activities. Due to the fact that the specifications for these aluminas were almost identical and no consistent correlation in respect of physical properties and activity could be discerned, it was concluded that other property differences must be responsible for the significant differences in activity. The aim of this project was to investigate the relative differences in the acidic/basic properties of different aluminas and to determine whether these could be the source of the different catalytic performances observed.

Isopropanol conversion is a commonly used test reaction to probe for the differences in acidic/basic properties of alumina and other surfaces. Isopropanol undergoes dehydration to propene and diisopropyl ether on acidic sites and is dehydrogenated to acetone on basic sites and, consequently, it was considered worthy of investigation to determine whether this reaction would be sensitive enough to discern differences in the surface acid/base properties of commercial γ-alumina typically employed as catalyst supports.

CHAPTER 2: LITERATURE REVIEW

2.1 ALUMINA PROPERTIES

Alumina is one of the most widely used catalyst supports in the petroleum industry due to its robust, porous nature and it being relatively inexpensive. Of special importance is its capacity for contributing acid-catalysed activity, which can be adapted to suit the requirements of a variety of catalytic processes (Benesi and Winquist, 1978).

2.1.1 INDUSTRIAL USES OF ALUMINA

Industrial uses include the following (Kirk-Othmer, 1992):

- *Catalytic Applications* - Alumina is used commercially in catalytic processes as catalyst, catalyst substrate, or as a modifying additive. In the Claus process, activated alumina is used as catalyst to remove sulfur from H_2S that originates from natural gas processing or petroleum refinery operations. The alumina is used as spheres of 5 mm diameter, which is a good compromise between high activity and low pressure drop for fixed bed application.

  The largest application for activated alumina is in catalysts for hydrotreating of petroleum derived streams. The catalysts are usually in the form of extrudates. Much attention has been given to optimising pore volume and pore size distribution of the activated aluminas used in different applications.

  Activated alumina is used as a modifying additive in the catalyst particles used in fluid catalytic cracking (FCC). Addition of alumina to the catalyst particles (typically zeolite, having a clay or alumina-silica binder system) has been reported to improve various properties.

Another catalytic application for promoted alumina is in automotive exhaust catalysts, which enhance oxidation of hydrocarbons and carbon monoxide, and reduce nitrogen oxide in exhaust gas.

✧ *Chromatographic applications* - Alumina is used in the separation of various organic compounds by normal phase chromatography because of its natural hydrophilic surface characteristics.

✧ *Membranes* - Membranes comprising activated alumina films less than 20 μm thick have been manufactured. These films are deposited from pseudoboehmite[1] and calcined to produce controlled pore sizes in the 2 to 10 nm range. Inorganic membrane systems, based on this type of film and supported on solid porous supports, have been introduced commercially in various separation processes in the chemical processing industry. These have better mechanical and thermal stability than organic membranes.

✧ *Adsorbent Applications* - One of the earliest uses for alumina was the removal of water vapour from gases. It is also used to selectively remove various species from gas and liquid systems. In refining and petrochemical operations, activated alumina is used to remove trace HCl from reformer hydrogen, fluorides from hydrocarbons produced by HF alkylation, and in a variety of other cleanup applications.

2.1.2 SOURCES OF ALUMINA AND INFLUENCE OF CONTAMINANTS

Aluminium is the most abundant metal in the earth's crust and the third most abundant element on earth. It comprises approximately 8.3 wt% of the earth's crust. Combined with oxygen and hydrogen to form $Al_2O_3 \cdot n\ H_2O$, aluminium is a major constituent of bauxite, which is the most commonly mined aluminium-bearing ore. Bauxite is a term used for ores that contain

[1] Pseudoboehmite differs in crystallite size and hydroxyl content from the alumina typically referred to as boehmite (Oberlander, 1984).

economically recoverable quantities of the aluminium hydroxide mineral gibbsite or the oxy-hydroxide forms boehmite and diaspore (Kirk-Othmer, 1992). Holleman and Wiberg (1964) defined bauxite as boehmite which is contaminated by iron hydroxide to varying degrees. World reserves of bauxite are estimated at 30 billion metric tons (Haupin, 1987).

Bauxite is mined by surface methods (open cut mining). In 1888 Karl Bayer developed a refining process for extracting alumina from bauxite in four stages: Digestion, Clarification, Precipitation and Calcination. The Bayer process is still used today (Poisson et al., 1987).

Precipitation of $Al(OH)_3$ from aluminium salts can be achieved by adjusting the pH. Aluminium is amphoteric i.e. it is soluble in both acidic and basic solvents. In solutions of pH below 2 it is present as solvated Al^{3+} and in basic solutions of pH above 12 it exists in the form of AlO_4^{5-} (aluminate ions) (Moulijn and van Leeuwen, 1996).

In the Bayer digestion step, bauxite ore, the mixed hydroxides of iron and aluminum, reacts with a sodium hydroxide solution to form soluble sodium aluminate. All the other constituents remain unsolubilised. Cooling after digestion and clarification enhances supersaturation of dissolved $Al(OH)_3$. The supersaturated solution is then seeded with fine gibbsite particles to initiate crystallization of the trihydroxide, called the Bayer hydrate. The remaining alkali solution is reconcentrated and subsequently reused in the digestion stage. The process is conducted so as to recover an easily filterable and calcinable product (Poisson et al., 1987).

In addition to the route above, there are other manufacturing routes. Starting from an aqueous acidic Al^{3+} solution of pH above 3, precipitation is achieved by increasing the pH via the addition of an alkali.

The first precipitate from acidic solutions is a gel-like substance containing minute crystals of boehmite (AlOOH). Filtering this without aging and then calcining at temperatures up to 600°C, produces an amorphous material. At temperatures higher than 1100°C, α-Al_2O_3 is formed (figure 2-1).

Precipitation from a basic solution of AlO_4^{5-} is initiated via the addition of acid. At pH below 11 precipitation of bayerite, a crystalline form of $Al(OH)_3$, occurs. Upon filtering, drying and calcining above 500°C, a phase known as η-Al_2O_3, is formed. At higher temperatures θ-Al_2O_3 will form, which converts to α-Al_2O_3 at temperatures above 1100°C.

If the slurry of bayerite is aged at temperatures in the region of 80 °C and a pH of approximately 8, crystalline boehmite is formed. Precipitation of crystalline boehmite may also be achieved by combining acidic and basic solutions of alumina salts to reach the required pH range. Upon heating the precipitate at increasing temperatures, it converts firstly to γ-Al_2O_3, then to δ-Al_2O_3 and finally at temperatures exceeding 1100°C, to α-Al_2O_3.

If bayerite is aged at high pH, gibbsite forms which, upon subsequent heating at progressively increasing temperatures, converts firstly to χ-Al_2O_3, then to κ-Al_2O_3 and finally to α-Al_2O_3 by treatment above 1100 °C.

Precipitation of crystalline boehmite may also be achieved by the mixing of acidic and basic solutions of aluminium salts to obtain a pH in the range of 6 to 8.

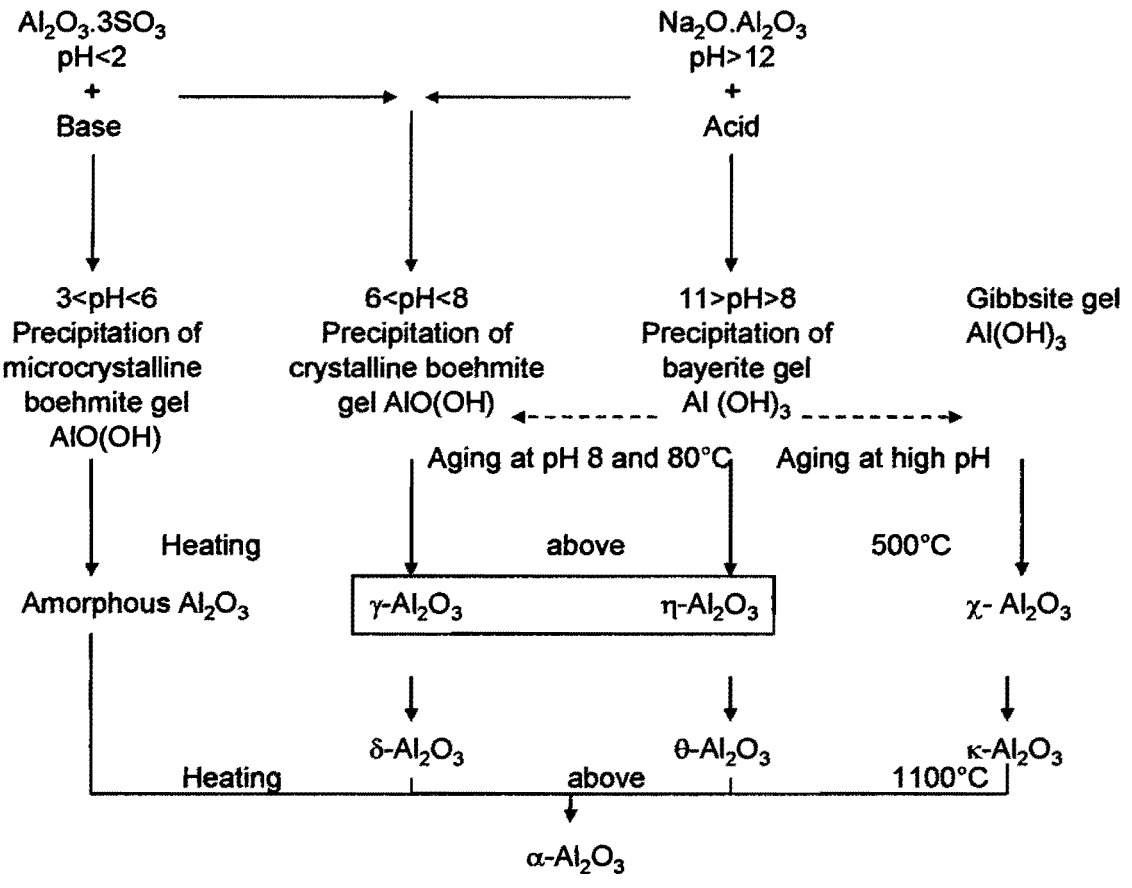

Figure 2-1 Schematic representation of the formation of the different forms of alumina (adapted from a drawing by Moulijn and van Leeuwen, 1996)

The important forms, in terms of use as catalyst supports, are γ-Al_2O_3 and η-Al_2O_3, particularly the former. These represent supports with low to high surface area (15-300 m^2/g) and high thermal stability for which the surface acidity can be controlled.

A third important source of aluminum oxyhydroxides is the hydrolysis of aluminum alcoholates in the Alfol process for the production of detergent alcohols (Weissermel and Arpe, 1997). This process involves the following steps:

$$Al + 2\ Al(C_2H_5)_3 + 1.5\ H_2 \rightarrow 3\ AlH(C_2H_5)_2$$

$$AlH(C_2H_5)_2 + H_2C{=}CH_2 \rightarrow Al(C_2H_5)_3$$

$$Al(C_2H_5)_3 + 3n\ C_2H_4 \rightarrow Al[(CH_2\text{-}CH_2)_n\text{-}C_2H_5]_3$$
$$(n = 1 \text{ to } \sim 11)$$

$$Al[(CH_2\text{-}CH_2)_n\text{-}C_2H_5]_3 + 1.5\ O_2 \rightarrow Al[O(CH_2\text{-}CH_2)_n\text{-}C_2H_5]_3$$

$$Al[O(CH_2\text{-}CH_2)_n\text{-}C_2H_5]_3 + 3\ H_2O \rightarrow 3\ CH_3(CH_2\text{-}CH_2)_nCH_2OH + Al(OH)_3$$

The very pure aluminum hydroxide produced as a co-product is used to make high purity Al_2O_3 for catalyst supports.

Weissenbacher et al. (1998) state that the majority of activated aluminas are produced by the rapid dehydration of aluminium trihydroxide feedstock. The rapid heating eliminates the formation of hydrothermal boehmite and forms an amorphous aluminum oxide without any loss of surface area. The process produces aluminas containing 3-12% water with surface areas of 200-350 m^2/g.

Processing of alumina products is tailored to optimize one or more key product properties, including surface area, purity, pore size distribution and particle size, shape or strength.

The properties of the different aluminum hydroxide and oxyhydroxide precursors for the preparation of active aluminas are summarized in table 2.1.

Table 2-1 Properties of different precursors used for active alumina preparation (Schüth and Unger, 1996)

Property	Bayer process	Precipitated hydroxide	Alcoholate hydrolysis
Raw material	Bauxite	Aluminum salt solutions	Aluminum alcoholates
Process	Digestion in NaOH and crystallisation	Neutralisation with acids or bases	Hydrolysis
Phase	Gibbsite	Pseudoboehmite, bayerite, nordstrandite, gibbsite	Pseudoboehmite
Size of primary particles (nm)	500-15000	10-1000	4-10
Main impurity	Na_2O	Chloride, sulfate, nitrate	Carbon (very low concentrations)
Weight loss on calcination (wt %)	35	18-40	22-28
Maximum of pore radius distribution (nm)	1.2-2.2	1.2-2.2	3.0-7.5
BET surface area (m^2g^{-1})	0.5-10	200-400	160-600

As can be seen from the discussion above, the production process will determine the type and levels of impurities that are present in the alumina product. This is substantiated by Narayanan et al. (1992) who state that the nature of alumina depends considerably on the precursor from which it is obtained by calcination, the calcination conditions and the amount of impurities. Lippens and Steggerda (1970) state that washing with dilute or even concentrated hydrochloric acid does not decrease the sodium content found in gibbsite produced via the Bayer process.

According to Tanabe (1970) it is well known that the addition of halogen to alumina enhances the acid strength of the solid, whereas the addition of potassium or sodium enhances the basic strength.

It is not uncommon to find that commercially available supports contain substances which can act as, or can generate, poisons for catalytically active metals. The presence of minute amounts of Na_2O has been found to decrease the catalytic effect of alumina for the dehydration of propanol and butanol (Lippens and Steggerda, 1970). Alumina, if prepared from sulfate solutions, may incorporate sulfate ions which are exceedingly difficult to remove by washing or even by calcination. Hydrogen atoms migrating to the support during catalyst reduction via spillover from a reducible component, may lead to the formation of hydrogen sulfide and this can produce very misleading results in activity tests (Richardson, 1989).

2.1.3 ECONOMIC ASPECTS

In 1990, U.S. production of activated aluminas was about 50 000 t/yr and bulk prices were mostly between $0.60 and $3.00/kg (Kirk-Othmer, 1992). The least expensive products are those derived directly from the Bayer-process. Aluminas of high purity (99.9%) are also available, but at much higher prices. Products for adsorbent purposes are generally less sophisticated and less expensive than products for catalytic applications.

The comparably high soda content of Bayer gibbsite (0.2-0.3% Na_2O) makes it unattractive for many catalytic applications. Gel-based products (i.e. those produced from precipitated hydroxides) are normally used where low soda levels are required. Gels prepared from inorganic salts or acid aluminate solutions contain less soda, typically in the region of 300 ppm.

Very pure alumina is obtained from aluminium alcoholate hydrolysis (Alfol process) (Weissermel and Arpe, 1997).

North American producers of aluminas include Alcoa, La Roche, Discovery and Alcan. Gel-based activated aluminas are produced by La Roche, Vista, and several of the major catalyst manufacturers. In Europe, principal suppliers are Rhône-Poulenc and Condea (Sasol Germany).

Most markets are mature. Global growth for most applications is expected to be about 1-3% per year (Kirk-Othmer, 1992).

2.1.4 CRYSTALLINE PHASES AND PHASE TRANSFORMATIONS

γ-alumina and η-alumina are also called active or transition aluminas (Kirk-Othmer, 1992). Transition alumina is probably the more accurate nomenclature because the various phases identified by x-ray diffraction are really stages in a continuous transition between the disordered structures immediately following decomposition of the hydrous precursors and the stable, most densely packed, crystalline α-alumina product of high temperature calcination (Kirk-Othmer, 1992). These materials are seldom phase pure and generally contain other transition aluminas as impurities. Their properties depend strongly on the type of starting material, the procedure chosen for thermal treatment and the process conditions such as temperature and pressure (Schüth and Unger, 1996).

Figure 2-2 shows the decomposition sequence for several hydrous alumina precursors and indicates the approximate temperatures at which the activated forms occur. This scheme differs from figure 2-1 through the introduction of a temperature scale in respect of thermal treatment and clearly indicates the effect of calcination temperature on phase formation. Starting from the hydrous precursors, heating causes dehydration and rearrangement leading to a series of transitional aluminas and finally α-Al_2O_3 (Schüth and Unger, 1996).

Starting from gibbsite or bayerite respectively, pathway (a), leading to boehmite and eventually γ-alumina, is favoured under 'severe' treatment conditions (see figure 2-2).

Pathway (b) in figure 2-2 is favoured under mild conditions, a route which circumvents the formation of the intermediate γ-alumina phase (Schüth and Unger, 1996).

Upon heating, boehmite gels exhibit a weight loss throughout the range 50-600°C due to the loss of structural water and gradual transformation to γ-Al_2O_3. This is a topotactic transformation (i.e. changes are limited to the internal structure) and is accomplished by internal condensation of protons and hydroxyls between boehmite layers. This removes half of the oxygens from the layers as water, effecting a collapse and rearrangement of the structure into the cubic close-packed form of γ-alumina.

The $\gamma \rightarrow \delta \rightarrow \theta$-$Al_2O_3$ transformations do not involve loss of water and thermal analysis indicates no weight loss above about 600°C.

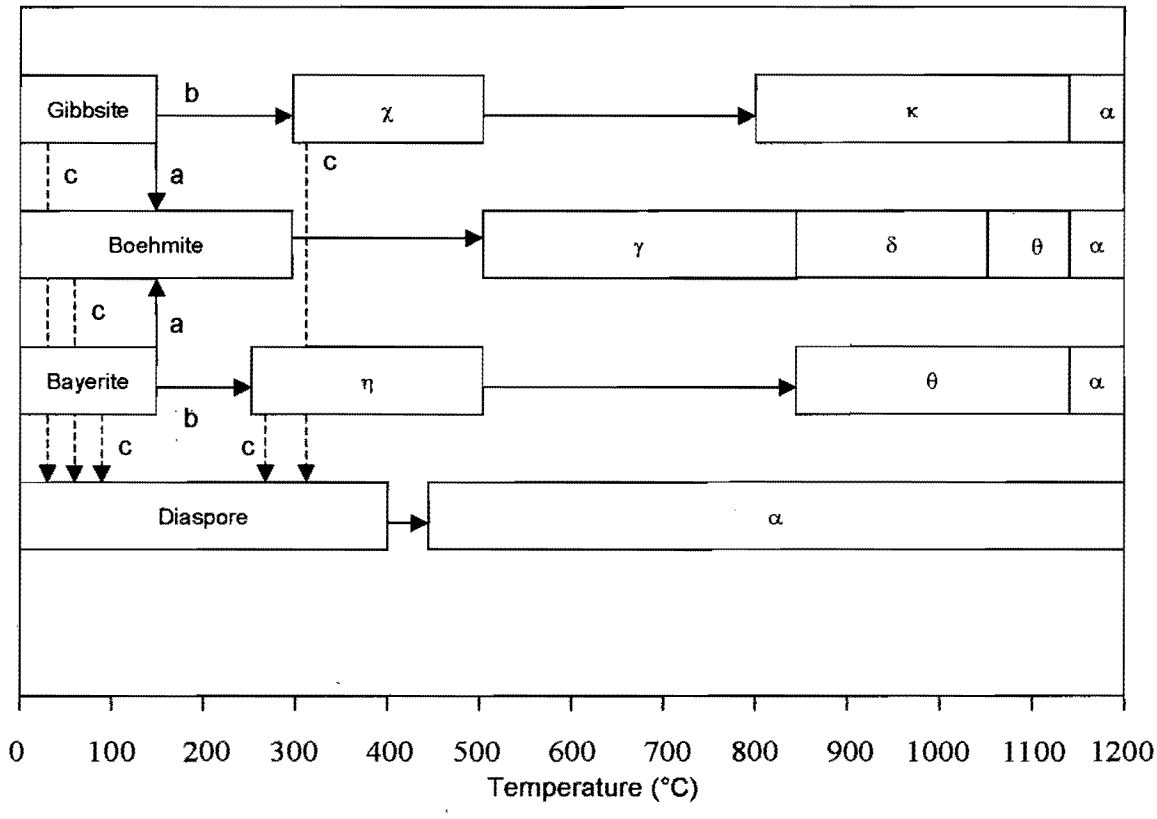

Figure 2-2 Decomposition sequence of hydrous aluminas (Schüth and Unger, 1996)

a) Pathway under severe treatment conditions (pressures exceeding 1 bar, moist air, heating rates higher than 1°C/min and crystallite sizes higher than 100 µm)

b) Pathway under mild treatment conditions (pressure of 1 bar, dry air, heating rates below 1°C/min and crystallite sizes below 10 µm)

c) Pathway under high water vapour pressure (142 bar, 275-425°C)

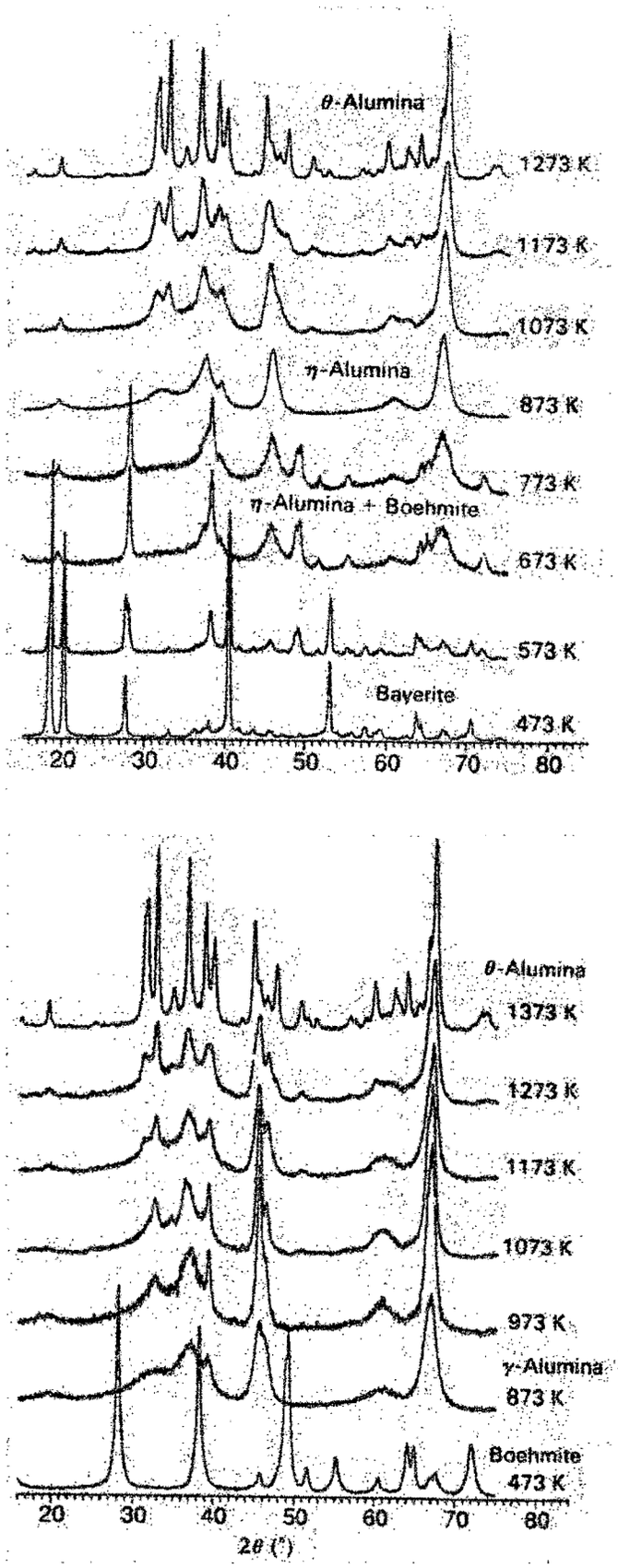

Figure 2-3 X-ray diffraction patterns of transition aluminas obtained with increasing calcination temperature starting from bayerite and boehmite, respectively (Brinker and Scherer, 1990)

With increasing temperature, the crystal structure becomes more ordered as can be seen from the X-ray diffraction patterns of figure 2-3 corresponding to the scheme given in figure 2-2. The final transformation to α-Al_2O_3 involves a reorganization of the oxygens into a denser, hexagonal close-packed configuration.

It has been reported that between 275 and 425°C and a water vapour pressure above 142 bar, all hydroxides and oxides are converted into diaspore, when seeding of this form is present. It is the only aluminium hydroxide that decomposes directly to α-alumina (at the strikingly low temperature of approximately 450°C) (figure 2-2). However, preparation of diaspore is so difficult that no viable application has been found (Lippens and Steggerda, 1970).

The oxygen lattice persists during dehydration and thus cation displacement in the lattice is the most important mechanism for the formation of the different forms of alumina. In going from the hydroxide stage to the α-alumina stage, both of which have aluminium atoms only in octahedral positions, intermediate phases having aluminium in tetrahedral positions are traversed (Lippens and Steggerda, 1970).

Therefore, during the transformation into α-alumina, the coordination of Al^{3+} changes from approximately 25% tetrahedral and 75% octahedral in γ-alumina to 100% octahedral in the α-phase. The tetrahedrally coordinated aluminum atoms are believed to be responsible for the catalytic activity of γ-alumina and therefore it is expected that the higher temperature phases will be less reactive than γ-alumina (Narayanan et al., 1992).

2.1.5 THE STRUCTURE OF ALUMINA

According to Knözinger and Ratnasamy (1978), the surface structure of alumina is of great importance with regard to determining the structure of supported catalytically active phases. Catalytically interesting aluminas are

generally poorly crystallized, which limits the use of typical methods used for structural investigations (Nortier et al., 1990). Moreover, the difficulty of preparing phase pure samples makes phase studies complex (Narayanan et al., 1992).

Powder X-ray diffraction has established that γ-alumina crystallises with a spinel-type structure comprising a cubic close-packed oxygen lattice with one-eighth of the tetrahedral and one-half of the octahedral interstices filled by the aluminium cations (the unit cell consists of 32 oxide ions with 21 $^{1}/_{3}$ aluminium ions arranged at random in the 16 octahedral and 8 tetrahedral positions of the spinel structure with 2 $^{2}/_{3}$ vacant cation positions). The 'sandwiching' of aluminium ions between the oxide planes in close packing apparently causes the characteristic lattice distortion of alumina (Dabrowski et al., 1970). It is the octahedral sites which are preferentially occupied by Al^{3+}, but it is the occupied tetrahedral sites which are believed to be the catalytically active centres (Knözinger and Ratnasamy, 1978).

The cation distribution is temperature-dependent and the tetrahedral positions are very irregularly occupied, hence, some influence on activity may be expected (Knözinger and Ratnasamy, 1978).

2.1.6 SURFACE MODELS – SURFACE HYDROXYLS

Active alumina adsorbs water, at room temperature, as undissociated molecules strongly hydrogen bonded to the underlying surface. At higher water vapour pressures, more water bonds in a multi-layer physical adsorption process but this may easily be removed by drying at approximately 120°C. It has been shown that water molecules that are not removed via this drying process react to form surface hydroxyl groups. This reaction is complete at about 300°C (Lippens and Steggerda, 1970). The OH^--groups on the surface of alumina behave as Bronsted-acid sites.

At higher temperatures these hydroxyls are gradually removed as water, leaving behind an oxygen ion in the form of an oxygen bridge:

This process results in the formation of an exposed Al-atom, which behaves as a Lewis acid site due to its electron-deficient character.

Peri (1965) studied the surface of γ-alumina by using gravimetric and infra-red data as a guide and control in a computerized simulation of the dehydration process. On dry γ-alumina, as obtained through thermal treatment, the exposed (100) plane contains only oxide ions (figure 2-4a). At low temperatures, a filled monolayer of OH^--ions can be formed (figure 2-4b).

During dehydration, adjacent OH^--ions combine as shown above. This combination proceeds at random, but only two-thirds of the OH^--groups can be removed in this manner without disturbing the local order at which point no adjacent hydroxy pairs remain on the surface. Further dehydration requires the creation of oxide and/or vacancy disorder.

Random removal of all hydroxyl pairs results in a surface as illustrated in figure 2-5. The remaining isolated hydroxyl groups cover approximately 10% of the surface and are found on five types of sites, having from zero to four oxygen nearest neighbours as illustrated in the figure (Tanabe, 1970) and as confirmed by infrared studies (Poisson, 1987). These five types of hydroxyl ion sites should vary in chemical properties, the A-site being the most basic and the C-site the most acidic (figure 2-5).

surface enolate, water and an oxygen vacancy. Experimental evidence in support of the latter proposal was provided by Chadwick and O'Malley (1987), who further suggested that the interpretation of Bowker was affected by the limited range of conditions investigated. Both proposed mechanisms would depend on the available surface hydroxyl groups which participate in the reaction.

Other authors suggest that the OH-bond of the alcohol is cleaved during adsorption, since ion pairs on the surface of MgO or other basic heterogeneous catalysts chemisorb alcohols heterolytically, as shown in figure 2-13 (Stone, 1990).

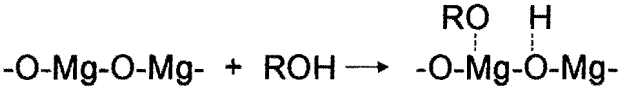

Figure 2-13 Heterolytic chemisorption of alcohol on MgO

Jain and Pillai (1967) proposed that during ether formation a second alcohol molecule interacts with an adsorbed molecule in a nucleophilic displacement reaction. The chemisorption of the oxygen on the acidic site polarises the C-O bond and makes the hydroxyl a better leaving group (figure 2-14).

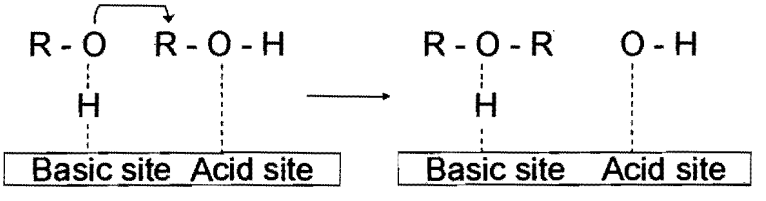

Figure 2-14 Mechanism for ether formation as proposed by Jain and Pillay, 1967

Knözinger et al. (1968) also suggested that a surface alcoholate group reacts with an alcohol molecule in the adsorbed phase by electrophilic attack on the hydroxyl oxygen.

2.2.2 INFLUENCE OF REACTION CONDITIONS

Dehydrogenation and dehydration of isopropanol over aluminas have been shown to be strongly affected by the experimental conditions, e.g. reaction temperature, alcohol partial pressure and other factors (Wang et al., 1999).

2.2.2.1 TEMPERATURE

In theory, the higher the temperature the more the selectivity shifts in favour of the reaction with the highest activation energy. Wang et al. (1999) reported that the total conversion of isopropanol over aluminas increased with increasing reaction temperature. The selectivity towards dehydrogenation decreased with increasing reaction temperature, while selectivity towards dehydration increased. Selectivity towards diisopropyl ether formation reached a maximum at 150°C and diminished at higher temperatures.

Narayanan et al. (1992) reported results from different aluminas tested in the form of Arrhenius plots for propene formation and total consumption of isopropanol. Ether formation was found to be a minor product on all the aluminas tested. It is also reported that the activation energies for propene formation and total consumption of 2-propanol range from 24-27 kcal/mol for γ-aluminas. As the temperature was increased above 202°C, DIPE formation showed a pronounced non-Arrhenius behaviour and the reaction rate decreased with increasing temperature. This was ascribed to the decreasing surface coverage of reactant alcohol, which affects the bimolecular reaction to ether formation much more strongly than the unimolecular reaction leading to propene.

The above explanation may, however, not be conclusive. Activation energies reported must be regarded as apparent activation energies incorporating adsorption enthalpies and equilibrium constants of the reactants. Moreover, the authors did not consider that the formation of DIPE from isopropanol is an equilibrium reaction, DIPE formation being unfavourable at elevated temperatures.

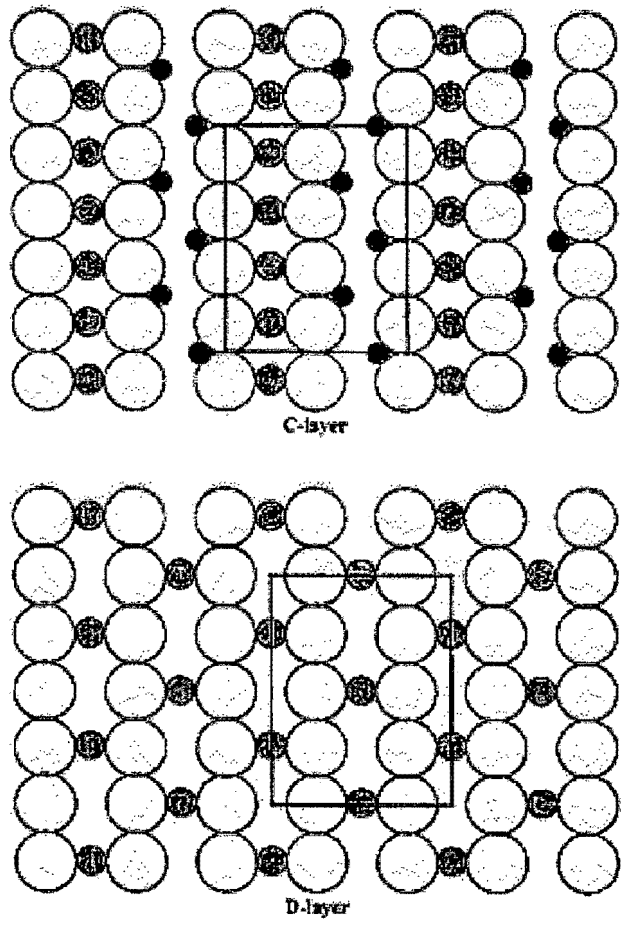

Figure 2-6 The cluster model for C- and D-layers of γ-alumina (Xia et al., 1999) [Large open circle = oxygen anions; medium, shaded circle = octahedral Al^{3+} ions, small, black circle = tetrahedral Al^{3+} ions, □ = unit cell]

For energetic reasons, only anion layers will terminate a crystallite and these surface layers will most favourably consist of hydroxyl groups. It is important to realise that five different OH^--configurations can be expected on the surface of aluminas (figure 2-7). Their occurrence is different on the different faces of the alumina crystals such that their relative concentration on the surface of a crystal depends on the relative contributions of the different crystal faces. The hydroxyl groups in these various configurations carry slightly differing net charges and, consequently they should exhibit different properties with the protonic acidity of the hydroxyl groups decreasing as their net charge becomes more negative. It follows that the bottom right configuration of figure 2-7 is the most acidic, corresponding to the ranking discussed in relation to figure 2-5.

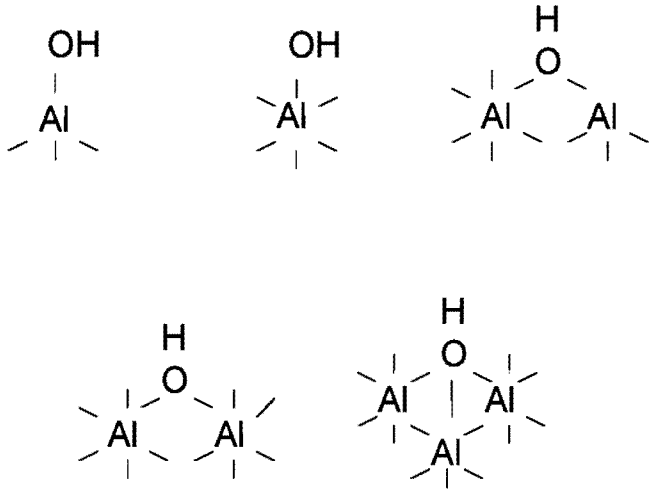

Figure 2-7 The five possible surface OH configurations (Knözinger and Ratnasamy, 1978)

The proton acidity and ease of removal of an hydroxyl group are regarded as important factors which govern the dehydroxylation process of alumina as previously described. This model assumes that the regular dehydroxylation process is governed solely by the relative basicities and protonic acidities of neighboring hydroxyl groups and their mutual orbital orientations in ideal exposed crystal faces. All in all, this model dramatically illustrates the heterogeneity of the γ-Al_2O_3 surface.

2.2 ACID/BASE CATALYSED CONVERSION OF ISOPROPANOL

Isopropanol conversion has often been applied for correlating chemical reactivity with physicochemical properties of solids (Pepe et al., 1985). Ai and Suzuki (1973) have reported that the dehydration of isopropanol is a good measure of acidity of some oxidation catalysts whose surface areas are so small that a gas adsorption method is insensitive for the determination of acidity. In 1797 four Dutch chemists (Bondt, Deiman, Paets van Troostwijk and Lauwerenburgh) discovered the catalytic dehydration action of alumina on alcohol. In 1901 Grigorieff's rediscovery of this catalytic dehydration reaction induced Ipatieff to systematically investigate catalytic dehydration in

to the dehydrogenation reaction, which he was already studying at that time (De Boer et al., 1967).

It is stated in the literature that alcohol dehydration does not require acid sites as strong as those necessary to catalyse, for example, skeletal isomerisation (Narayanan et al., 1992). The alcohol dehydration activity is therefore expected to be more closely related to the total number of active sites.

The possible routes for the reaction are (figure 2-8):

i) Isopropanol dehydration to propene,

ii) Condensation to diisopropyl ether and

iii) Isopropanol dehydrogenation to acetone.

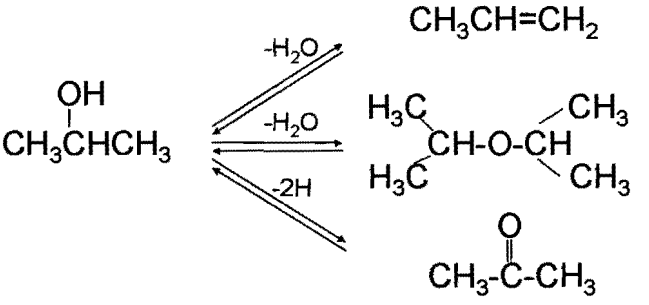

Figure 2-8 Possible reaction routes for isopropanol conversion

Dehydration to propene is said to take place on acid sites, while dehydrogenation to acetone is mediated by basic sites (El-Jamal et al., 1988). Both these reactions are parallel first-order reactions according to Pepe et al. (1989). Tanabe (1981) states that the activity for dehydrogenation of isopropanol to acetone is proportional to the acidity and basicity of a catalyst, since the dehydrogenation is considered to proceed by a concerted mechanism.

It depends on the catalyst system whether the hydrogen, which is abstracted in the dehydrogenation step is released as molecular hydrogen, H_2, or transferred to other molecules. The former requires a 'port hole', which is not necessarily available on alumina catalysts (Roessner, 2002). The latter

results in the formation of a saturated product, e.g. propane from propene via ionic H-transfer.

All steps must be regarded as reversible.

2.2.1 REACTION MECHANISMS PERTAINING TO ISOPROPANOL CONVERSION

Cortez et al. (1992) state that strong acid sites are involved in both the ether and olefin formation. Parry (1963) states that no Bronsted acidity was found to be present on alumina surfaces after calcination and that it could be concluded that the acid sites involved in dehydration are Lewis acid sites. It must, however, be kept in mind that the reaction produces water at low temperature and this could cause the (re)-formation of Bronsted acid sites.

Cortez et al. (1992) also state that the ether and olefin products would be produced via different mechanisms: a concerted one involving an acid-base pair for the ether (E_2 mechanism) and a single acid site for the olefin (E_1 mechanism). Their results also indicate that DIPE formation takes place mainly on the stronger acid sites, whereas olefin formation could take place on any acid site (weak or strong). This is substantiated by Fiedorow et al. (1980) who found that for alumina doped with 0.3 wt% sodium, no strong acid sites could be detected, yet the catalyst still produced a substantial olefin yield.

Acetone formation was found to occur on basic sites (Cortez et al., 1992).

Also, dehydration of a secondary alcohol under acidic conditions proceeds via the E_1 pathway (Fox and Whitesell, 1997). Dehydration is facilitated by acid via protonation of the hydroxyl group forming water, a good leaving group. A secondary carbocation is produced and upon abstraction of the β-hydrogen, propene is formed (figure 2-9).

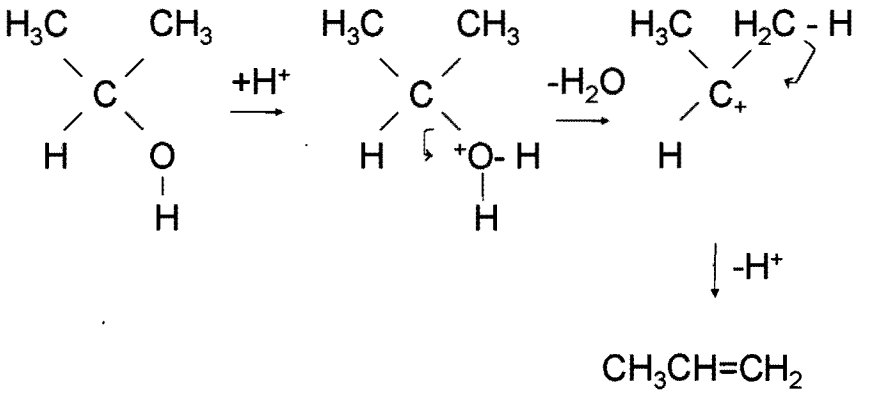

Figure 2-9 Dehydration of a secondary alcohol via E_1 pathway (Fox and Whitesell, 1997)

Pines and Manassen (1966) suggested that olefins are formed by the adsorption of alcohol on the acidic site through the oxygen atom of the alcoholic hydroxyl group, thereby polarizing the C-O bond. Breakage of the C-O bond and the abstraction of β-hydrogen by a nucleophile seem to occur in a concerted manner.

Fikis et al. (1978) suggested that propene formation occurs via an E_2 type mechanism on adjacent vacant surface sites (figure 2-10).

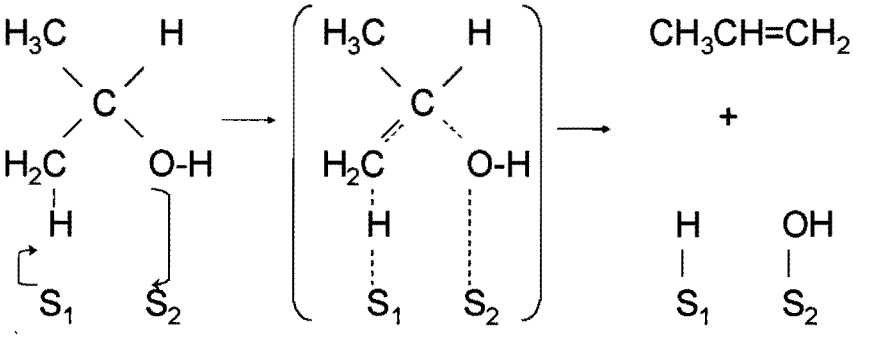

Figure 2-10 E_2 type mechanism of propene formation (Fikis et al., 1978)

Knözinger and Scheglila (1970) proposed an E_2 type mechanism for the dehydration of primary, secondary and tertiary alcohols over alumina below 200°C. At higher temperatures, depending on the reactant structure, dehydration was thought to proceed via an E_1 type mechanism.

A two-point adsorption intermediate has also been proposed for acetone formation (Fikis et al., 1978). One site is a hydroxyl group, which may have formed as an adsorbed species from a dehydration reaction. The adsorbed intermediate species will be located at sites offering H or OH and, consequently, will be related primarily to the presence of 'acidic' species in the solid surface (figure 2-11).

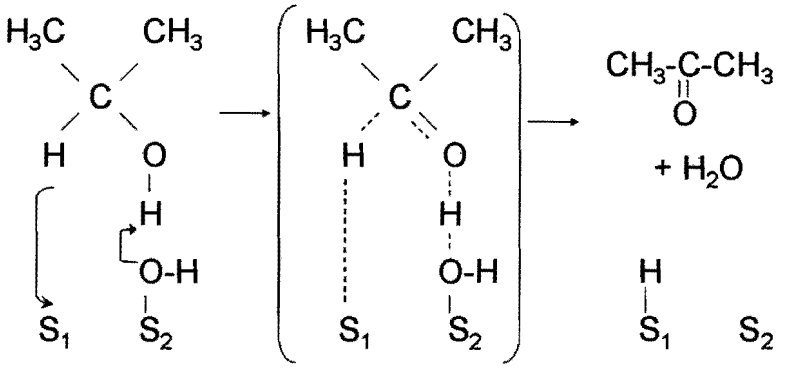

Figure 2-11 Mechanism of acetone formation (Youssef et al., 1992)

The mechanism shown in figure 2-11 does not regenerate the initial catalytic surface, but accumulates hydrogen. The authors do not address the question of how the surface hydrogen is removed. Bowker et al. (1985) report that surface dehydrogenation involves dissociation of hydrogen. Griffin and Yates (1982) have shown that such a reaction is possible below room temperature on zinc oxide.

Noller et al. (1984) proposed a mechanism for dehydration and dehydrogenation and specified the kind of surface sites involved in catalysis. The main features are that all interactions take place between an electron pair acceptor (Lewis acid) and an electron-pair donor (Lewis base). They proposed that the electron pair acceptor site induces the abstraction of OH^- and the electron pair donor site, the abstraction of H^+ (figure 2-12).

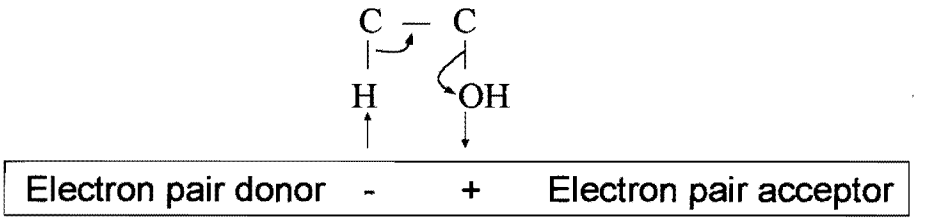

Figure 2-12 Mechanism for dehydration and dehydrogenation (Noller et al., 1984)

In the mechanisms proposed by Fikis (1978) and Noller (1984) both acid and base sites are involved, the difference being the sequence of bond scission. It is the strongest interaction that determines the first step and, hence, the mechanism.

In the case of strong solid acids, the interaction of the surface electron pair acceptor with the OH group of the alcohol is strong and leads to the OH group being abstracted in the first step. The carbocation is formed immediately. For basic catalysts, the strong interaction between the surface electron pair donor and the β-H of the alcohol, leads to the β-H being abstracted in the first step with intermediate carbanion formation.

TPD studies by Noller (1984) showed that the products arising from dehydration and dehydrogenation, i.e. propene and acetone, respectively, exhibit desorption maxima at the same temperature. Therefore, they concluded that these are evolved from the same adsorption sites.

Two other mechanisms have also been proposed. Bowker et al. (1985) proposed that dehydrogenation reaction proceeded via elimination of the α-hydrogen from an adsorbed isopropoxy species, whereas dehydration occurs via a reaction between an adsorbed isopropanol and a surface hydroxyl group leading to an adsorbed isopropoxy species, water and an oxygen vacancy. Mazanec (1986) and Koga et al. (1980) propose the dehydrogenation reaction to proceed via β-hydrogen elimination leading to a surface enolate, while the dehydration proceeds via a reaction between an adsorbed isopropoxy species and a surface hydroxyl group leading to a

surface enolate, water and an oxygen vacancy. Experimental evidence in support of the latter proposal was provided by Chadwick and O'Malley (1987), who further suggested that the interpretation of Bowker was affected by the limited range of conditions investigated. Both proposed mechanisms would depend on the available surface hydroxyl groups which participate in the reaction.

Other authors suggest that the OH-bond of the alcohol is cleaved during adsorption, since ion pairs on the surface of MgO or other basic heterogeneous catalysts chemisorb alcohols heterolitically, as shown in figure 2-13 (Stone, 1990).

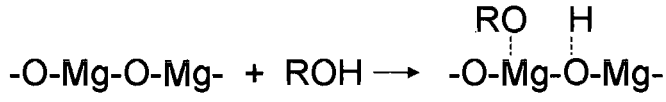

Figure 2-13 Heterolytic chemisorption of alcohol on MgO

Jain and Pillai (1967) proposed that during ether formation a second alcohol molecule interacts with an adsorbed molecule in a nucleophilic displacement reaction. The chemisorption of the oxygen on the acidic site polarises the C-O bond and makes the hydroxyl a better leaving group (figure 2-14).

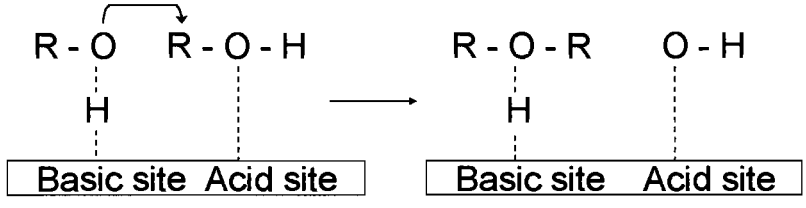

Figure 2-14 Mechanism for ether formation as proposed by Jain and Pillay, 1967

Knözinger et al. (1968) also suggested that a surface alcoholate group reacts with an alcohol molecule in the adsorbed phase by electrophilic attack on the hydroxyl oxygen.

2.2.2 INFLUENCE OF REACTION CONDITIONS

Dehydrogenation and dehydration of isopropanol over aluminas have been shown to be strongly affected by the experimental conditions, e.g. reaction temperature, alcohol partial pressure and other factors (Wang et al., 1999).

2.2.2.1 TEMPERATURE

In theory, the higher the temperature the more the selectivity shifts in favour of the reaction with the highest activation energy. Wang et al. (1999) reported that the total conversion of isopropanol over aluminas increased with increasing reaction temperature. The selectivity towards dehydrogenation decreased with increasing reaction temperature, while selectivity towards dehydration increased. Selectivity towards diisopropyl ether formation reached a maximum at 150°C and diminished at higher temperatures.

Narayanan et al. (1992) reported results from different aluminas tested in the form of Arrhenius plots for propene formation and total consumption of isopropanol. Ether formation was found to be a minor product on all the aluminas tested. It is also reported that the activation energies for propene formation and total consumption of 2-propanol range from 24-27 kcal/mol for γ-aluminas. As the temperature was increased above 202°C, DIPE formation showed a pronounced non-Arrhenius behaviour and the reaction rate decreased with increasing temperature. This was ascribed to the decreasing surface coverage of reactant alcohol, which affects the bimolecular reaction to ether formation much more strongly than the unimolecular reaction leading to propene.

The above explanation may, however, not be conclusive. Activation energies reported must be regarded as apparent activation energies incorporating adsorption enthalpies and equilibrium constants of the reactants. Moreover, the authors did not consider that the formation of DIPE from isopropanol is an equilibrium reaction, DIPE being unfavourable at elevated temperatures.

De Boer et al. (1967) state that the intermolecular dehydration of two molecules of ethanol to diethyl ether on alumina exhibits a lower activation energy than the intramolecular dehydration to the olefin. At temperatures below 260°C, the ether is practically the only product, while at temperatures above 300°C the products are almost entirely ethylene and water, consistent with the general statement given above.

2.2.2.2 PARTIAL PRESSURE OF THE ALCOHOL

Narayanan et al. (1992) determined the reaction order of propene formation by studying the variation in reactivity with increasing partial pressure of isopropanol. A figure was produced showing propene formed as a function of isopropanol partial pressure at three different temperatures. While there was a negligible change in reactivity with pressure at 150°C and 180°C, the reactivity was more sensitive to partial pressures at 200°C, with a sharp fall off as partial pressure is lowered below 13 mbar. In the normal operating regime of 60-67 mbar partial pressure, it is shown that the reaction is essentially zero order with respect to isopropanol concentration.

De Boer et al. (1967) showed, for the conversion of ethanol, that olefin formation tends to exhibit zero order behaviour at alcohol partial pressures higher than about 40 mbar (figure 2-15). They concluded that a saturation of the surface with chemisorbed ethanol molecules is reached under these conditions, leading to a zero order dependency for the direct production of olefin from alcohol. Simultaneously, diethyl ether is produced. This reaction involves two alcohol molecules and leads to the steadily increasing curve in figure 2-15.

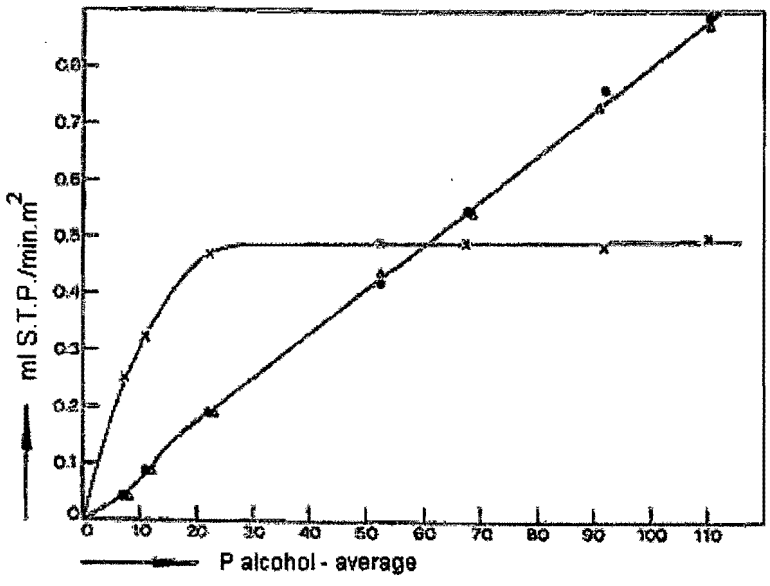

Figure 2-15 Experimental results from conversion of ethanol over γ-alumina (De Boer et al., 1967)

Two reaction mechanisms may be considered. If the reaction follows the Langmuir-Hinshelwood scheme, where both reactant species are adsorbed, the order of the ether production reaction should also tend to zero at the same partial pressure as does the ethylene production reaction (curve B in figure 2-16).

If however, the reaction proceeds according to a Eley-Rideal scheme, where one reactant is adsorbed and the second resides in the gas phase, an initially second order response, changing into first order when the alcohol adsorption becomes saturated would be expected (curve A in figure 2-16). The extrapolation of the linear part of this curve to zero pressure, should cut the vertical axis below zero, as for curve A. Curve C was the combination of these.

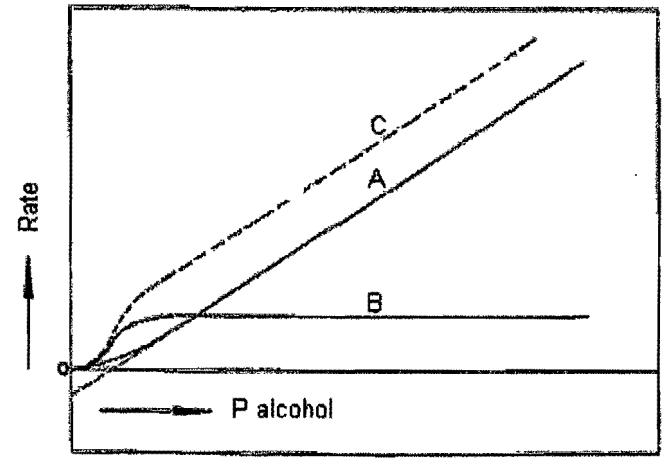

Figure 2-16 Schematical explanation of the curve obtained for ether production (De Boer et al., 1967)

The observed response for the production of ether (curve C in figure 2-16), indeed, has the character of a second order reaction at low alcohol partial pressure changing to a linear response at roughly the same pressure as where the ethylene production becomes zero order.

Extrapolation of the experimental response to zero pressure, intersects the vertical axis above zero (corresponding to curve C). By considering the intercept of the extrapolated lines, the authors came to the conclusion that both Langmuir-Hinshelwood and Eley-Rideal mechanisms proceed simultaneously.

2.2.3 INFLUENCE OF ALUMINA CHARACTERISTICS

2.2.3.1 STRUCTURE

Pines and Haag (1960) studied the effect of alumina structure on catalytic activity. Samples of increasing crystallinity were produced via pretreatment at temperatures varying from 400 to 1000°C. They found that cyclohexene isomerisation activity per unit surface area reached a maximum for calcination temperatures around 600°C (found to be primarily η-alumina) and the activity declined over twenty-fold when the calcination temperature exceeded 800°C.

They also reported that the hydroxyl content of these samples did not differ significantly.

MacIver et al. (1964) studied the activity of γ- and η-alumina for different acid-catalysed reactions. Their results indicated that the two aluminas had different catalytic properties and, since they were structurally different, the authors suggested that the difference in structure is a significant factor governing the catalytic behaviour of alumina. In keeping with this conclusion, Pepe et al. (1988) state that alumina catalysed isopropanol conversion is structure dependent.

Narayanan et al. (1992) tested the effect of alumina structure on alcohol dehydration. They found that dehydration was the favoured reaction over all the aluminas tested except a δ-phase alumina prepared by arc-evaporation, which favoured the dehydrogenation reaction to acetone and considered to be due to high levels of tetrahedral aluminium in this material. The results also showed that γ-alumina was three to five times more reactive than the other aluminas tested.

2.2.3.2 ALKALI IMPURITIES

The poisoning effect of alkali metal addition to alumina has been studied by several authors, who have different interpretations of the origin of the phenomenon. Chuang and Dalla Lana (1972) state that the catalytic behaviour of NaOH-impregnated alumina can be ascribed to an ion exchange between Na ions and the acidic OH groups of the alumina surface. The role of alumina can be altered from that of a dehydrating catalyst to one of a dehydrogenating catalyst by impregnating with NaOH (Deo et al., 1971).

Pines and Haag (1960) reported that the activity of active aluminas for alcohol dehydration as well as double-bond and skeletal isomerisation is poisoned by impregnation with sodium hydroxide or sodium chloride. Approximately 1.5 wt% sodium was required to render the impregnated catalysts inactive for

isomerisation and dehydration. However, sodium impregnation was not found to affect product selectivity.

The method of sodium incorporation was found to be important. When incorporating sodium during precipitation, the sites responsible for skeletal isomerisation were selectively poisoned. The authors indicated that the alkali metal ions added to the alumina surface poison the Lewis acid sites and gave rise to an acid/base surface complex (Pines and Haag, 1960):

$$-\mathrm{Al}\begin{matrix}/\\ \\ \backslash\end{matrix} + \mathrm{NaOH} \rightarrow \begin{matrix}|\\ [-\mathrm{Al}-\mathrm{OH}]^{-}\ \mathrm{Na}^{+}\\ |\end{matrix}$$

Jiratova and Beranek (1982) found that the strong acid sites of alumina are selectively poisoned by sodium addition.

Fiedorow and Dalla Lana (1980) report that the poisoning effect of Li and Na ions upon the Lewis acid sites increases with an increase in the ionic radii (i.e. basicity) of the alkali metal ion.

Alkali-metal doping has been shown also to modify the selectivity of other alcohol conversion reactions. The main reaction of propanol on γ-alumina is that of dehydration, which involves the least acidic of the surface hydroxyl groups. Added alkali-metal was found to suppress olefin production in the reaction of propanol over alumina catalysts (Deo and Dalla Lana, 1969). Once these sites have been suppressed by doping with sodium hydroxide, the dehydrogenation reaction involving the aluminum ions becomes dominant.

Narayanan et al. (1992) also reports that for γ-aluminas, sodium poisoning appears to play a major role in the declining dehydration activity with isopropanol conversion.

2.2.3.3 CALCINATION CONDITIONS

MacIver et al. (1964) found that the activity of γ- and η-alumina towards double bond isomerisation of 1-pentene, increased with increasing

pretreatment temperature. A slight decrease was reported at the highest temperature (900°C). The activities for skeletal isomerisation of 1-pentene passed through a maximum at a pretreatment temperature of 600-700°C.

Pines and Haag (1960) investigated the effect of calcination temperature on the activity of alumina towards skeletal isomerisation of cyclohexene. They found that maximum catalytic activity occurs at a calcination temperature of 600-700°C.

Wang et al. (1999) reported that isopropanol conversion levels reached a maximum for samples calcined at 600°C and decreased with higher pretreatment temperatures. Temperature pretreatment effects phase transformation (section 2.1.4). The prevalent phase, after treatment at 600°C, would be γ-alumina and is reported by Narayanan et al. (1992) to be most active (section 2.2.3.1). Pretreatment at higher temperature would give rise to less active phases and, consequently, lower conversion levels as reported by Wang et al. (1999).

CHAPTER 3: OBJECTIVES OF THIS STUDY

Literature describes the surface of alumina as highly heterogeneous and does not give a clear description of what are typically the properties that can be expected from these surfaces.

The objective of this study was to investigate the use of isopropanol conversion as a probe reaction to determine the presence of differences in surface properties, in particular acidic/basic properties. Given the influence of production route and subsequent calcination conditions on the nature of the resulting structural and surface properties of alumina, the following key question was posed:

Is the isopropanol conversion reaction sensitive to changes in surface properties across the range of materials and pre-treatment temperatures of industrial interest?

CHAPTER 4: EXPERIMENTAL DETAIL

The aluminas used during the experiments originated from three different manufacturers namely: Sasol Germany (formerly Condea), Axens (formerly Procatalyse) and La Roche. The details of the brands are given in table 4-1.

Table 4-1 Alumina information

Supplier	Grade
Condea	Puralox SCCa
Procatalyse	SPH 538 MP
La Roche	V900

4.1 ALUMINA CALCINATION

4.1.1 BULK CALCINATION AT CONSTANT TEMPERATURE

Each brand was calcined at five temperatures in the range 750°C to 950°C. Calcinations were carried out in a quartz calcination tube with a central thermocouple (see appendix A-1 for more detail of the design). The calcination procedure is detailed in table 4-2. Airflow was maintained throughout the procedure, inclusive of the cooling down period.

Table 4-2 Calcination conditions

Mass of alumina (g)	40-50
Airflow (l/min)	1.7
Heating rate (°C/min)	1.6
Time at final temperature (hr)	16

The mass of the calcination tube, containing the alumina sample, was determined before and after the calcination procedure. The change in mass could therefore be calculated. All calcined samples were stored in a desiccator to avoid the re-adsorption of water.

4.1.2 THERMOGRAVIMETRIC ANALYSIS

Thermogravimetric analysis (TGA) was conducted on a Mettler TGA/SDTA851e balance. A sample of approximately 50 mg was weighed into a 70 µl platinum pan and the procedure followed, as set out in table 4-3.

Table 4-3 TGA conditions

Mass of alumina (g)	0.05
Nitrogen flow (ml/min)	100
Starting temperature (°C)	ambient
Heating rate (°C/min)	15
Final temperature (°C)	1200

4.1 ALUMINA CHARACTERISATION

4.2.1 IMPURITIES

4.2.1.1 SODIUM AND SILICON DETERMINATION

The sodium and silicon content was determined by Atomic Emission Spectroscopy (AES). A sample was digested in a mixture of 6 ml HCl, 2 ml HNO_3 and 1 ml HBF_4, in an Ethos Plus microwave oven at a temperature of 180°C (15 min to completion). An analytical sample was prepared by diluting the digested mixture to sufficient volume. Analysis was conducted on a Vista AX CCD Simultaneous ICP-AES.

4.2.1.2 SULPHUR DETERMINATION

The sulphur content was determined as SO_2 evolved when combusting the sample at 1350°C in a pure oxygen atmosphere using a Leco SC-432 sulphur analyser.

4.2.2 SURFACE AREA AND PORE VOLUME

The surface area and total pore volume were measured by nitrogen adsorption via the BET method using a Micromeretics Tristar 3000 instrument. Approximately 0.25 g of sample was de-gassed by heating it to 200°C in a nitrogen flow, overnight, prior to analysis.

4.2.3 ACIDITY

Ammonia-Temperature Programmed Desorption was performed using a Micromeritics Autochem 2910 with a sample size of approximately 0.15 g and desorbed ammonia detection by a thermal conductivity detector. Table 4-4 describes the procedure followed.

Table 4-4 NH_3-TPD procedure

Step	Atmosphere	Flowrate (ml/min)	Heating rate (°C/min)	Temperature (°C)	Time at temperature (min)
Degassing	He	50	5	ambient - 120	10
	He	50	10	120 - 250	30
NH_3 adsorption	4-5% NH_3 in He	50	-	100	60
Flushing	He	50	-	100	30
Desorption	He	50	10	100 - 750	-

4.2.4 ZETA POTENTIAL

Zeta potential (a measure of the overall charge present on the surface of an oxide as a function of the pH) was determined using a Malvern Zetasizer 4. Approximately 0.1 g of ground sample was added to 50 ml of 0.05 M KCl solution and shaken well, followed by pH adjustment in the acid and alkaline ranges using 0.1 N HCl and KOH respectively. Sufficient time was allowed for pH stabilization prior to analysis.

Data workup involved averaging the results of 3 measurements.

4.2.5 CRYSTAL PHASE (XRD)

Samples were analysed via x-ray diffraction with a Phillips Automatic X-ray powder diffractometer. The conditions used during analyses were as follows:

Table 4-5 XRD conditions

Source	Copper tube
Start angle (°)	5
End angle (°)	75
Step size (°)	0.05
Scan speed (°/sec)	0.03

4.3 CATALYTIC ACTIVITY

4.3.1 THE CONVERSION OF ISOPROPANOL

The conversion of isopropanol was used to compare the alumina samples and to determine the influence of the calcination temperature on catalytic activity and selectivity. These tests were carried out in the gas phase in a fixed bed reactor.

4.3.2 REACTOR SYSTEM

A schematic diagram of the experimental set-up is shown in figure 4-1. The reactor system consists of a fixed bed reactor, preceded by a preheater/vaporiser filled with 4 mm glass beads. The feed was introduced via an isocratic pump (Rheos 4000 HPLC pump). Argon and hydrogen were supplied to the reactor via Brooks mass flow controllers. Liquid and gas feed lines combined immediately before the preheater/vapouriser.

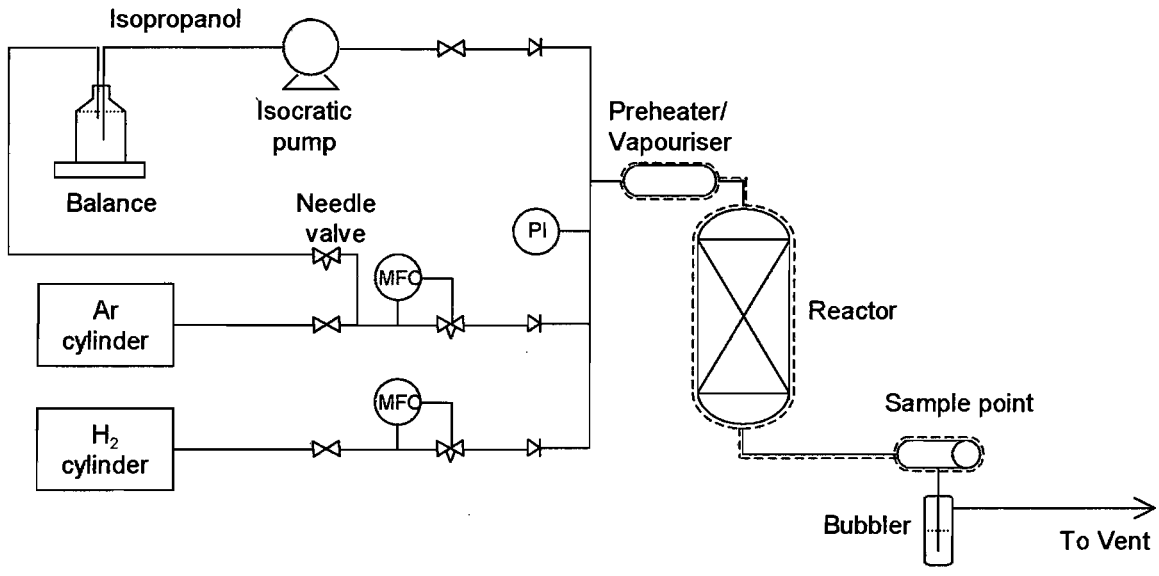

Figure 4-1 Process flow diagram for the test reaction (---- = heated)

4.3.2.1 FEED STORAGE FLASK

The isopropanol feed was stored in a 500 ml glass container and placed on a balance (Mettler Toledo PB1853). As a result of initial findings suggesting some degree of feed oxidation (appendix A-6), a small flow of argon gas was bubbled through the isopropanol feed so as to strip oxygen from the liquid. The balance reading was taken before and after each run, so that the feed rate could be calculated.

4.3.2.2 FEED PUMP CALIBRATION

The isocratic pump was calibrated by making use of the balance to confirm the amount of liquid feed introduced into the system (appendix A-2).

4.3.2.3 GAS FLOW METER CALIBRATION

The mass flow controllers were calibrated by using a Ritter drum-type gas meter (TG1-14571-pvc) and a stopwatch. The temperature and atmospheric pressure were noted and the flows were normalised to standard temperature and pressure. Calibration data are provided in appendix A-3.

4.3.2.4 PREHEATER/VAPORISER

The preheater/vaporiser consisted of a 150 ml stainless steel sample bomb, filled with 4 mm glass beads to increase the surface area for vaporisation.

4.3.2.5 REACTOR AND REACTOR LOADING

The experiments were conducted in a stainless-steel double-wall fixed bed plug-flow reactor (figure 4-2). The reactor insert tube (14 mm diameter and 200 mm in length) contained the catalyst bed and was located in the slightly larger external reactor body so as to ensure the whole bed was located in the isothermal region (figure 4-2 and section 4.3.2.7). The temperature was controlled by a heating mantle and a thermocouple was used to monitor the internal temperature just below the catalyst bed.

The special design of the reactor allowed the reactor insert tube to be removed, unloaded and reloaded with new catalyst, while the external reactor body was kept in place and the temperature of the heating mantle and external tube was kept at the reaction temperature.

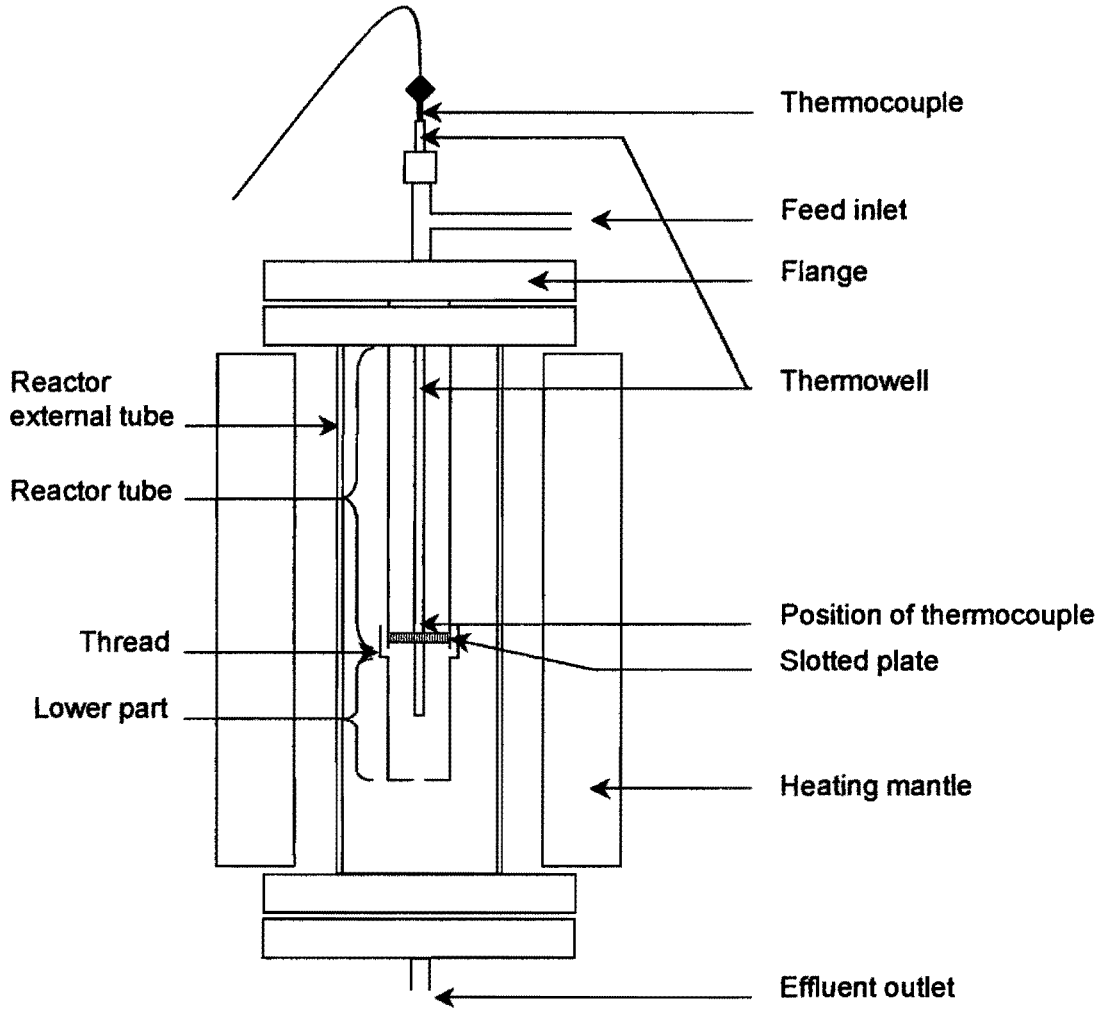

Figure 4-2 Schematic configuration of reactor

The reactor insert tube was loaded with catalyst in an upside-down position so as to eventually achieve a packed bed configuration as per figure 4-3.

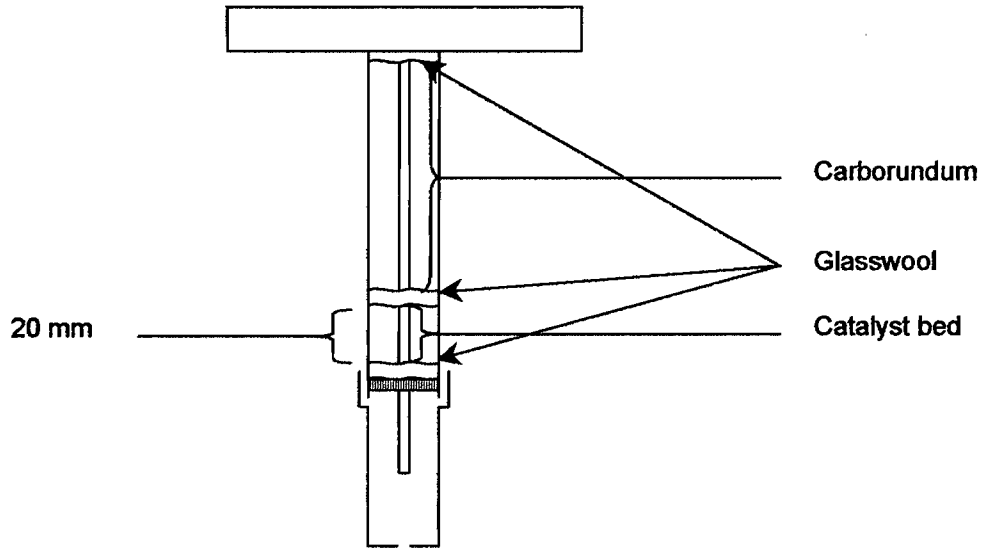

Figure 4-3 Schematic configuration of catalyst packing

4.3.2.6 CATALYST PREPARATION

All the catalysts were supplied in powder form (60 to 80 μm) and were used as such. No diluent was applied in the catalyst bed.

4.3.2.7 REACTOR ISOTHERMAL ZONE

The temperature profile of the reactor was determined under typical reaction conditions of temperature and gas flow. For this purpose the reactor was loaded as described above, but carborundum was loaded instead of catalyst. The thermocouple was pushed down to its lowest point and then pulled out 0.5 cm at a time, recording the steady-state temperature as shown in figure 4-4.

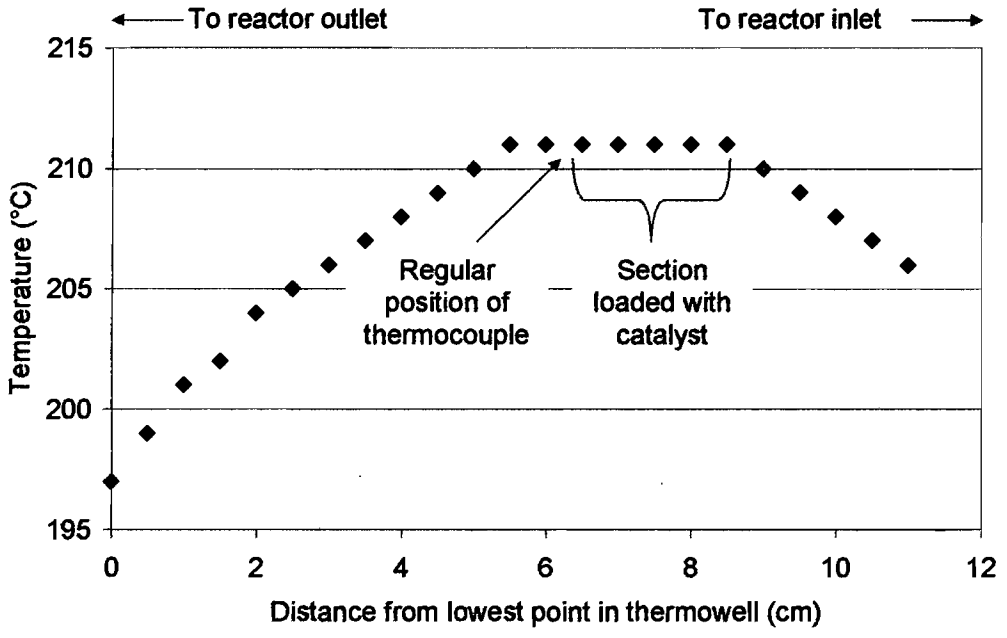

Figure 4-4 Temperature profile in reactor

The catalyst bed was positioned in the area identified as isothermal.

4.3.2.8 EXPERIMENTAL PROCEDURE

All runs were conducted according to the same procedure. After loading the reactor and establishing carrier gas flow, enough time was allowed for the temperature to reach the setpoint and stabilise. The isocratic pump was started and the balance tarred. During most runs a single sample of the product was taken after 50 min (see sections 4.3.4.1 and 4.3.4.2 for details on sampling). Thereafter, the pump was stopped and the reactor was flushed with carrier gas for 30 min, before the reactor insert tube was removed from the reactor and the next catalyst loaded (see section 4.3.2.5).

Multiple sampling during a long term (19 hrs) run proved that steady-state performance was achieved after 50 min time-on-stream and that a 50 min sample was representative (see section 5.3.1.2 and appendix A-12).

4.3.3 EXPERIMENTAL CONDITIONS

The conditions used during all runs are provided in table 4-6.

Table 4-6 Experimental conditions

Mass of catalyst	3 g
Temperature	200°C
Pressure	Atmospheric (0.85 bar)
Feed	Isopropanol[1]
Pump rate	0.0037 $l.h^{-1}$
LHSV	1 h^{-1}
Carrier gas	Argon or Hydrogen
Carrier gas flow rate	15 $l.h^{-1}$ (STP)
Isopropanol:Carrier gas	1:13.3 molar ratio

4.3.4 PRODUCT SAMPLING AND ANALYSIS

A special sampling point was installed downstream of the reactor. The essence of this device was a soft septum, which allowed the extraction of gaseous/vaporous samples from the reactor effluent using evacuated ampoules or gas syringes. Details of this sampling technique are provided in appendix A-4.

4.3.4.1 AMPOULE SAMPLING

Initially, samples of the product were collected with ampoules (appendix A-4). Sampling through this method introduced inconsistencies, which were ascribed to compounds introduced from outside, because of an unfortunate combination of external factors (appendix A-6). Ampoule sampling was, hence, abandoned and unless indicated, all analyses presented in this study were obtained via syringe sampling.

[1] Manufactured by Rochelle Chemicals, Batch no 2076, 99.7% Purity, 0.05% ketones. Note that GC analyses of the isopropanol used in fact revealed about 2 wt% acetone, see appendix A-6.

4.3.4.2 SYRINGE SAMPLING

Due to the problems experienced with the ampoule method, later samples were taken by using a gas syringe (100 µl VICI Pressure-lok® Precision Analytical gas syringe). The needle of the syringe was inserted through the septum of the sampling point and a sample was withdrawn. To eliminate contamination, the syringe was filled and emptied six times with the fully vaporised effluent stream before the final sample was taken.

The feed mixture contained about 9 vol% isopropanol vapour in argon or hydrogen carrier gas. Isopropanol was still the major and also the least volatile constituent of the product mixture. Vapour pressure values (appendix A-5) predicted a dew point of the reactor effluent below 35°C. Therefore the gas syringe was heated in an oven (set at 50°C) in order to avoid any product condensation.

4.3.4.3 GAS CHROMATOGRAPHIC ANALYSIS

A Chrompack CP9000 Gas Chromatograph fitted with a Petrocol column was used to analyse the content of the ampoules and syringes. Gas chromatography conditions are summarised in table 4-7.

Table 4-7 Gas chromatography conditions

Gas Chromatograph	Chrompack CP9000
Column	Petrocol D8-150
Carrier gas	Hydrogen
Head pressure	200 kPa
Split	1:100
Initial oven temperature	-60°C
Heating rate	50°C/min to -20°C
	2°C/min to 220°C
Final temperature	220°C
Hold time	80 min

A typical GC trace is shown in figure 4-5 and peak identification is listed in table 4-7. Note that the acetone peak is quite small with significant tailing.

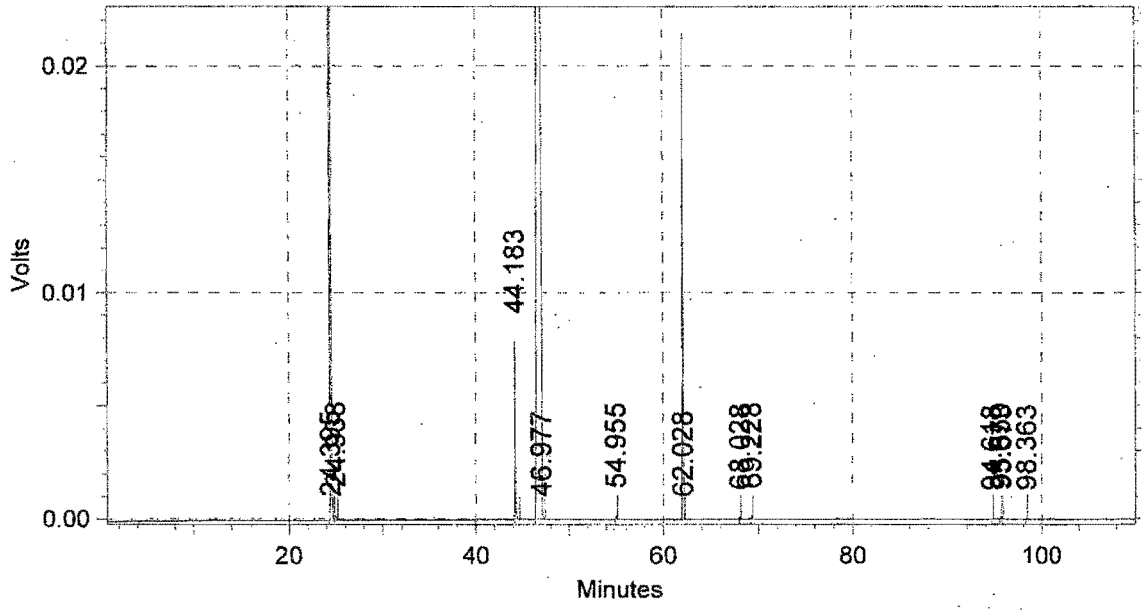

Figure 4-5 Typical GC trace of isopropanol containing product

Table 4-8 Identity of GC peaks

Product I.D.	Retention time (min)
Propene	24.395
Acetone	44.183
Isopropanol	46.977
Diisopropyl ether	62.028

4.3.5 DATA WORK-UP

4.3.5.1 PRODUCT COMPOSITION

The GC analysis of the product was reported as peak area. These values were divided by the individual mass specific response factors for the different molecules, to report them in a form proportional to mass.

$$M_i \sim Area_i / f_i$$

The relative response towards carbon atoms has been found to be as follows (Callanan, 2000):

All C in hydrocarbons	1.0	
R-C(=O)-R	0	(C=O double bond)
R_2-CH-OH	0.55	(C-O single bond)
R_2-CH-O-R	0.55	(C-O single bond)

The response factors for the compounds were calculated relative to propene, which was considered to have a response factor of 1. The mass specific response factor, f, for a compound i was therefore calculated as follows:

$$f_i = \frac{(C_{response,i} \cdot MC_i) / (C_i \cdot MM_i)}{(C_{response,propene} \cdot MC_{propene}) / (C_{propene} \cdot MM_{propene})}$$

Where f_i = response factor for molecule i

C_i = number of carbon atoms in molecule i

$C_{responce,i}$ = number of carbon atoms responded to by FID

- propene = 3
- isopropanol = 2.55
- diisopropyl ether = 5.1
- acetone = 2

MM_i = molecular mass of molecule i

MC_i = mass of carbon in molecule i

The values of the mass specific response factors, f_i, as derived from the above, are as follows:

Propene	1.00
Isopropanol	0.60
Diisopropyl ether	0.70
Acetone	0.48
Others	1.00

A small amount of other components were also found in the product and lumped together under the caption 'others'. These were treated as olefins and therefore a response factor of 1, as for propene, was used.

4.3.5.2 CONVERSION, SELECTIVITY AND YIELD

In order to express conversion, selectivity and yield in mole % the mass percent product compositions were converted on the basis of equivalent moles of isopropanol feed, i.e. a factor of 2 was incorporated in the expression for diisopropyl ether, since two moles of alcohol are consumed to make one mole of ether. Moles of 'others' were expressed in terms of moles alcohol consumed as well.

Isopropanol conversion results are presented in two forms throughout this study. In the case where acetone is not considered a product of the reaction, but rather as an inert component of the feed, acetone is discounted from the feed and effluent stream analyses, with the remaining components normalised to 100% and the conversion, selectivity and yield are defined on a molar basis as follows:

$$\text{Conversion} = 1 - \text{moles isopropanol}_{out} / \text{moles isopropanol}_{in}$$

$$\text{Selectivity} = \frac{\text{moles of isopropanol consumed in product}_i}{\text{moles isopropanol}_{in} - \text{moles isopropanol}_{out}}$$

$$\text{Yield} = \text{Selectivity} \cdot \text{Conversion}$$

In the case where all components other than isopropanol are considered to be products of the reaction, calculations are conducted according to the above definitions, but the nomenclature employed are pseudo-conversion, pseudo-selectivity and pseudo-yield, respectively.

4.3.5.3 NORMALISING TO CATALYST SURFACE AREA

Conversion values were normalised in order to eliminate any effects caused by differences in the surface area. The correct method would require calculating the rates and relating these to the surface area or eventually calculating turn-over-numbers. However, since conversions obtained ranged from 5 to 35%, the initial rate method would not be valid and calculating rate constants would require detailed knowledge of the kinetics of the reactions. Although, assuming the kinetics to be of 1st order might be reasonable for the formation of acetone and propene, this assumption is incorrect for diisopropyl ether formation (Heese, 1998). Conversions are therefore normalised to a reference area as follows:

$$X_{norm} = X_{measured} \cdot Area_{ref} / Area_i$$

Where X_{norm} = normalised conversion

$X_{measured}$ = conversion without surface area considerations

$Area_i$ = surface area of the alumina used

$Area_{ref}$ = surface area of a hypothetical reference sample (averaged surface area of all alumina samples studied)

It should be noted that the above procedure of normalisation did not change the conversion values significantly (section 6.3.3.2).

4.3.6 EXPERIMENTS CONDUCTED

Table 4-9 lists the set of experiments included in this study. These experiments were conducted using a syringe as sampling device as described in section 4.3.4.2.

Table 4-9 List of the experiments carried out using H_2 carrier gas and a syringe as sampling device

Run number	Alumina	Calcination temperature (°C)
C0 C19 C21 C36	Blank	
C1 C38	Condea	As received
C4 C37	Condea	750
C14 C26	Condea	800
C9 C30	Condea	850
C8 C31	Condea	900
C3 C25	Condea	950
C11	Procatalyse	As received
C6 C33	Procatalyse	750
C5 C34	Procatalyse	800
C16 C24 C41	Procatalyse	850
C13 C27	Procatalyse	900
C10 C29	Procatalyse	950
C15	La Roche	As received
C12 C28 C39	La Roche	750
C7 C32	La Roche	800
C2 C35	La Roche	850
C17 C23	La Roche	900
C18 C20 C22 C40	La Roche	950

CHAPTER 5: RESULTS

5.1 ALUMINA CALCINATION

5.1.1 BULK CALCINATION AT CONSTANT TEMPERATURE

All samples displayed a loss of mass upon calcination. The results are depicted in figure 5-1 (see appendix A-7 for the tabulated results).

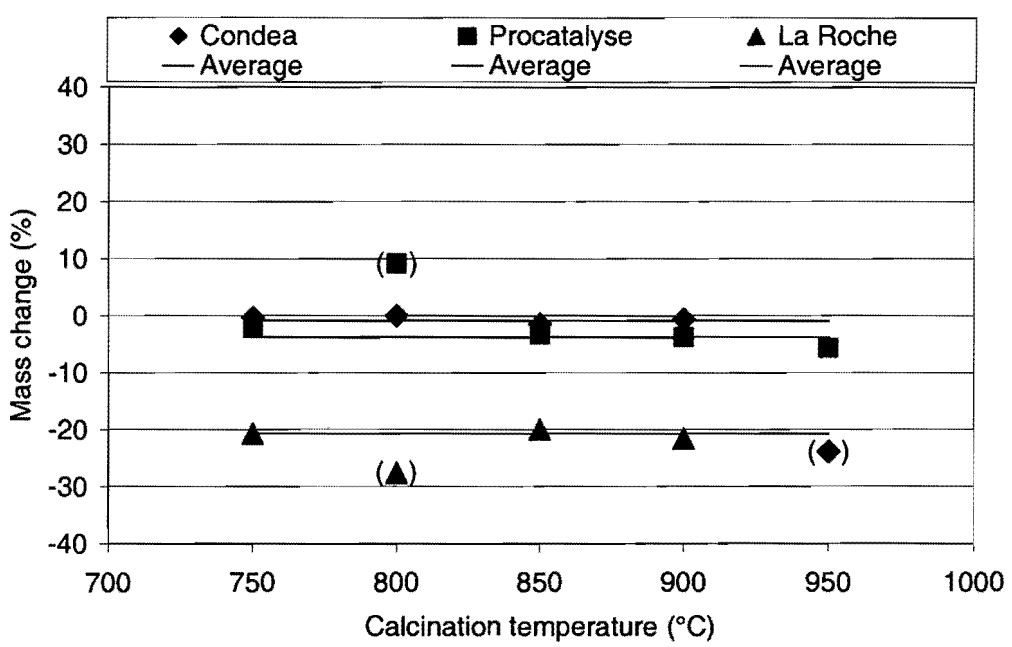

Figure 5-1 Percentage mass change as a function of calcination temperature

Both the Condea and Procatalyse varieties of alumina display no or very minor mass loss upon calcination in the range 750°C to 950°C. Moreover, the mass loss is roughly constant in this range.

The La Roche alumina exhibits a comparably high mass loss of approximately 20% when calcined in the range 750°C to 950°C. Here too the effect of calcination temperature is small.

5.1.2 THERMOGRAVIMETRIC ANALYSIS

The results obtained from TGA are presented in figure 5-2a to c.

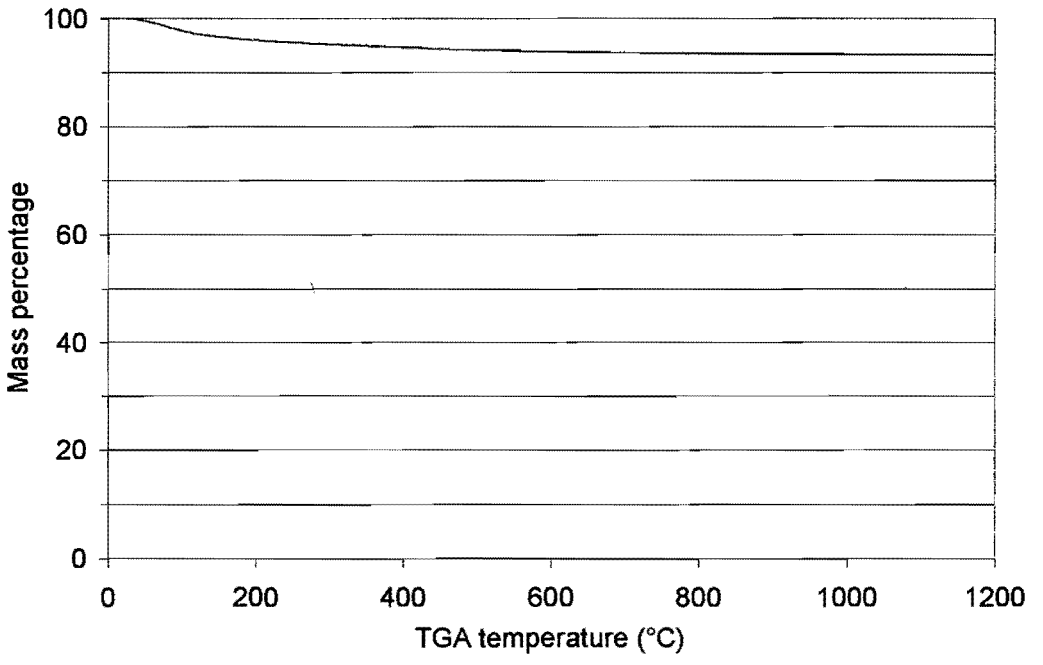

Figure 5-2a TGA results for Condea sample

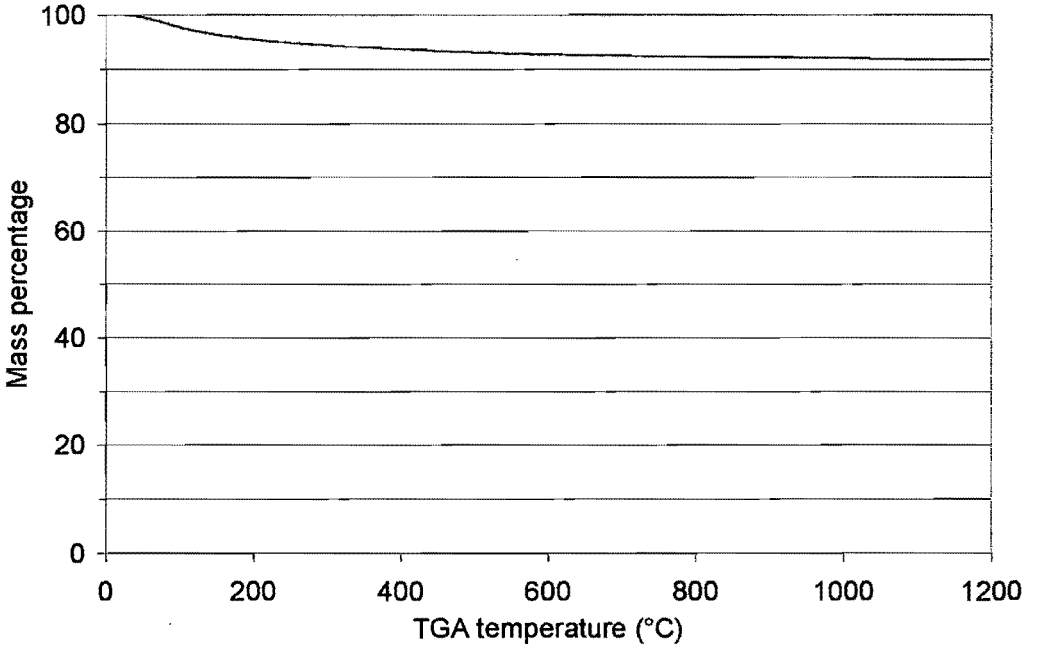

Figure 5-2b TGA results for Procatalyse sample

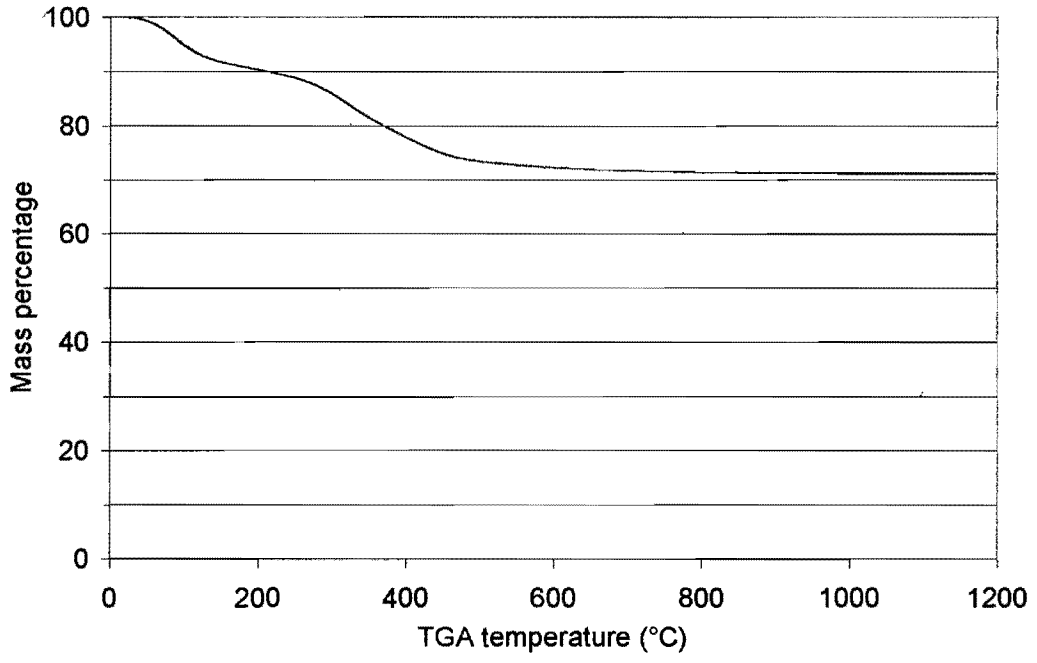

Figure 5-2c TGA results for La Roche sample

Comparison of the mass lost during bulk sample calcination and TGA (table 5-1) indicates that the observed mass loss is significantly higher for the TGA measurements. Samples were taken directly from the desiccator to be calcined, while those employed for TGA were stored in containers which did not exclude atmospheric air. It is therefore quite possible that the additional mass loss may be due to moisture which adsorbed prior to analysis.

Table 5-1 Comparison of mass loss upon bulk sample calcination and TGA

Alumina sample	Average loss during calcination (%)	Loss during TGA (%)
Condea	0.8	6.4
Procatalise	3.7	7.6
La Roche	20.7	28.4

5.2 ALUMINA CHARACTERISATION

5.2.1 IMPURITIES

As discussed in sections 2.1.2 and 2.2.3.2, the presence of impurities may change the characteristics of a support. Levels of sodium, silicon and sulfur are reported in table 5-1.

Table 5-1 Impurities present in the alumina types

Alumina	Na as Na_2O (ppm)		Si as SiO_2 (ppm)		S as sulfate (ppm)	
	By manu-facturer	AES Analysis	By manu-facturer	AES Analysis	By manu-facturer	By com-bustion
Condea	50	200	350	14700	~	<100
Procatalyse	90	500	1100	3700	2800	1000
La Roche	500	700	700	3700	~	300

~ Information not available

The impurity levels reported by the manufacturers are much different to those obtained from the various analyses. The reason for these discrepancies are unknown and, consequently, any evaluation of catalytic performance in respect of impurity levels needs to consider both sets of data.

Chemical analyses showed the presence of 700 ppm Na_2O in the uncalcined sample of La Roche alumina. On calcination 20% weight loss takes place, which means the Na_2O content increases to 880 ppm. Similarly, for Condea the content increases to 202 ppm and for Procatalyse to 520 ppm.

5.2.2 SURFACE AREAS AND PORE VOLUMES

The BET surface area and pore volumes of the untreated and calcined samples are reported in figures 5-3 and 5-4. The tabulated results are reported in appendix A-8.

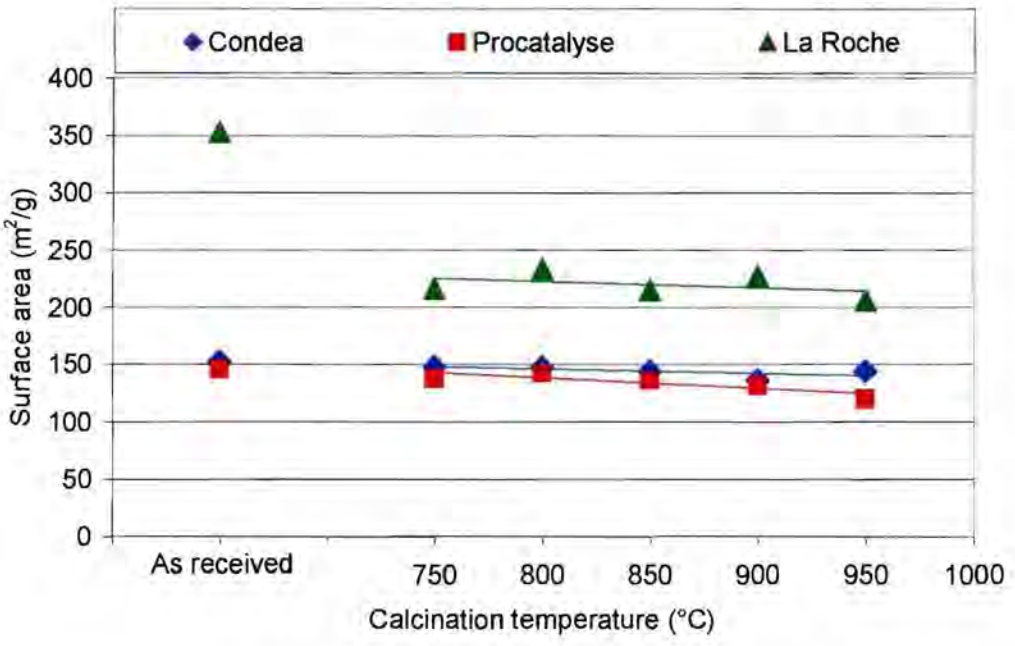

Figure 5-3 Surface area versus calcination temperature

A huge decrease of the BET surface area is observed for the La Roche sample upon calcination at 750°C. For the other two alumina varieties, the surface area does not change significantly upon calcination.

The trend observed for all three aluminas indicates a slight decrease in the surface area as the temperature of calcination increases in the range 750°C to 950°C. Whereas the surface areas of both the Condea and Procatalyse aluminas are very similar, the La Roche sample has a much higher surface area, even after calcination.

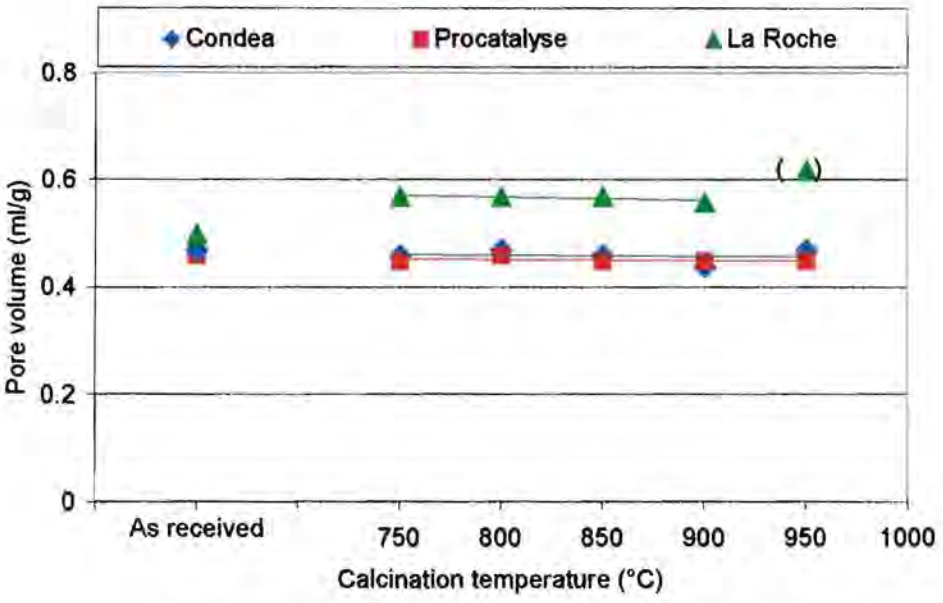

Figure 5-4 Pore volume versus calcination temperature

Consistent with the surface area data, pore volumes did not change substantially upon calcination at 750°C, except in the case of the La Roche sample. Moreover, for all samples no change in pore volume occurs with increasing calcination temperature in the range 750-950°C. Calcined La Roche alumina exhibits a significantly higher pore volume than the other alumina samples.

The pore size distribution was measured for one sample each of Condea and La Roche alumina, calcined at 850°C and 900°C, respectively.

Table 5-3 Results from pore size distribution determinations

Alumina	Calcination temperature (°C)	Range of pore sizes (nm)	Maximum of distribution curve (nm)
Condea	850	4-20	9
La Roche	900	3-50	7

The pore size distribution range was significantly narrower for Condea alumina than for La Roche alumina (see appendix A-9).

5.2.3 AMMONIA-TEMPERATURE PROGRAMMED DESORPTION

The NH_3-TPD results could be quantified with regard to the temperature of the maxima of the two main desorption peaks, whereas peak integration results were unreliable. The NH_3-TPD traces for all the samples calcined at different temperatures are presented in figure 5-5a to c.

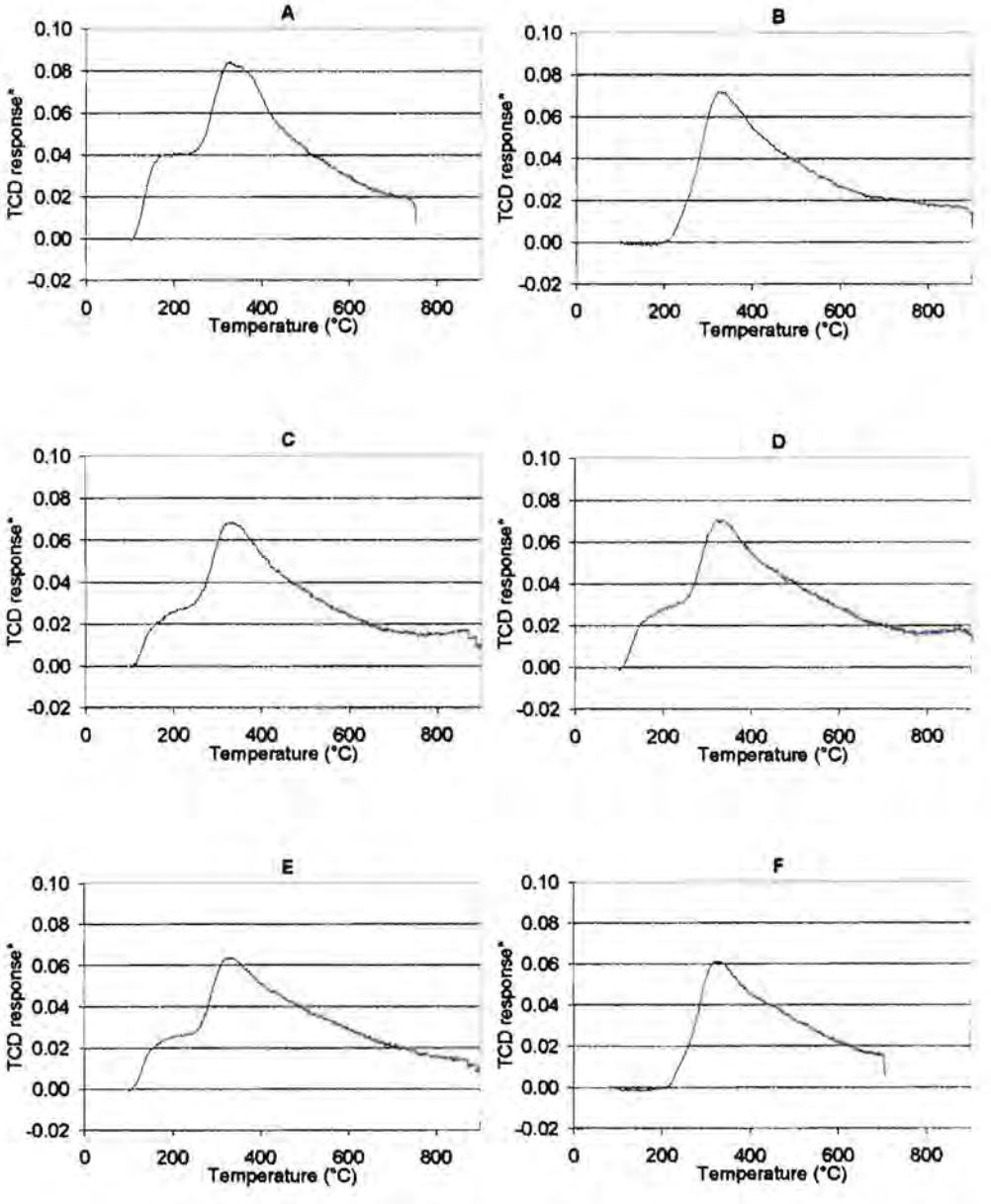

Figure 5-5a NH_3-TPD traces for Condea samples calcined at different temperatures: A – as received, B – 750°C, C – 800°C, D – 850°C, E – 900°C and F – 950°C [* - arbitrary units]

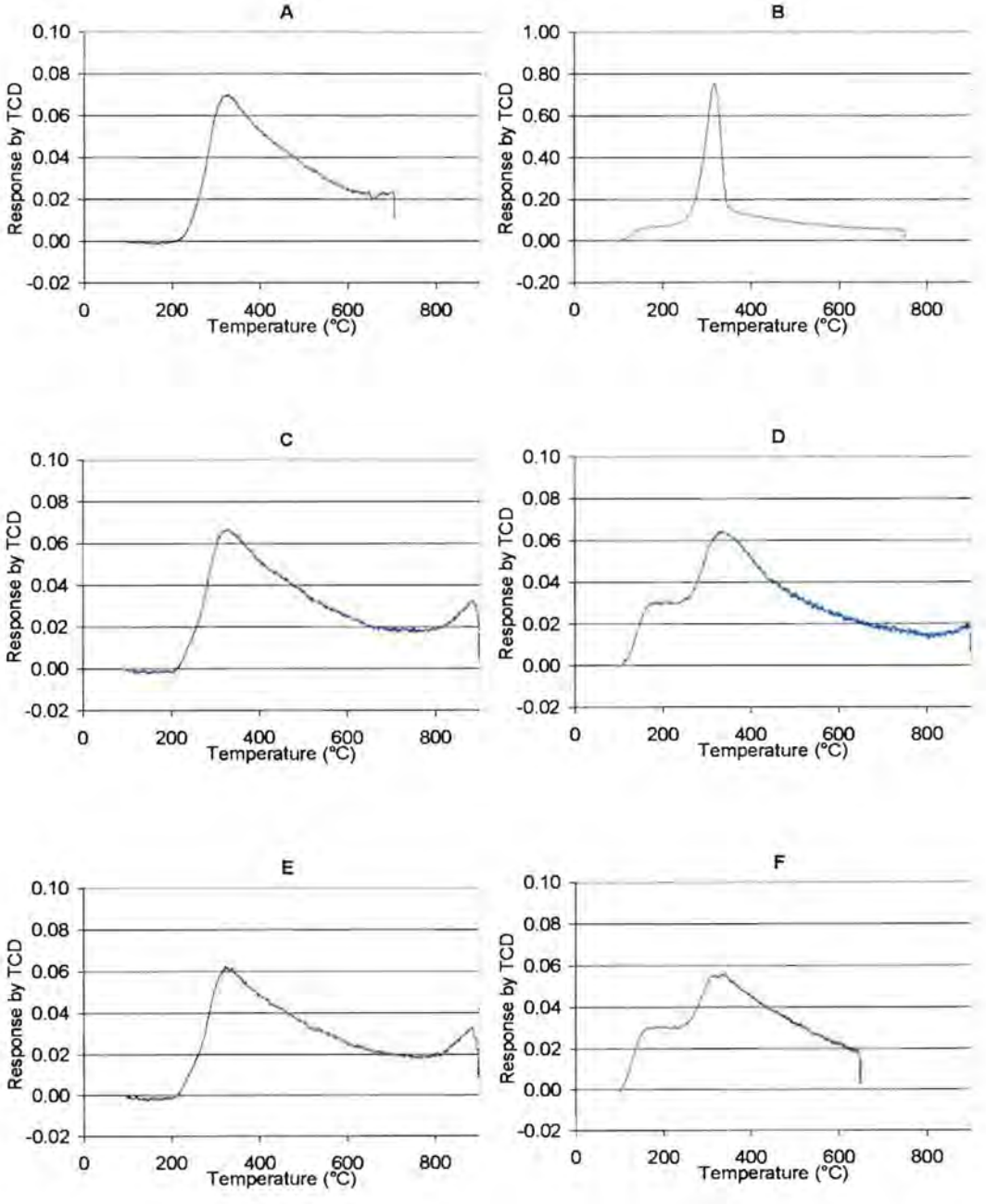

Figure 5-5b NH_3-TPD traces for Procatalyse samples calcined at different temperatures: A – as received, B – 750°C, C – 800°C, D – 850°C, E – 900°C and F – 950°C [* - arbitrary units]

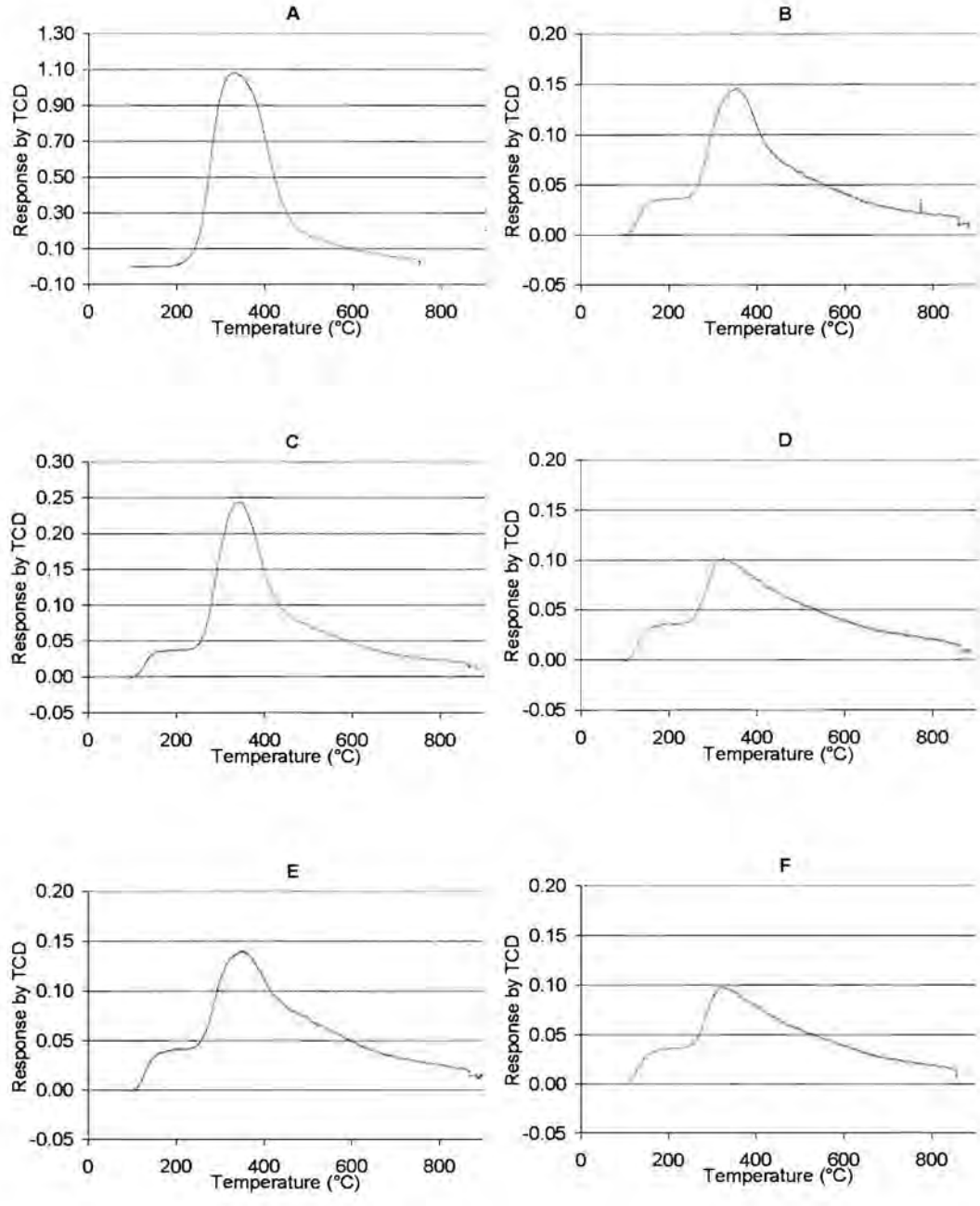

Figure 5-5c NH_3-TPD traces for La Roche samples calcined at different temperatures: A – as received, B – 750°C, C – 800°C, D – 850°C, E – 900°C and F – 950°C [* - arbitrary units]

Most samples exhibited a plateau in the region of 150-250°C, followed by a steep increase in NH_3 desorption. A maximum is reached in the region above 300°C and as the temperature further increases an exponential decline is

observed. In most cases the decrease continues to a level below that of the initial plateau.

Two peaks were identified by the data evaluation software applied. Peak A – small and generally quite unresolved under the 'plateau' with a maximum around 245°C and peak B – ranging from 250°C to 500°C with a maximum around 330°C. Peak A results from physisorbed or hydrogen bonded NH_3 and as such is not representative of strong acidity and is consequently of no significance. A summary of the TPD results is given in table 5-4.

Table 5-4 Maximum temperatures of the peaks observed in ammonia-TPD

Alumina	**Calcination temperature (°C)**	**Temperature peak B (°C)**
Condea	As received	323
	750	328
	800	324
	850	322
	900	323
	950	329
Procatalyse	As received	329
	750	319
	800	327
	850	340
	900	329
	950	338
La Roche	As received	330
	750	353
	800	345
	850	325
	900	352
	950	326

For all three aluminas it is observed consistently that the decline, following the maximum of the major peak B, becomes less steep with an increase in calcination temperature (see section 6.1.4).

5.2.4 ZETA POTENTIAL

Zeta potential is a measure of the total overall charge of all ions that are present on the surface of a material at a certain pH. It can be used as an indication of the presence of impurities, since these influence the position of the point of zero charge (also known as the isoelectric point). The intrinsic error associated with this method is ±5 mV zeta reading (Harris, 2002).

The results are depicted in figures 5-6a to c.

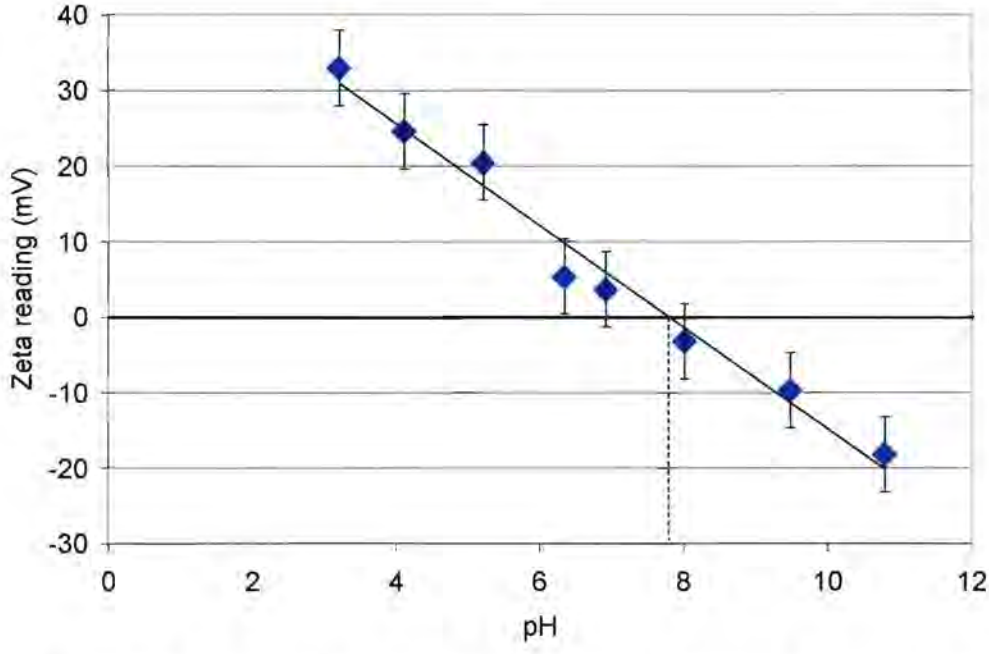

Figure 5-6a Plot of Zeta potential versus pH for Condea alumina as received

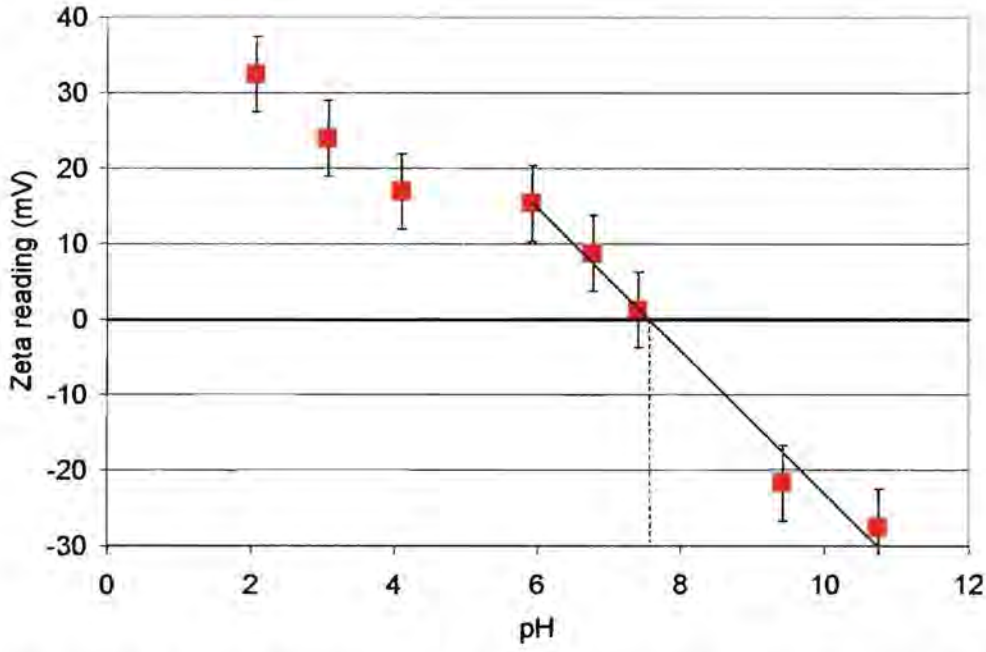

Figure 5-6b Plot of Zeta potential versus pH for Procatalyse alumina as received

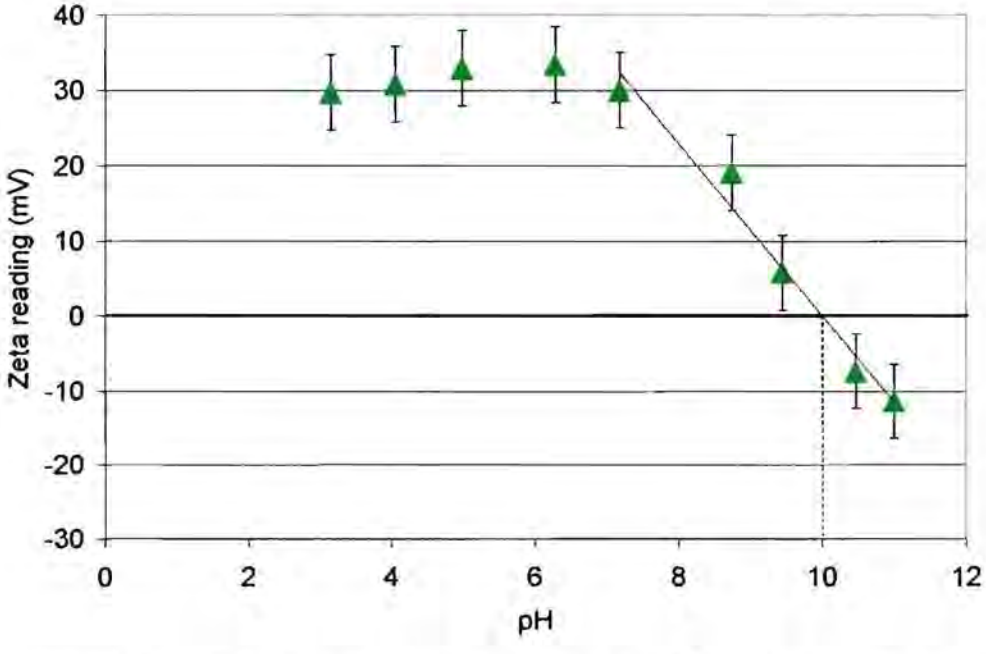

Figure 5-6c Plot of Zeta potential versus pH for La Roche sample as received

The isoelectric point was found to be very similar (pH=7.8 and 7.6) for the Condea and Procatalyse samples, while that for the sample from La Roche was much higher (pH=10). Upon calcination of the latter sample, a decrease was observed in the isoelectric point (figure 5-6d).

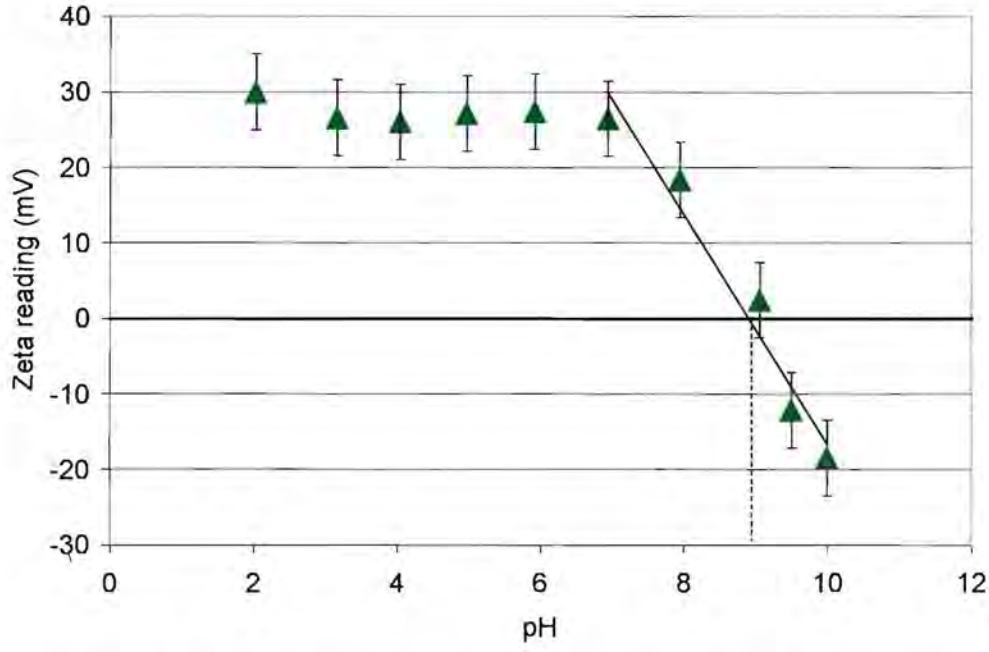

Figure 5-6d Plot of Zeta potential versus pH for La Roche sample calcined at 750°C

5.2.5 X-RAY DIFFRACTION

It was shown that the Condea and Procatalyse samples, 'as received', consist mainly of γ-alumina (Al_2O_3). The sample from La Roche, 'as received', consists of boehmite (AlOOH). XRD traces are presented in figures 5-7a to c.

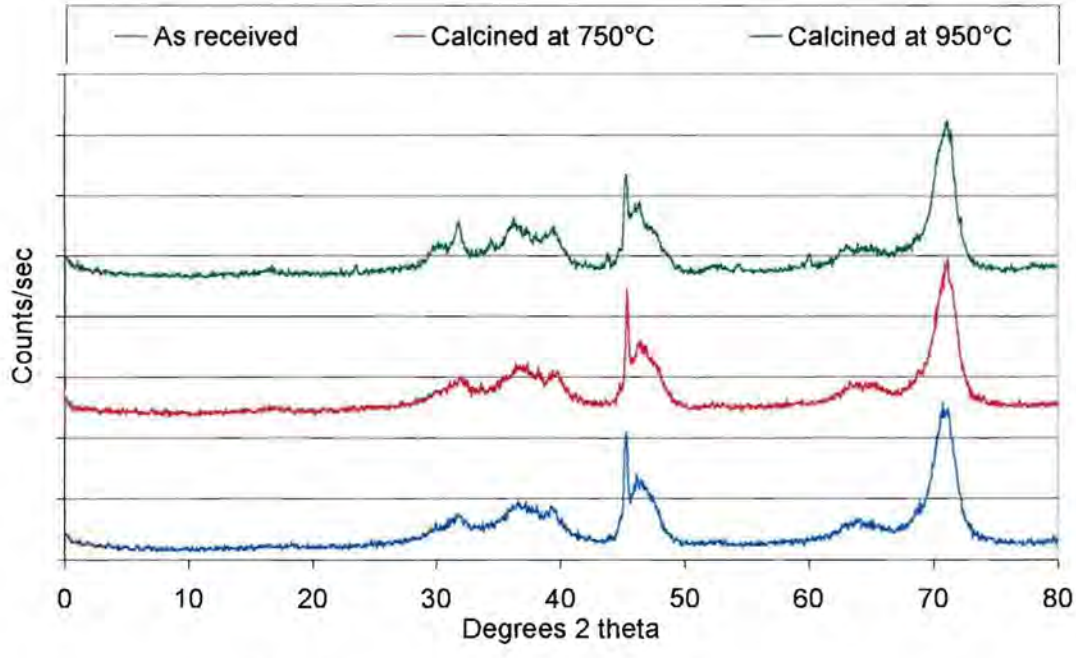

Figure 5-7a X-ray diffraction patterns of Condea samples

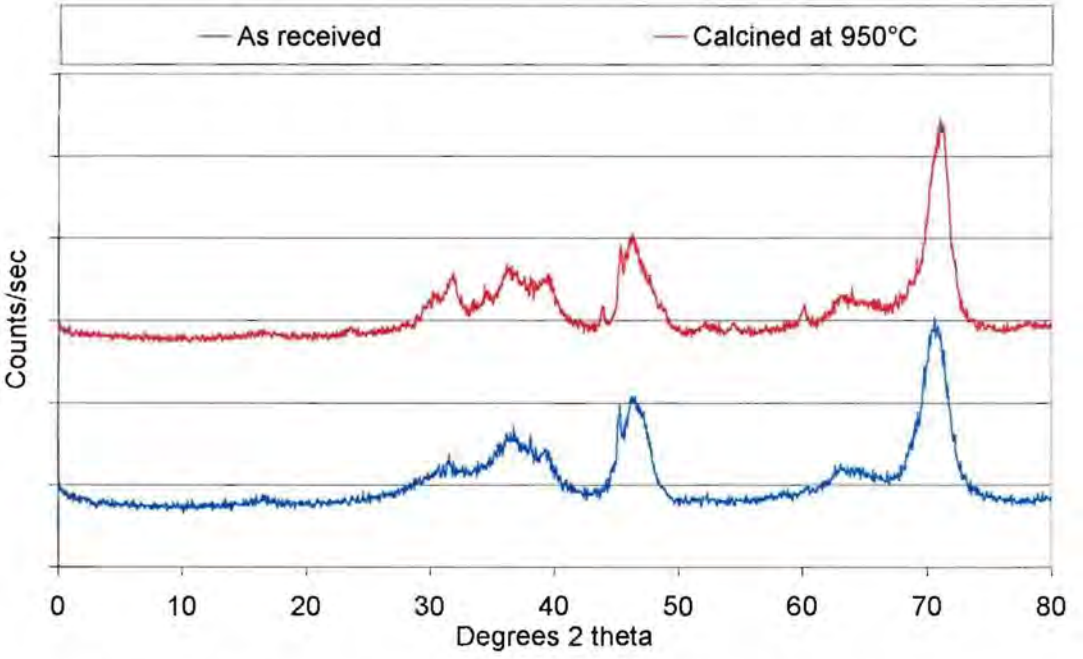

Figure 5-7b X-ray diffraction patterns of Procatalyse samples

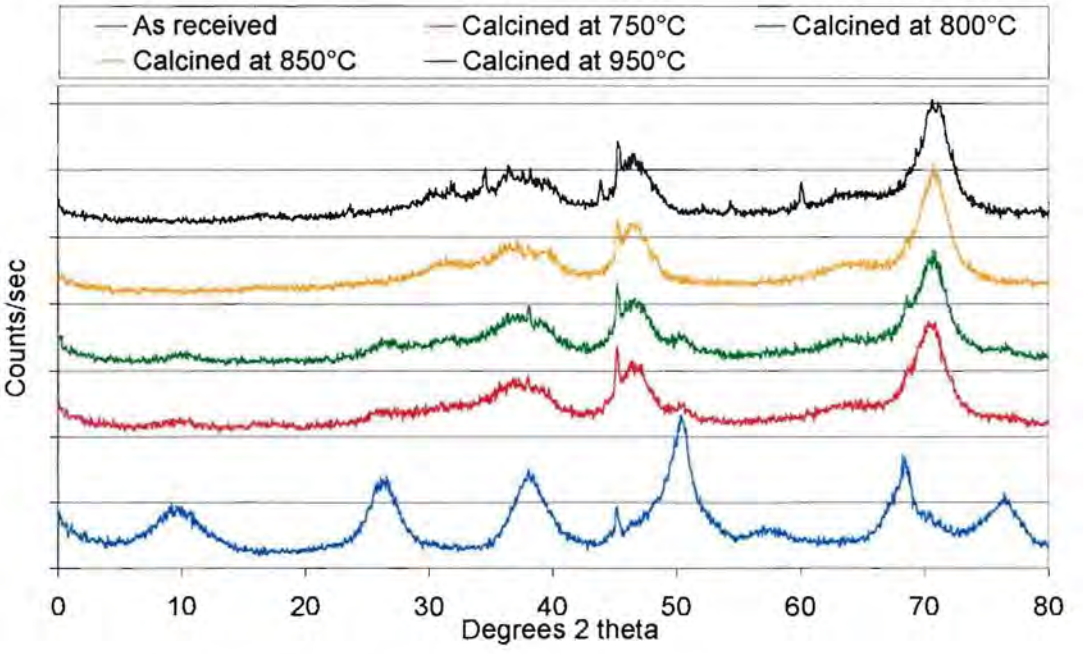

Figure 5-7c X-ray diffraction patterns of La Roche samples

Calcining the Condea sample to 750°C did not produce any observable changes in the XRD pattern, whereas upon calcination at 950°C, peaks representing α- and δ-phases of alumina in addition to the γ-phase can be observed.

The XRD pattern of the Procatalyse sample calcined at 950°C also showed the presence of the α- and δ-phases, in addition to the γ-phase.

Calcination of the La Roche sample to 750°C induced a drastic change in the XRD pattern. The sample underwent a phase change from boehmite to the γ-phase, but the presence of the former is still observable up to a calcination temperature of 800°C. After calcining at 850°C, γ-alumina is the major phase present and as in the case of the other varieties, calcination at 950°C produced a mixture of γ-, δ- and α-alumina phases.

5.3 ISOPROPANOL CONVERSION

The major components found in the reactor effluent stream were in all cases: propylene, diisopropyl ether (DIPE) and acetone, together with unconverted isopropanol. Traces of other compounds were observed in the gas chromatogram and were collectively grouped as 'others'. A table containing the detailed results is provided in appendix A-10.

For purposes of presenting the results of the isopropanol conversion experiments in this chapter, acetone is considered a product of the reaction. It will, however, be argued (sections 5.3.1 to 5.3.3 and 6.2) that acetone levels in the reactor effluent are indistinguishable from contaminant levels in the feed and, consequently, that it is best considered an 'inert' component, at least in so far as the experiments conducted over the alumina catalysts of this study. Therefore, results presented in this chapter are presented as pseudo-conversion, pseudo-selectivity and pseudo-yield, according to the definitions of section 4.3.5.2.

5.3.1 ANALYTICAL REPRODUCIBILITY

5.3.1.1 BLANK EXPERIMENT

The product analyses for a number of injections of samples from a blank run (i.e. reactor filled with carborundum), using a gas syringe, were processed as described in section 4.3.5. Results are provided in appendix A-11.

It is clear from the results that analyses are reproducible. Scatter is moderate. Note that the results indicate an acetone content of approximately 1.5 mol% acetone in the feed.

5.3.1.2 EXPERIMENT OVER CATALYST

One of the experiments with Condea alumina, calcined at 750°C, was extended to just over 19 hours. Five samples were taken at approximately 1 hour intervals and the last sample was taken 19h10min from the start of the experiment. The analyses were processed as described in section 4.3.5 and the data used to produce the figures in appendix A-12.

From the figures, the reproducibility of gas chromatographic analysis can be considered good.

5.3.1.3 REPRODUCIBILITY OF EXPERIMENTS

Most of the experiments were repeated to determine the reproducibility of individual experiments. Results from all the repeated experiments are plotted in figures 5-6a to 5-9c. Note that the chronological order of these experiments was random, as can be derived from figures 5-6a to c.

It can clearly be seen from the figures that the amount of scatter produced through repetition of individual experiments is much greater than obtained for repetition of analyses of a single experiment or a blank experiment (section

5.3.1.1 and 5.3.1.2). Therefore analysis can be excluded as a possible cause of this data scatter.

Catalyst samples for repeat experiments were taken from the same calcination batch and results from repeat experiments showed a random deviation (see figures 5-6a to 5-9c). This excludes calcination or the uptake of moisture during storage from possible reasons for the scatter. There are indications, which may suggest that the loading of the reactor (see section 4.3.1.5) might have produced some irregularities in the catalyst bed, resulting in irreproducible channelling effects and, consequently, direct effects on conversion. This hypothesis is supported by the results, since the values of pseudo-yield and pseudo-conversion, respectively, scatter significantly more than the pseudo-selectivity.

Due to the huge deviations in the pseudo-yield for the samples from Procatalyse alumina, calcined at 850 and 950°C (figures 5-8a and 5-8b) and the discontinuity in the pseudo-selectivity (figure 5-8c), it was decided to ignore these two samples in the discussion of results.

5.3.2 ISOPROPANOL CONVERSION OVER DIFFERENT ALUMINA SAMPLES

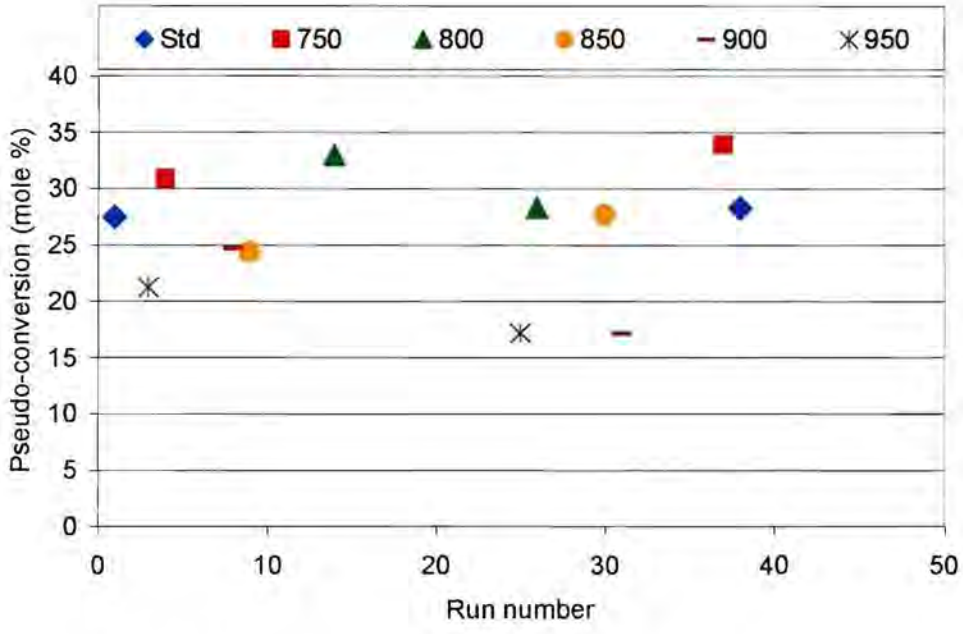

Figure 5-8a Pseudo-conversion of isopropanol over Condea alumina calcined at various temperatures in chronological order [Std refers to the sample as received and the numerical value refers to the calcination temperature]

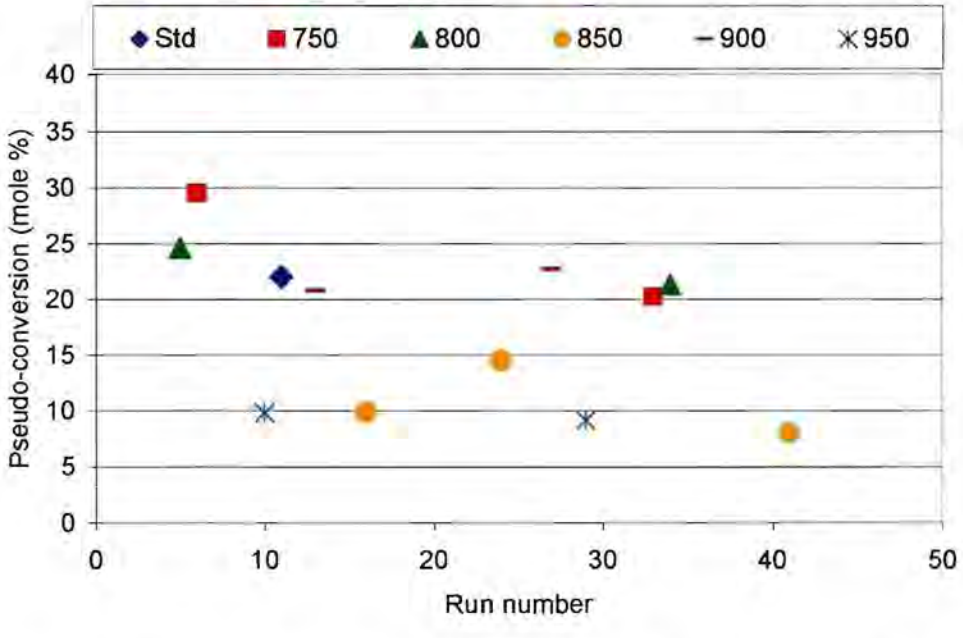

Figure 5-8b Pseudo-conversion of isopropanol over Procatalyse alumina calcined at various temperatures in chronological order [Std refers to the sample as received and the numerical value refers to the calcination temperature]

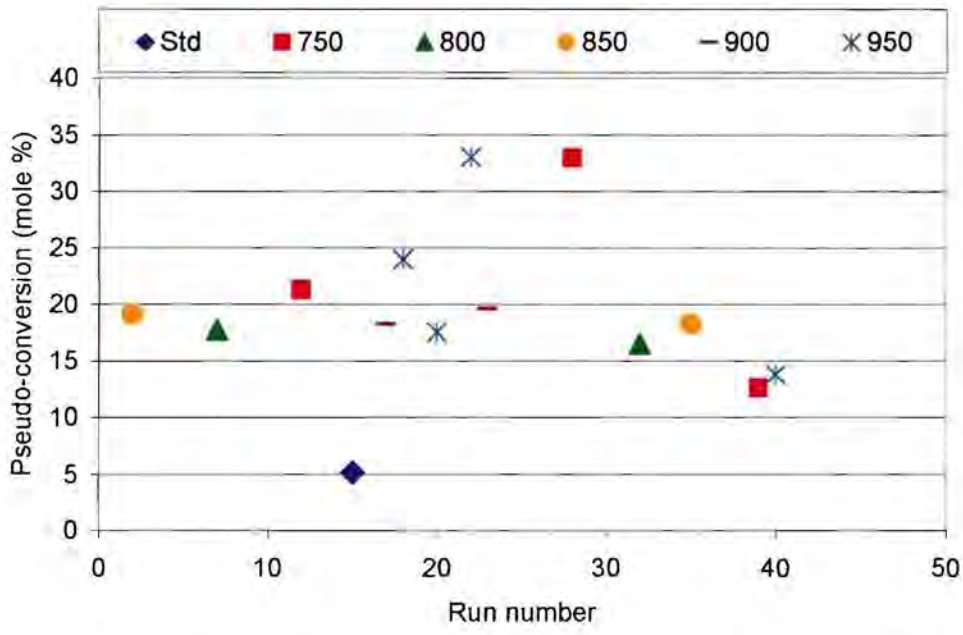

Figure 5-8c Pseudo-conversion of isopropanol over La Roche sample calcined at various temperatures in chronological order [Std refers to the sample as received and the numerical value refers to the calcination temperature]

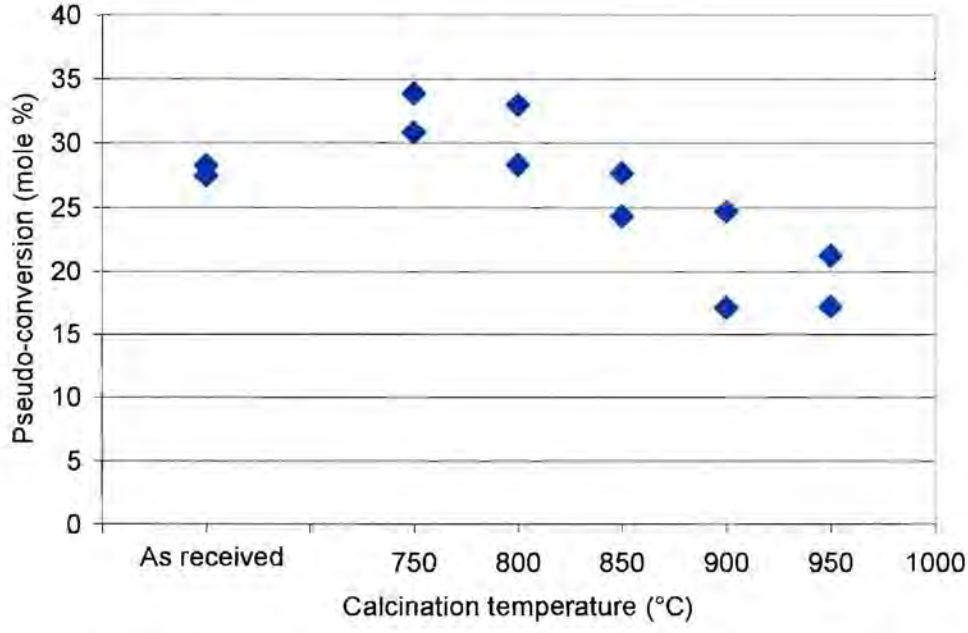

Figure 5-9a Pseudo-conversion of isopropanol over Condea alumina calcined at various temperatures

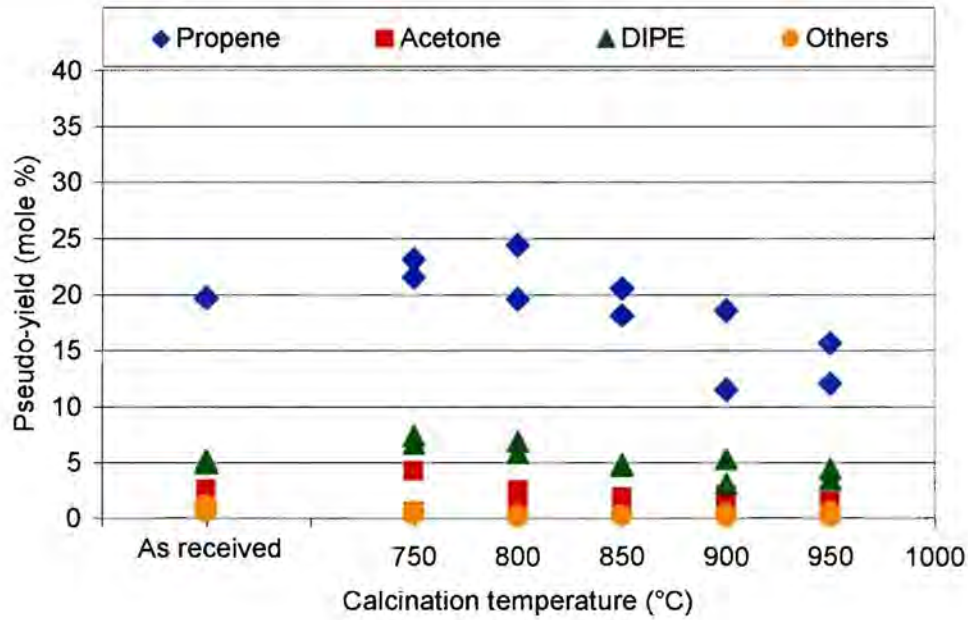

Figure 5-9b Pseudo-yield over Condea alumina calcined at various temperatures

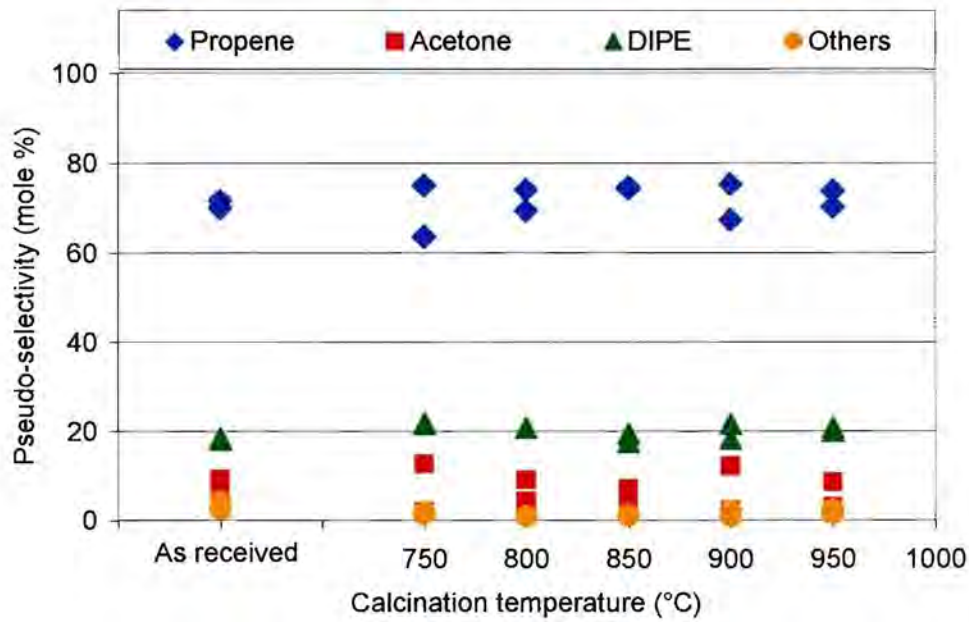

Figure 5-9c Pseudo-selectivity over Condea alumina calcined at various temperatures

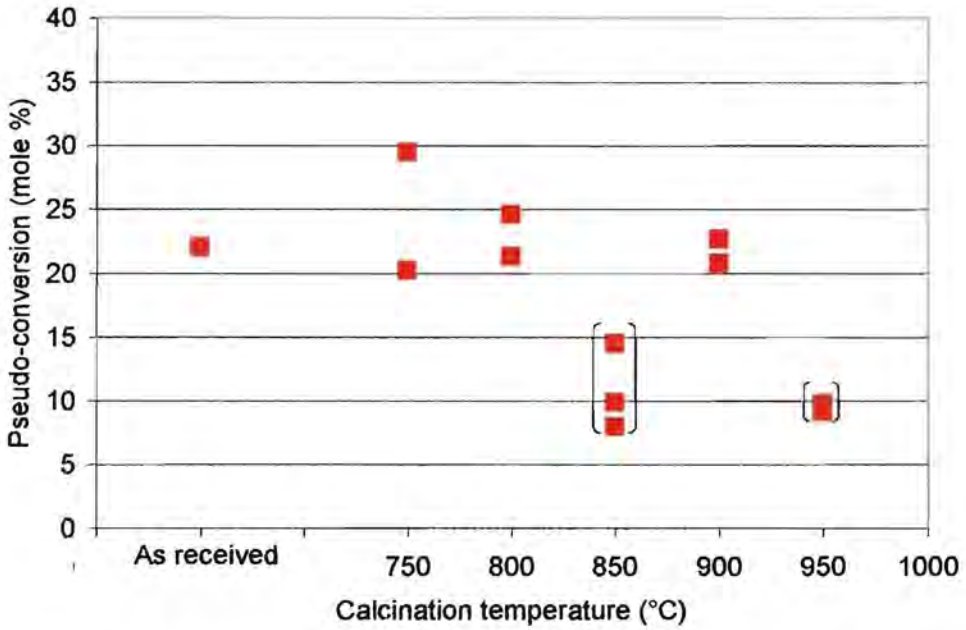

Figure 5-10a Pseudo-conversion over Procatalyse alumina calcined at various temperatures

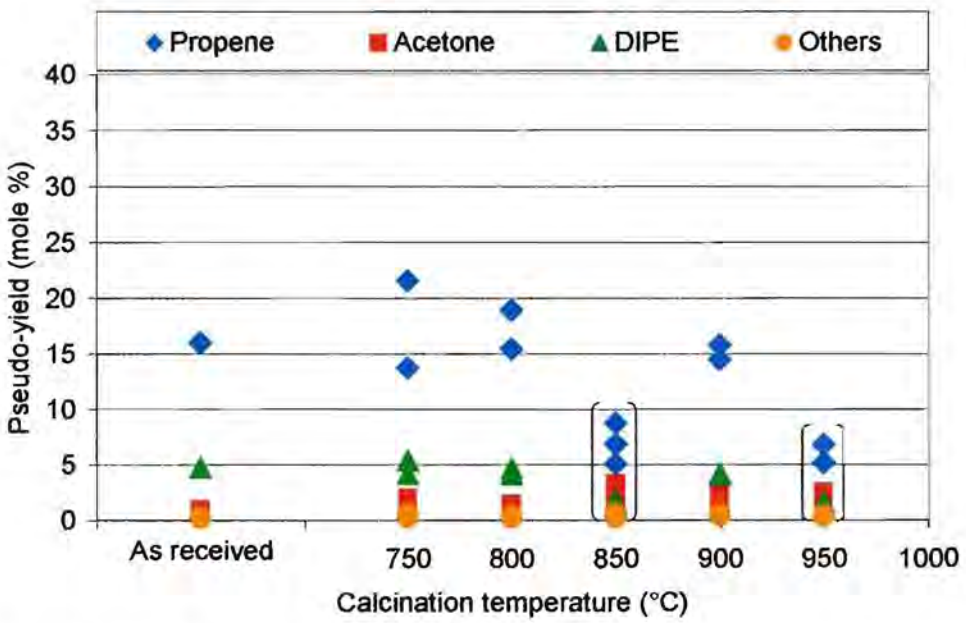

Figure 5-10b Pseudo-yield over Procatalyse alumina calcined at various temperatures

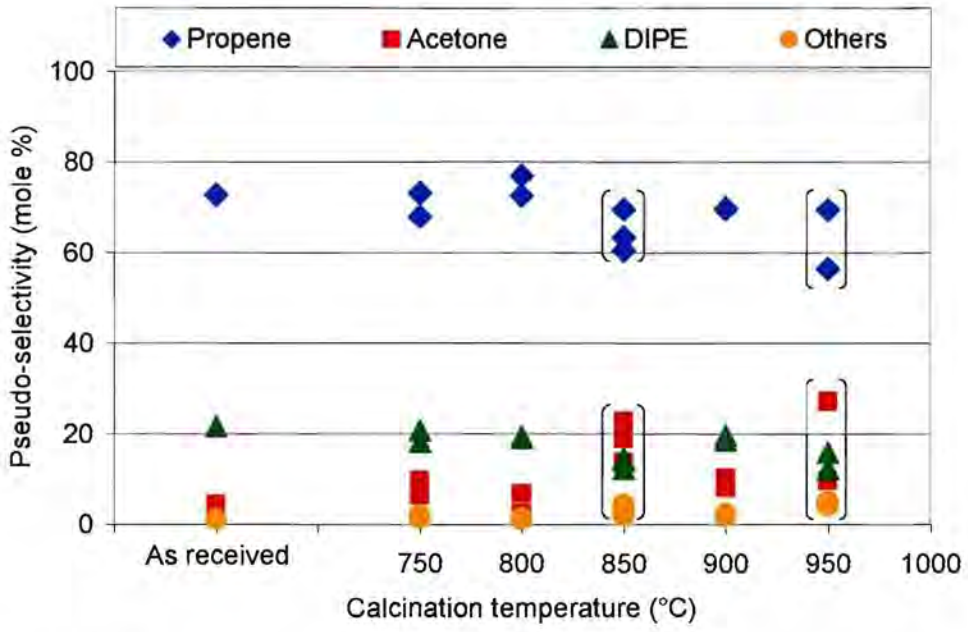

Figure 5-10c Pseudo-selectivity over Procatalyse alumina calcined at various temperatures

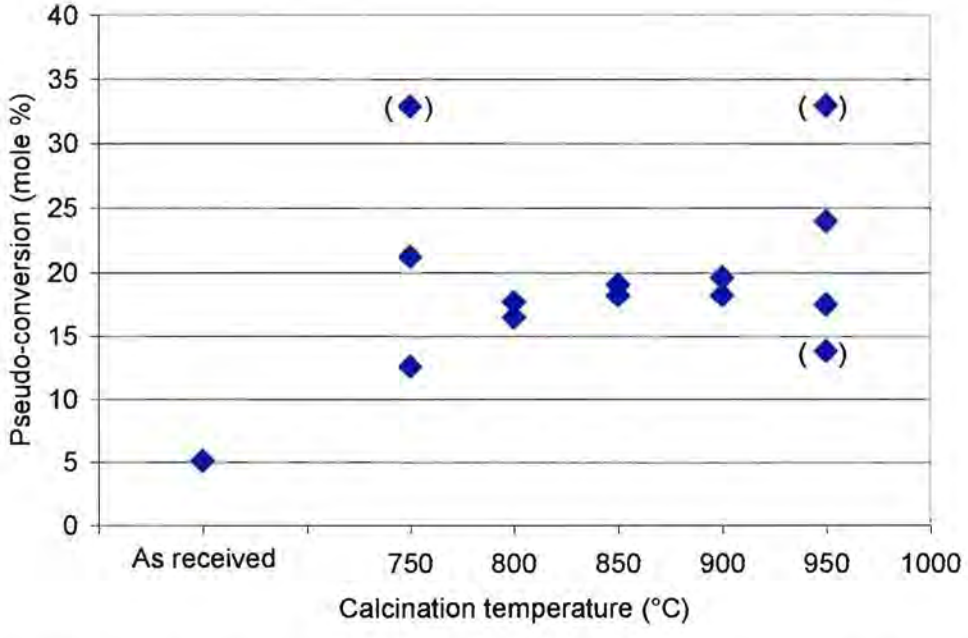

Figure 5-11a Pseudo-conversion over La Roche sample calcined at different temperatures

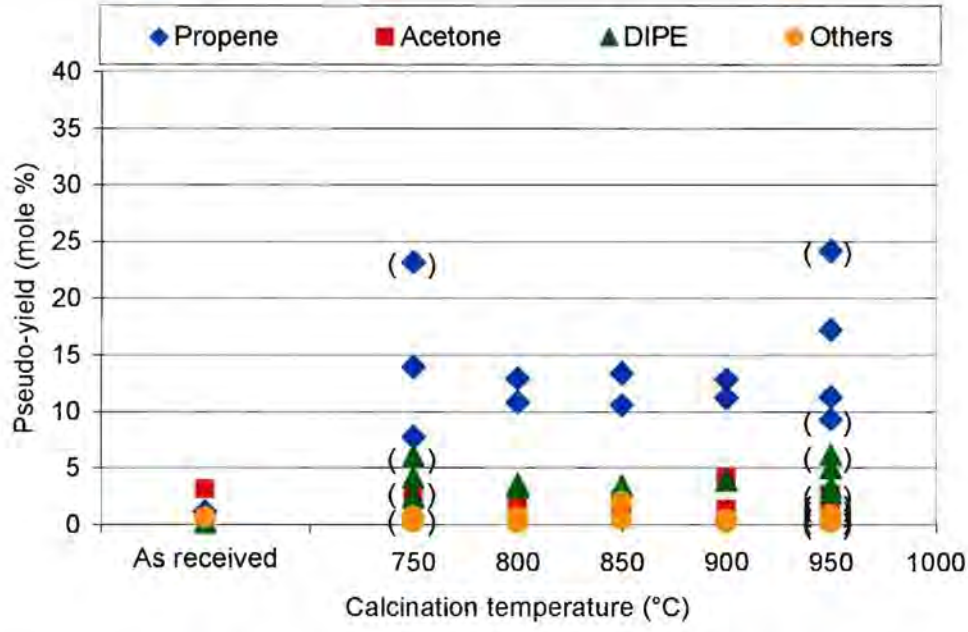

Figure 5-11b Pseudo-yield over La Roche sample calcined at various temperatures

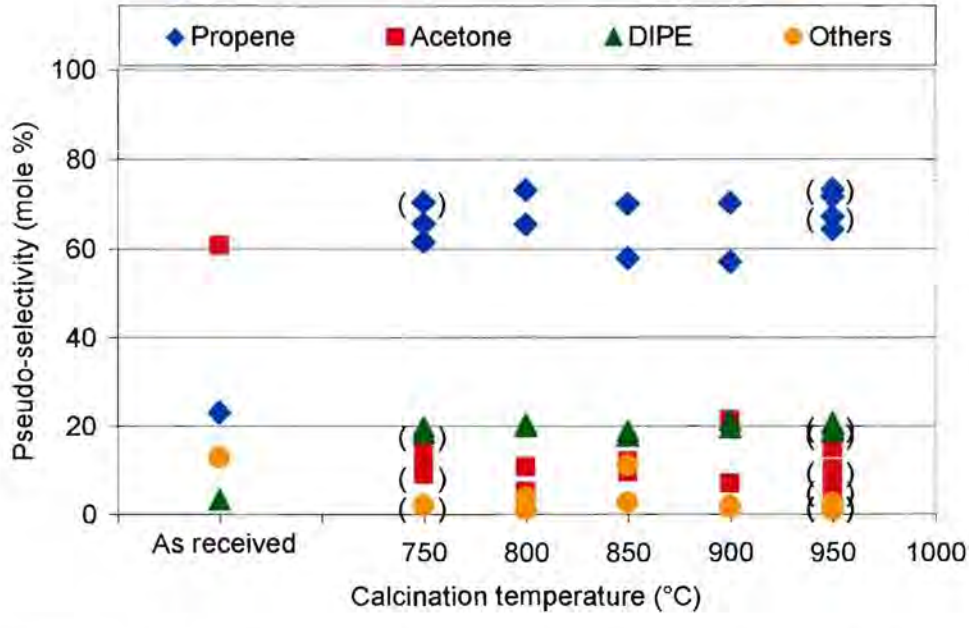

Figure 5-11c Pseudo-selectivity over La Roche sample calcined at various temperatures

Inspection of figures 5-9a, 5-10a and 5-11a reveals that the 'as received' samples of Condea and Procatalyse alumina do not display behaviour much different to the calcined samples. However, in the case of La Roche, the 'as

received' sample (identified as boehmite) exhibited a much lower activity than did the calcined materials.

For samples calcined at 750°C the activity declines as Condea > La Roche > Procatalyse. Activity declined with increasing calcination temperature for the Condea and Procatalyse samples, whereas the opposite is true, with activity rising slightly with increasing calcination temperature for the La Roche samples.

All the samples displayed a similar activity of approximately 20% conversion at the highest calcination temperature used (950°C).

When considering the percentage of different compounds found (figures 5-9b, 5-10b and 5-11b) it can be seen that propene predominated, followed by DIPE, acetone and 'others'. The trends for the percentage of propene and DIPE formed as a function of increasing calcination temperature, follow those observed for activity, i.e. significantly decreasing for Condea samples, moderately decreasing for Procatalyse samples and slightly increasing for La Roche samples.

The data for acetone were much affected by scatter, but apparently no trends of similar significance to those observed for propene and DIPE were present. No significant trend could be observed for the remaining (other) products.

When considering selectivity as a function of calcination temperature, no clear trend is to be found. In particular, acetone levels were found to be the most irregular.

As seen in figures 5-8a to c, the experiments were conducted in a totally random sequence and any trends observed are not due to artificial effects.

5.3.3 ACETONE LEVELS

5.3.3.1 ACETONE LEVELS AS A FUNCTION OF SODIUM CONTENT OF ALUMINA

Assuming that acetone was formed over basic sites, acetone production may be linked to the amount of sodium present in the aluminas. The relationship between the Na_2O content (see table 5-2) and the amount of acetone formed is shown in figure 5-12 on a dry sample weight basis. No trend is observed.

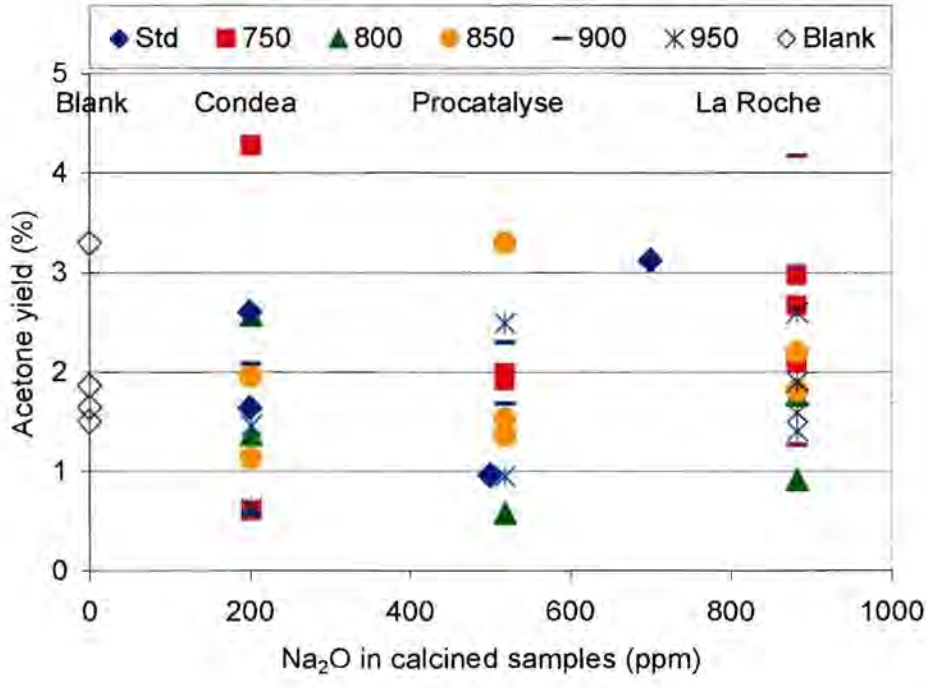

Figure 5-12 Acetone yield as a function of Na_2O content for all experiments

There is also no trend present that can be ascribed to a temperature effect. The acetone 'produced' simply reflects experimental scatter.

5.3.3.2 INFLUENCE OF CHRONOLOGY ON PERCENTAGE OF ACETONE FOUND

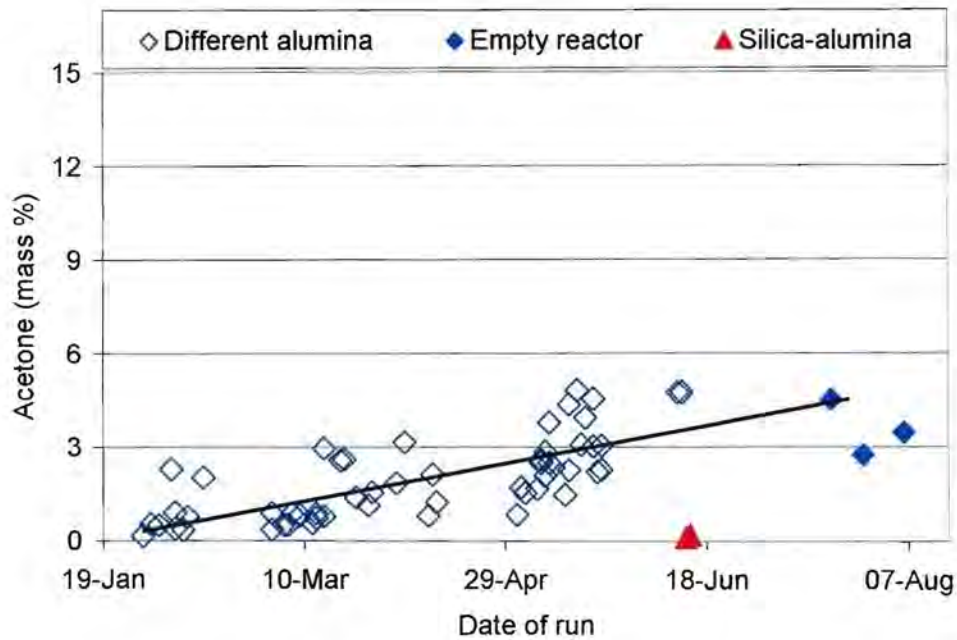

Figure 5-13a Increase in acetone level with passage of time for sampling via ampoules

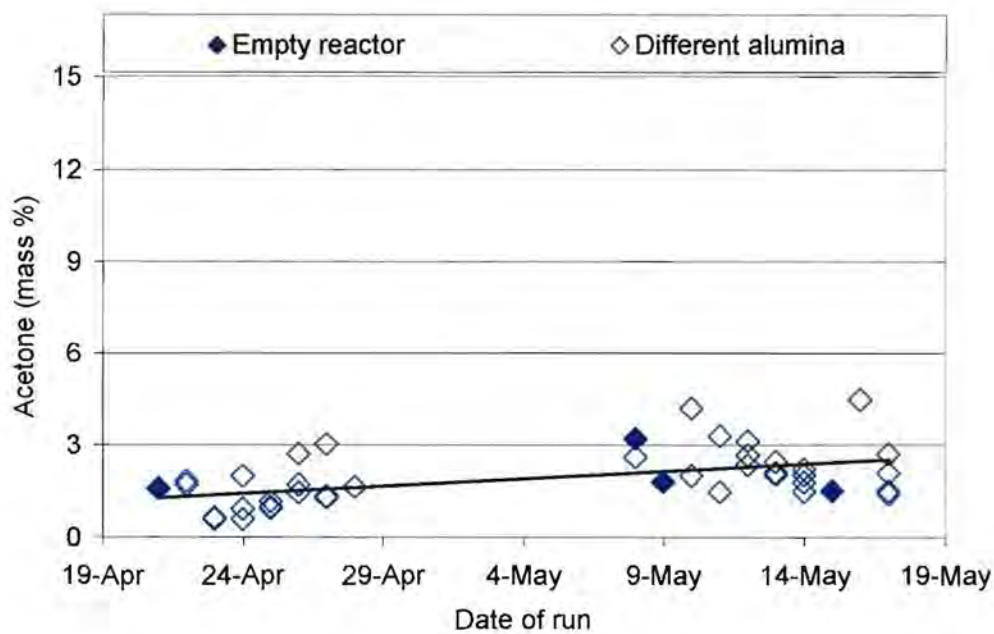

Figure 5-13b Increase in acetone level with passage of time for sampling via syringe

Viewing the experiments conducted in a chronological order, indicates an increasing acetone level with passage of time, emphasized by the trendline fitted. The large degree of scatter is again very prominent. Results from the blank runs clearly lie in the same range.

CHAPTER 6: DISCUSSION

A discussion of the results from the physico-chemical characterisation of the alumina samples is presented first, followed by a discussion of the results of the test reaction.

6.1 PHYSICO-CHEMICAL CHARACTERISATION OF THE ALUMINAS

6.1.1 XRD

XRD identified 'as received' La Roche 'alumina' in fact to be boehmite, crystalline AlOOH (figure 5-7c, section 5.2.5). Brinker and Scherer (1990) report that boehmite starts transforming into γ-alumina at 300°C. The XRD pattern of the La Roche sample calcined at 750°C, indeed indicated mainly γ-alumina (Al_2O_3) with some remnants of the boehmite structure still observable (figure 5-7c). XRD identified 'as received' Condea and Procatalyse samples to be γ-alumina with traces of boehmite structure still evident (figure 5-7b and c, section 5.2.5).

Phase transformation diagrams (section 2.1.4) indicate that γ-alumina starts transforming into δ-alumina at 850°C. It is therefore expected that the samples subjected to a calcination temperature of 850°C and/or higher would have δ-alumina present as a major phase. XRD results indeed show that a group of peaks appear in the XRD pattern of all samples calcined at higher than 850°C, which can be ascribed to δ-alumina (figure 5-6a to c, section 5.2.5).

6.1.2 WEIGHT LOSS THROUGH CALCINATION AND TGA

The following discussion refers to results obtained from bulk calcination (sections 4.1.1 and 5.1.1) at different temperatures as well as from Thermogravimetric Analysis (TGA) (sections 4.1.2 and 5.1.2).

Condea and Procatalyse alumina samples displayed an average weight loss of 0.8 and 3.7%, respectively, over the range of calcination temperatures used, whereas TGA results indicated a total loss of 6.4 and 7.6%, respectively (table 5-1). The weight losses during TGA occurred at approximately 100°C and above 150°C no significant additional losses were observed (figure 5-2a and b). It is therefore assumed that the losses are due to the removal of physically adsorbed water. The differences between the TGA and the calcination results are therefore explained as due to the samples being stored in a desiccator before calcination, while those for TGA were exposed to ambient air prior to analysis.

A higher weight loss was observed for the boehmite sample from La Roche. Stoichiometric calculations predict that a transformation of boehmite (AlOOH), into γ-alumina (Al_2O_3), would correspond to a loss of 15% in weight through the release of crystal water. In fact a loss of 20-30% was observed (table 5-1). The additional weight loss may be due to the loss of physically adsorbed water. Samples taken from the desiccator directly and calcined at the various temperatures showed an additional weight loss of 5% only, whereas after being stored in contact with ambient air prior to TGA analysis, the additional weight loss was 15%.

Weight loss as a function of temperature for the boehmite sample clearly shows two regions (figure 5-2c). The first part of the weight loss occurred at approximately 100°C and is ascribed to physically adsorbed water. The second step, in the region 250-450°C, with the highest loss rate at about 350°C, is ascribed to the loss of the crystal water, i.e. the transformation from boehmite to alumina:

$$2AlOOH \rightarrow Al_2O_3 + H_2O \quad (-15\% \text{ by weight})$$

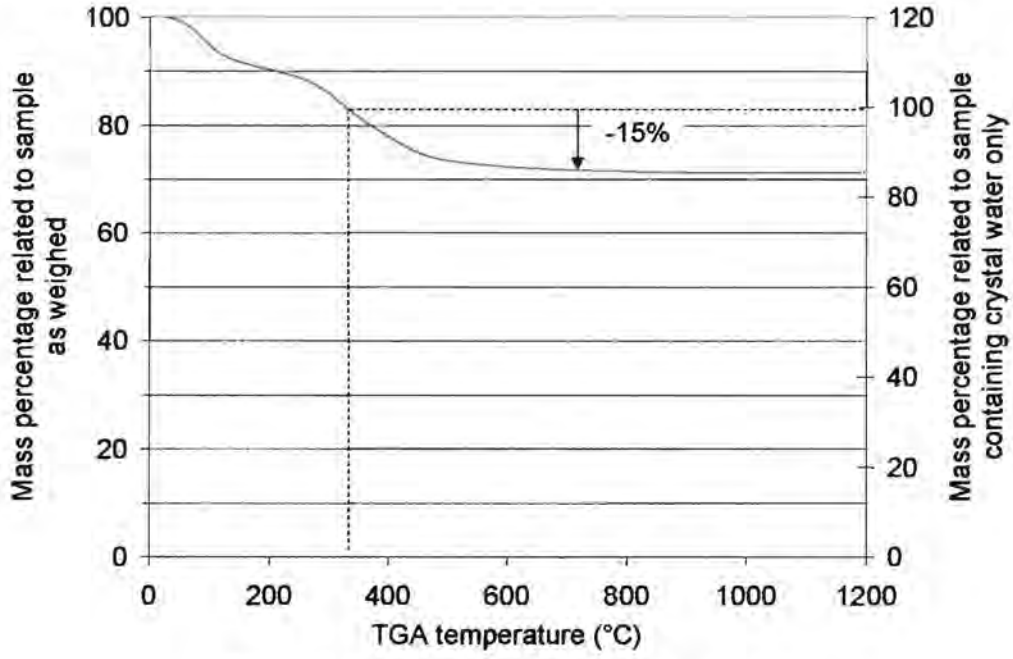

Figure 6-1 TGA results for La Roche sample

Indeed, based on the constant final weight of the sample achieved at high calcination temperature (figure 6-1), the second step matches the stoichiometric weight loss from boehmite to alumina corresponding to the above equation.

Consistent with the findings of Brinker and Scherer (1990) on boehmite, no significant additional weight loss was observed above 750°C (section 2.1.3). Correspondingly, the γ-alumina samples from Condea and Procatalyse did not show any influence of calcination temperature on weight loss in the range 750-950°C (figures 5-1 and 5-2a and b).

6.1.3 SURFACE AREA, PORE DIAMETER DISTRIBUTION AND PORE VOLUME

Except for the La Roche sample where calcination as such has a significant effect ($AlOOH \rightarrow Al_2O_3$), different calcination temperatures have no effect on the BET surface area and pore volume (figures 5-3, 5-4 and appendix A-8). Sintering, which is the change from small macroscopic structure elements to larger macroscopic structure elements, does not seem to occur up to 950°C. Sintering effects can thus not be responsible for the decline in catalytic activity

observed with increasing calcination temperature (section 5.3.2).

Analysis of the pore diameter distribution was only performed on La Roche and Condea samples that had been subjected to calcination. The adsorption/desorption curves (appendix A-9, figures A-9a and b) initially exhibited a moderate, almost linear increase in the volume adsorbed up to p/p_0 of approximately 0.5 and approximately 0.6 for the La Roche and Condea samples, respectively. Between p/p_0 of 0.6 and 0.9 and up to the final volume adsorbed, the adsorption isotherm for the La Roche sample shows a steep increase, suggesting a rather broad pore size distribution in the upper range. For the Condea sample a much steeper increase in adsorbed volume was observed within a range of only 0.1 p/p_0 units around 0.8 p/p_0. This suggests a rather narrow pore size distribution, in the upper range.

The maximum of the pore size distribution for the Condea sample is at a diameter of 9 nm, while for the La Roche sample it is at approximately 7 nm.

A small amount of hysteresis was found to be present in the adsorption-desorption isotherms. This effect is related to characteristics of the pores present and the particular shape of the isotherms indicates the presence of ink-bottle-shaped capillaries (Thomas and Thomas, 1997). However, the amount of hysteresis present, being small, is indicative of quite uniformly shaped and sized pores, particularly in the Condea sample.

This fact is substantiated by the figures for pore diameter distribution (appendix A-9), which show that the pore diameters of the Condea sample lie over a very small range (table 6-1). The mean pore diameter for the alumina derived from the La Roche boehmite sample is significantly smaller but the distribution is spread over a much wider range.

Table 6-1 Relative half height pore diameter distribution range (see appendix A-9 for full details)

Sample	Mean diameter	Relative half height diameter range
Condea	9.1	3.1
La Roche	6.7	12.3

The smaller pores for the La Roche sample result in a much higher BET surface area, which is 144 and 228 m^2/g for the Condea and La Roche samples, respectively.

The smallest existing pore diameter reported by the BET method is approximately 2 nm (figure A-11c and d). The critical diameter of isopropanol, which was used as the reactant in catalytic testing, is approximately 0.4 nm (Phala, 2002) and it is therefore assumed that the feed molecules for the catalytic testing had access to the entire surface reported by this method.

6.1.4 TEMPERATURE PROGRAMMED DESORPTION OF AMMONIA

Quantitative results for NH_3-TPD proved to be somewhat erratic. Therefore only significant qualitative trends will be discussed.

For all three aluminas, the major ammonia desorption peak is observed with a maximum at approximately 330°C (table 5-4). This peak is ascribed to NH_3 bound to strong acid sites. No trend can be identified in respect of calcination temperature. No significant difference is apparent for samples of different origin (the differences in average temperatures calculated for each series of calcined samples, Condea 325°C, Procatalyse 335°C and La Roche 340°C, are clearly within the range of experimental scatter).

Normalisation of the TPD curves to the maximum of the major peak, B, shows that the decline following the maximum of peak B becomes, systematically, less steep with increasing calcination temperature, as shown in figures 6-2a to c (regardless of the two arbitrary exceptions). Considering that the sample size was always the same (0.15 g), this indicates that the nature of the

acid sites changes with calcination temperature, i.e. changes occur that either destroy part of the weaker acid sites, desorbing around 330°C, or give rise to stronger acid sites. The former results in a flatter shape of the desorption peak, the latter results in a relatively slower release of adsorbed ammonia giving rise to a less steep slope. Since the quantitative results from peak integration were quite erratic, it is not possible to distinguish these two causes. However, since isopropanol conversion activity declines with increasing calcination temperature, the former may be the case. It must be kept in mind that the sample size, which also effects the peak shape, was the same for all TPD experiments.

The very strong sites may not readily be ascribed to Lewis sites since the calcined samples were exposed to ambient air, i.e. moisture, during loading to the TPD instrument.

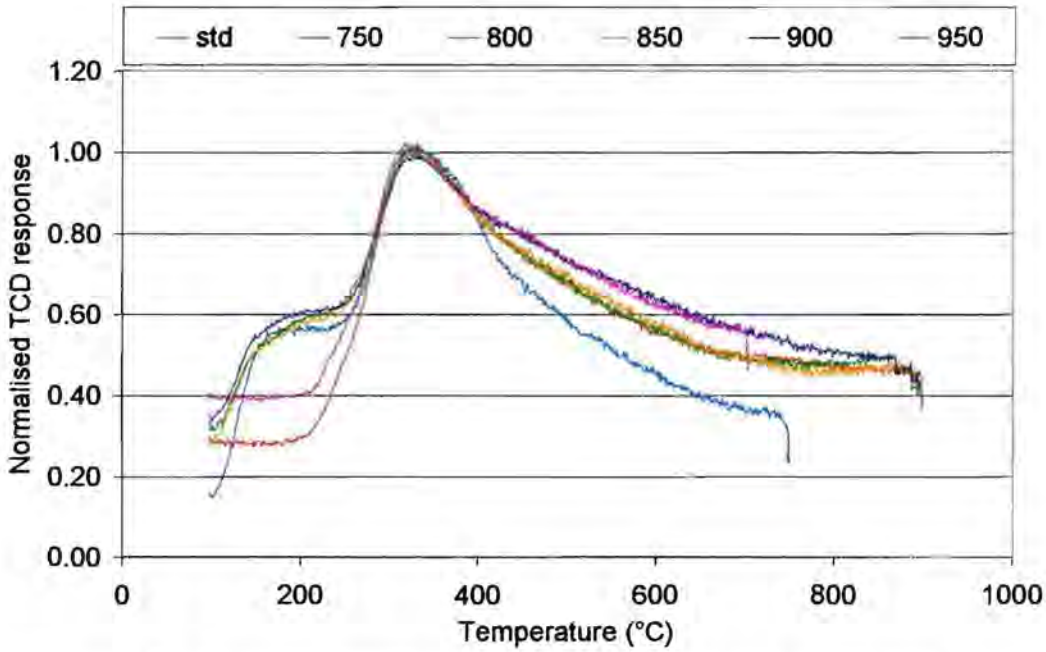

Figure 6-2a Normalised TPD results for Condea samples calcined at different temperatures

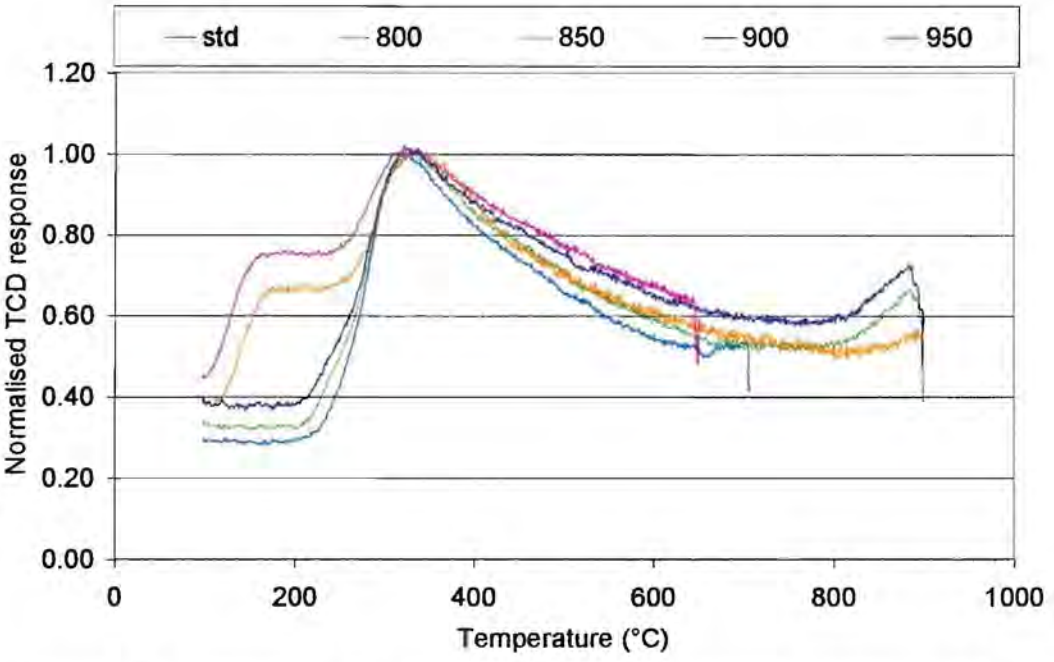

Figure 6-2b Normalised TPD results for Procatalyse samples calcined at different temperatures

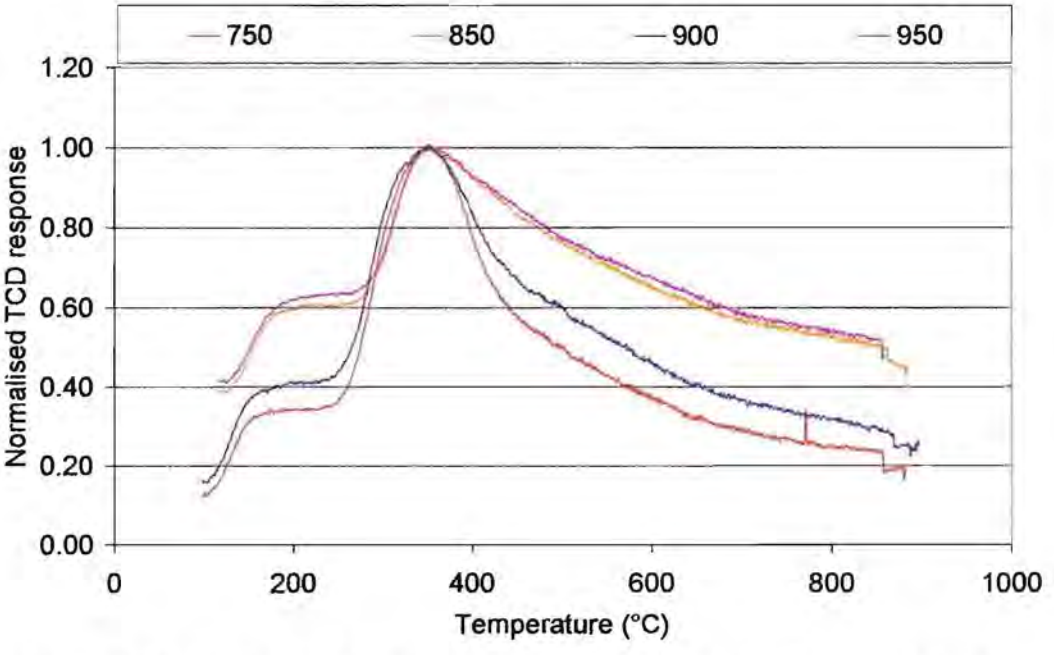

Figure 6-2c Normalised TPD results for La Roche samples calcined at different temperatures

One would expect a large volume of water being released or exchanged for ammonia as the temperature is increased during the TPD-analysis of the 'as

received' La Roche sample (identified as boehmite AlOOH). The release of crystal water from the boehmite, however, was found to start at 250°C and to peak at approximately 350°C (see section 5.1.2 and figure 6-1) which corresponds almost exactly to the major peak for NH_3 desorption. (Note that physically adsorbed water would have been driven off through heating at 200°C prior to NH_3 adsorption.)

6.1.5 ZETA POTENTIAL

The zeta potential measures the charge of the surface of the alumina particles in an aqueous environment, indicated by the pH of the isoelectric point. Results are shown in figures 5-6a to c. The large difference in the behaviour of the 'as received' La Roche sample (pH = 10) compared with the other two (pH around 7.7), is due to the former being boehmite (AlOOH) in contrast to the latter samples, which are alumina (Al_2O_3).

Calcination of the boehmite at 750°C, resulted in a shift of the iso-electric point to pH of about 9 (figure 5-6d). This would indicate that a decrease of surface hydroxyl groups occurred as a result of the calcination procedure, which would be expected since significant restructuring, loss of BET surface and partial dehydration occur during calcination.

6.2 FINDINGS IN RESPECT OF ACETONE FORMATION

Isopropanol conversion as a probe reaction for acid and basic sites was the major objective of this study. Literature states that basic and acid sites on solid materials, catalysts and catalyst supports, can be identified via the decomposition of isopropanol to acetone on basic sites, and/or propene and diisopropyl ether (DIPE) on acid sites, respectively (section 2.2). Literature also states that acetone yields and selectivities over alumina in most cases studied were quite low or that no acetone formed at all.

Acetone was present in all product mixtures obtained from experiments. Results presented in chapter 5 (section 5.3.1.1) however indicate clearly that

there is already a significant amount of acetone present in the feed, for both series of experiments A and C (argon carrier gas/ampoule sampling and hydrogen carrier gas/syringe sampling - see data points from blank runs in figures 5-13a and b).

When the content of acetone in the total reactor effluent is regarded as a function of the calcination temperature of the different alumina samples, no significant trend can be observed (note that the order of the experiments was random, see section 5.3.3). Moreover, it was observed that no significant differences appear between the three varieties of alumina studied. Furthermore, no significant difference appears between the acetone content in product samples and the acetone content in samples from blank runs, i.e. feed samples.

The presence, in the feed, of relevant percentages of acetone as well as the seemingly pronounced scatter in respect of acetone contents in the product stream of all experiments, obscures the detection of any small differences or trends which may possibly be present.

When considering the results from conversion experiments in chronological order (figures 5-13a and b), it appears that the level of acetone found is not different from blank runs (except over amorphous silica-alumina where all feed acetone is converted). It also appears that the level of acetone is constantly increasing with the passage of time during the period over which the set of experiments were conducted. Apparently, the acetone content is influenced by exposure of the feed to external influences e.g. light.

It would therefore be misleading to consider the acetone to be a product of isopropanol conversion.

The only clear result with respect to the acetone is observed over amorphous silica-alumina, when all feed acetone is consumed (propably through acid catalysed aldol addition).

Therefore, all further discussion on isopropanol conversion over the aluminas of this study is based on results where acetone is disregarded as a product of the reaction (i.e. acetone is considered to be an inert).

6.3 ISOPROPANOL CONVERSION

In view of the discussions above (sections 5.3 and 6.2) the following presentation of isopropanol conversion results is presented treating acetone as an inert component. Consequently, data are presented in terms of conversion, selectivity and yield as per discussion of section 4.3.5.2.

6.3.1 THERMODYNAMICS

Comparison of thermodynamic calculations with the product indicates that hydrogen is inert with regard to acetone conversion (more detail in appendix A-13). Equilibrium distributions calculated for inert carrier gas show that acetone formation, in addition to propene formation, is not thermodynamically limited.

DIPE is not thermodynamically stable, although kinetically DIPE formation is possible. Its formation is of a temporary nature only and will revert back to isopropanol and eventually convert to propene at high conversion.

6.3.2 TIME-ON-STREAM BEHAVIOUR FOR ISOPROPANOL CONVERSION

Results from section 5.3.1.2 are discussed here to elucidate the time-on-stream behaviour of isopropanol conversion over a Condea alumina sample calcined at 750°C. Note that acetone is no longer considered a product.

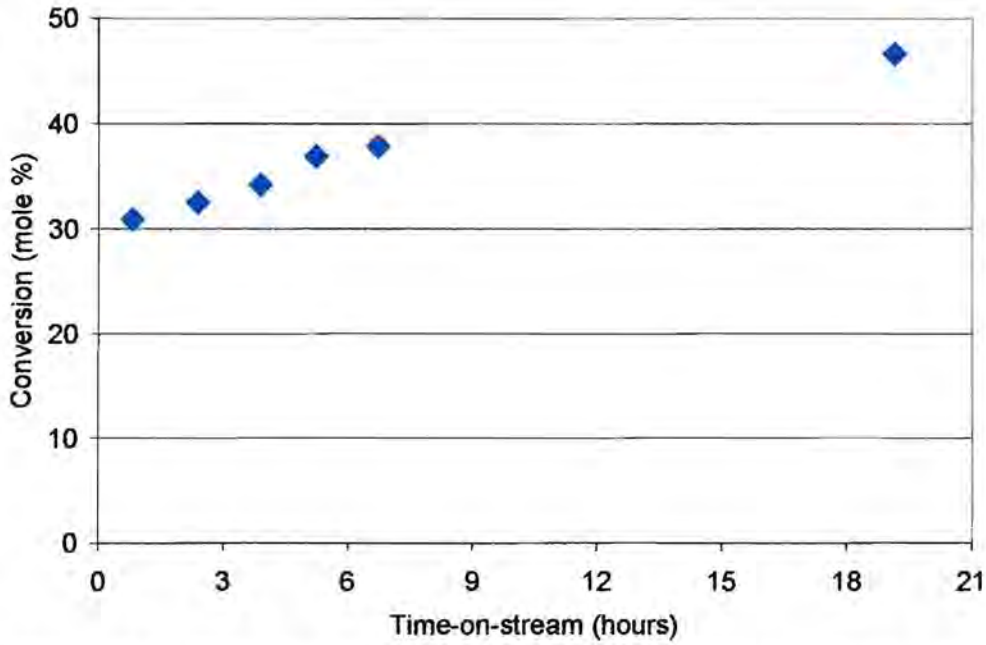

Figure 6-3a Conversion as a function of time-on-stream over Condea alumina calcined at 750°C

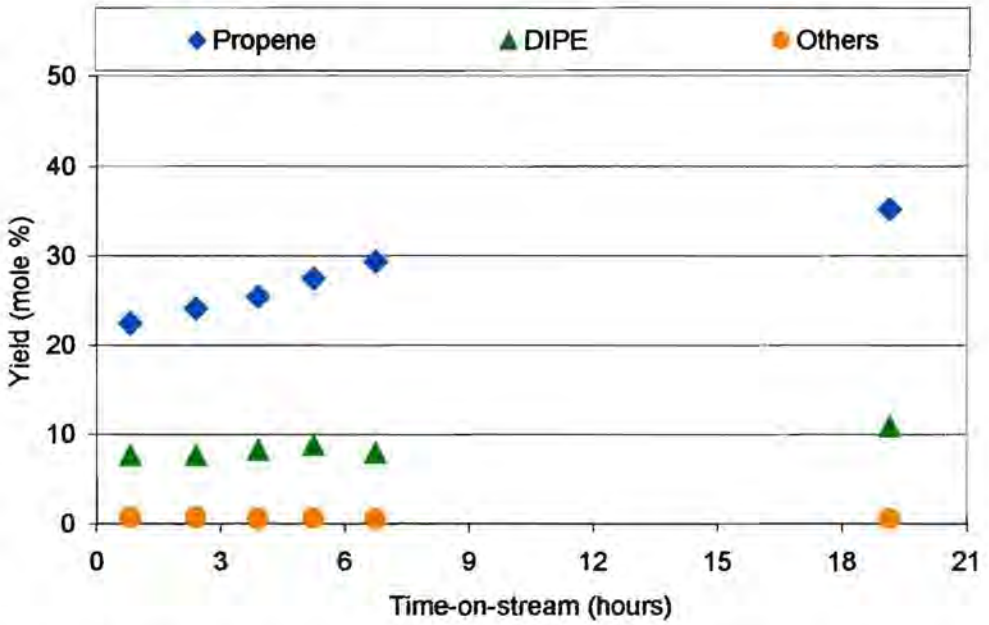

Figure 6-3b Yield as a function of time-on-stream over Condea alumina calcined at 750°C

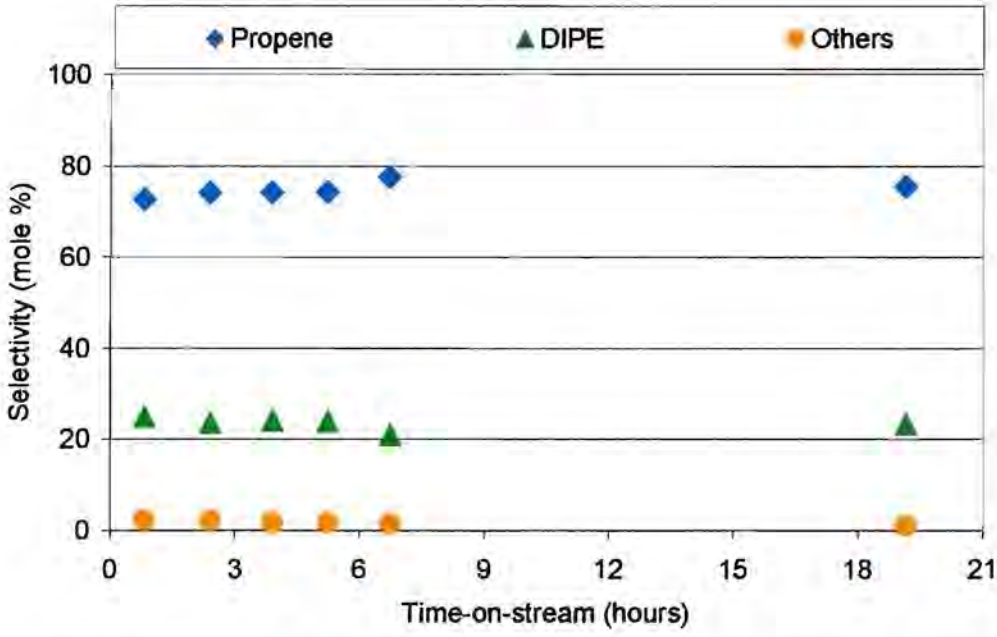

Figure 6-3c Selectivity as a function of time-on-stream over Condea alumina calcined at 750°C

Figures 6-3a and b clearly demonstrate that no deactivation occurred during the 19h run. In fact, a substantial increase in the activity can be observed. This change in activity may be caused by changes in the number and/or type of acid sites present, possibly as a result of the influence of water that is produced during the reaction.

Selectivity towards the different compounds remained constant (figure 6-3c), suggesting that the catalyst acid site strength distribution did not change with time-on-stream.

6.3.3 INFLUENCE OF CALCINATION TEMPERATURE

6.3.3.1 CONVERSION

The discussion below is based on the average values calculated from repeated experiments (excluding the values in brackets) from figures 5-9a, 5-10a and 5-11a in section 5.3.1.3. Also note that the acetone was excluded.

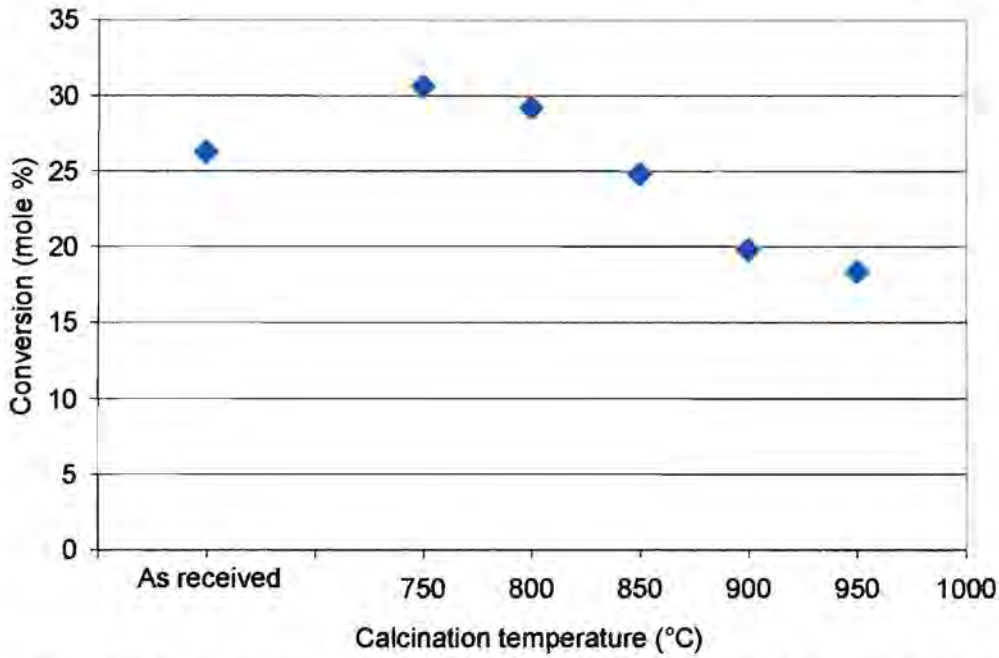

Figure 6-4a Isopropanol conversion over Condea alumina calcined at different temperatures

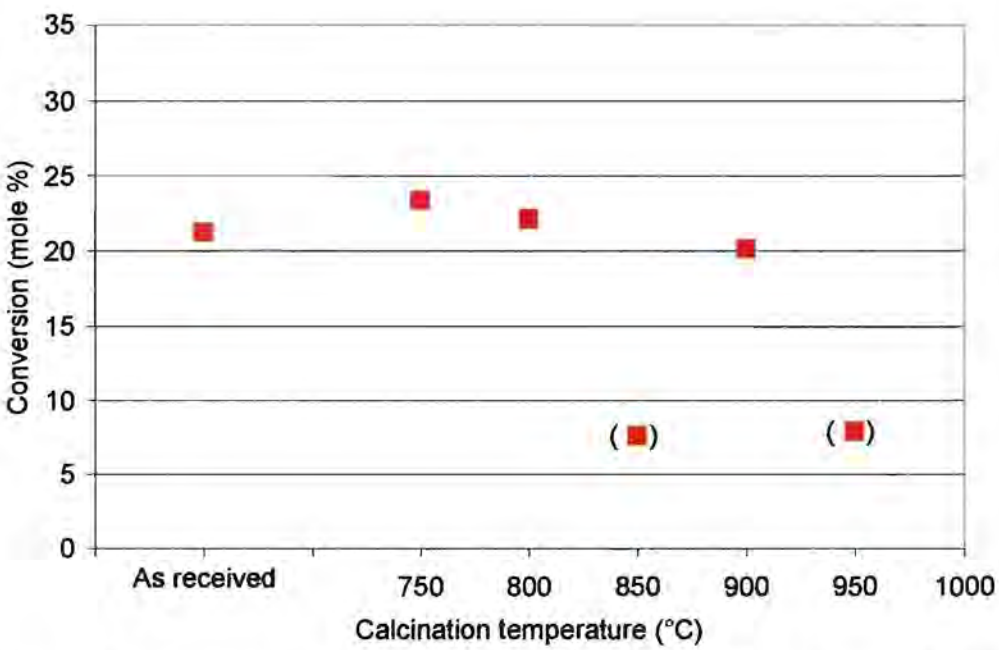

Figure 6-4b Isopropanol conversion over Procatalyse alumina calcined at different temperatures

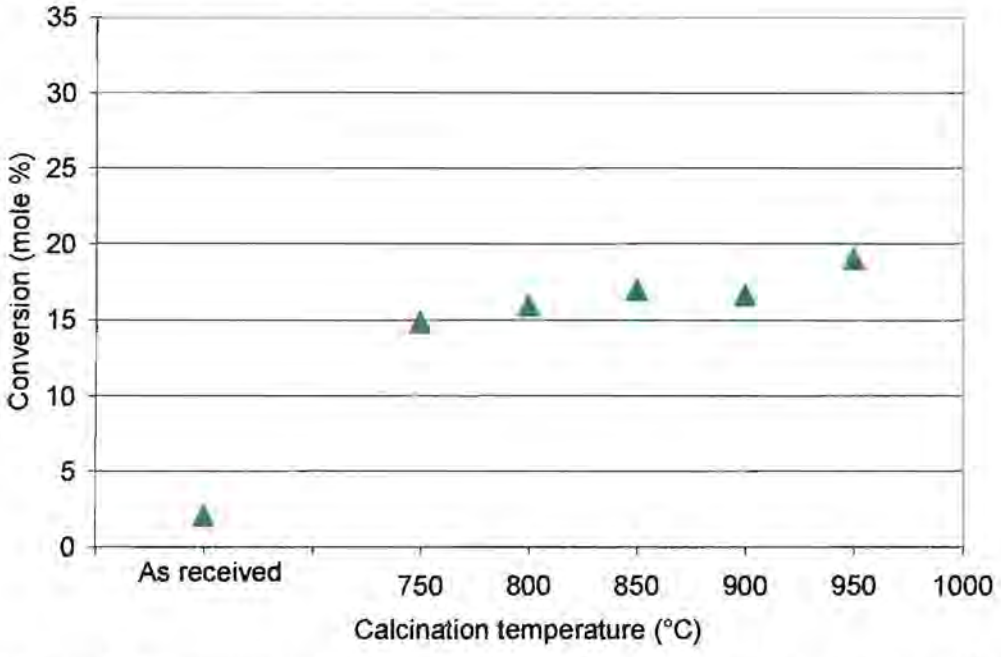

Figure 6-4c Isopropanol conversion over La Roche alumina calcined at different temperatures

From figures 6-4a to c, it is clear that the activity of all aluminas and the boehmite increases through calcination at 750°C. The activity of Condea alumina decreases significantly with a further increase in calcination temperature. Figure 6-4b in respect of Procatalyse alumina shows two apparently suspect data points for 850 and 950°C, such that the decrease in activity with increasing calcination temperature is only gradual; the identical low values and the general comparative trends presented in figure 6-8b, underlying the suspicions in respect of the 850 and 950°C data points. For the La Roche sample, the activity appears to increase continuously, although only slightly, with increasing calcination temperature.

The effect of calcination temperature, in particular with the more active alumina samples from Condea and Procatalyse, corresponds to literature, where maximum activity was reported for calcination temperatures around 600-700°C with a decline in activity arising from treatment at higher temperatures (section 2.2.2.3).

In figure 6-5, conversions over the three samples are compared. A

pronounced difference in activity is observed for the samples 'as received', as well as for the samples calcined at the lowermost temperature applied (750°C). But activities are quite similar, once samples had been calcined at very high temperatures (900°C and higher).

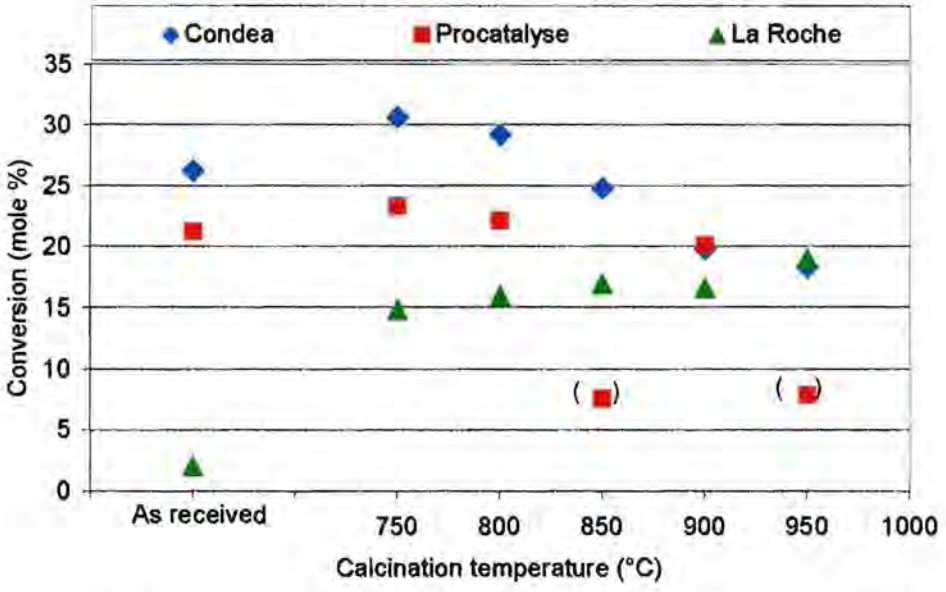

Figure 6-5 Comparison of conversions over Condea, Procatalyse and La Roche aluminas

Note that scatter (apart from the strikingly out-of-range points) is significantly reduced compared to corresponding figures including acetone.

6.3.3.2 ACTIVITY NORMALISED TO SURFACE AREA

The effect of surface area was eliminated as described in section 4.3.4.3 by relating the BET surface areas of all the different and differently pre-treated catalysts to a hypothetical average surface area.

Both the original and normalised conversions are shown in figures 6-6a to c. In figure 6-7 the normalised conversions are compared.

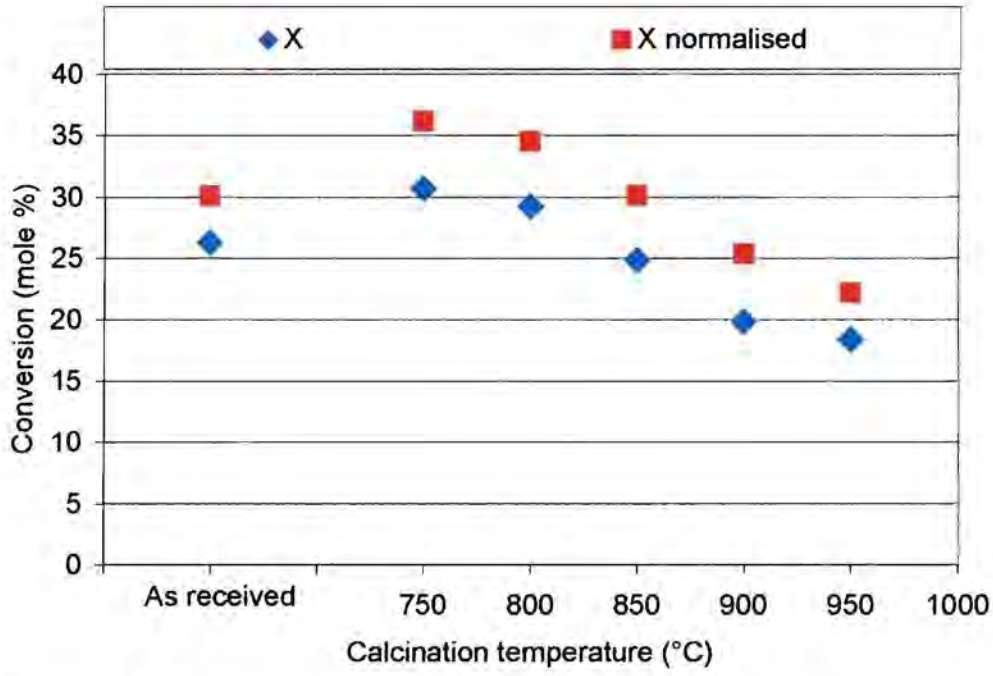

Figure 6-6a Isopropanol conversion and normalised conversion over Condea alumina calcined at different temperatures

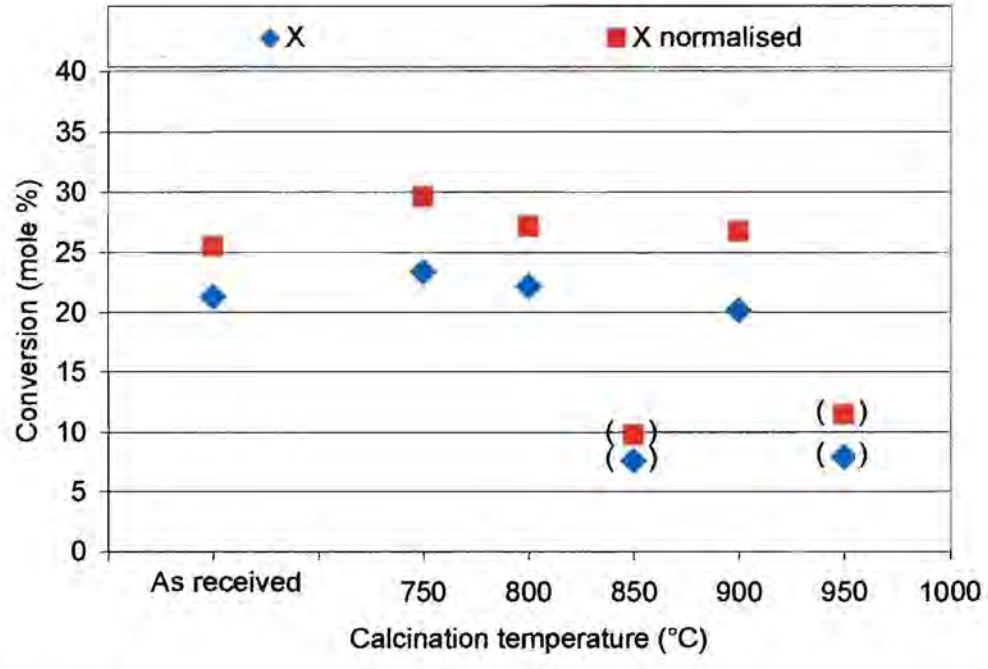

Figure 6-6b Isopropanol conversion and normalised conversion over Procatalyse alumina calcined at different temperatures

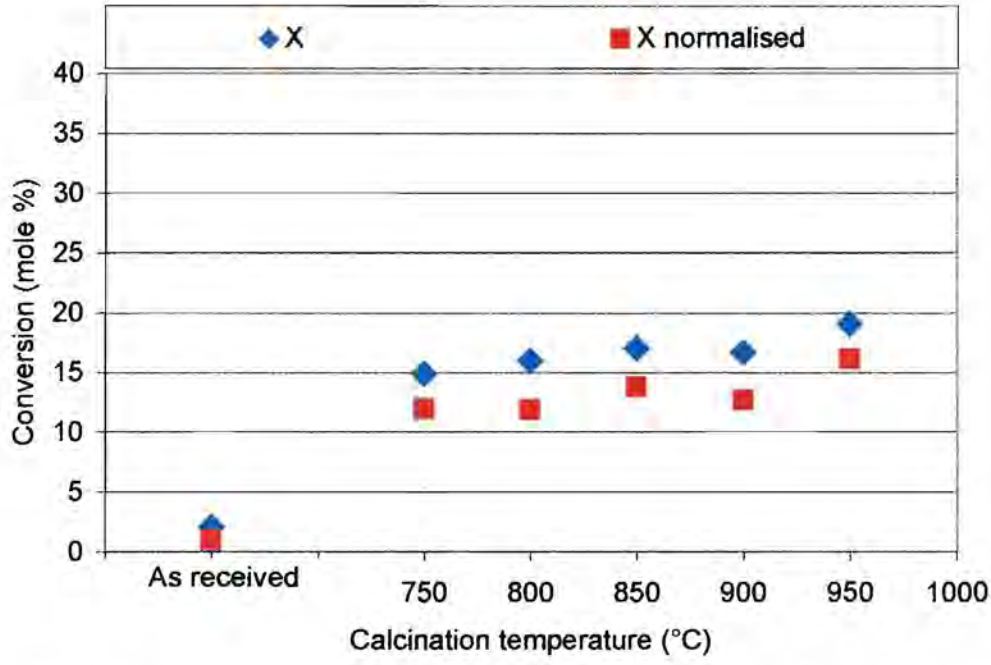

Figure 6-6c Isopropanol conversion and normalised conversion over La Roche alumina calcined at different temperatures

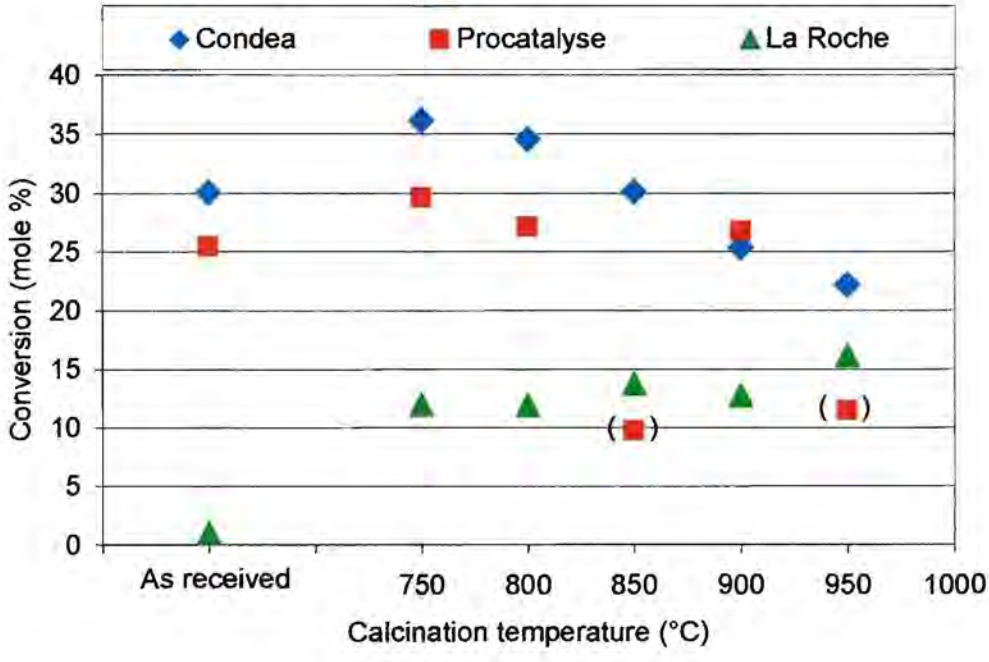

Figure 6-7 Comparison of normalised conversions over Condea, Procatalyse and La Roche aluminas

From figures 6-6a to c and 6-7 it is clear that the differences and the changes in activity with calcination temperature are not only due to differences in the surface area. Condea and Procatalyse aluminas still showed a similar relative difference in conversion with the samples calcined at low temperature, while the La Roche sample shows an even lower relative activity when the conversion levels were normalised with respect to BET surface. The trends with calcination temperature remained similar for all three, since the BET surface was found to remain essentially unchanged with increasing calcination temperature (section 6.1.3).

6.3.3.3 YIELDS

The yields of different products obtained for the three aluminas studied as a function of calcination temperature are presented in figures 6-8a to c. Since DIPE is a condensation product from two isopropanol molecules, yields are expressed based on mole % isopropanol.

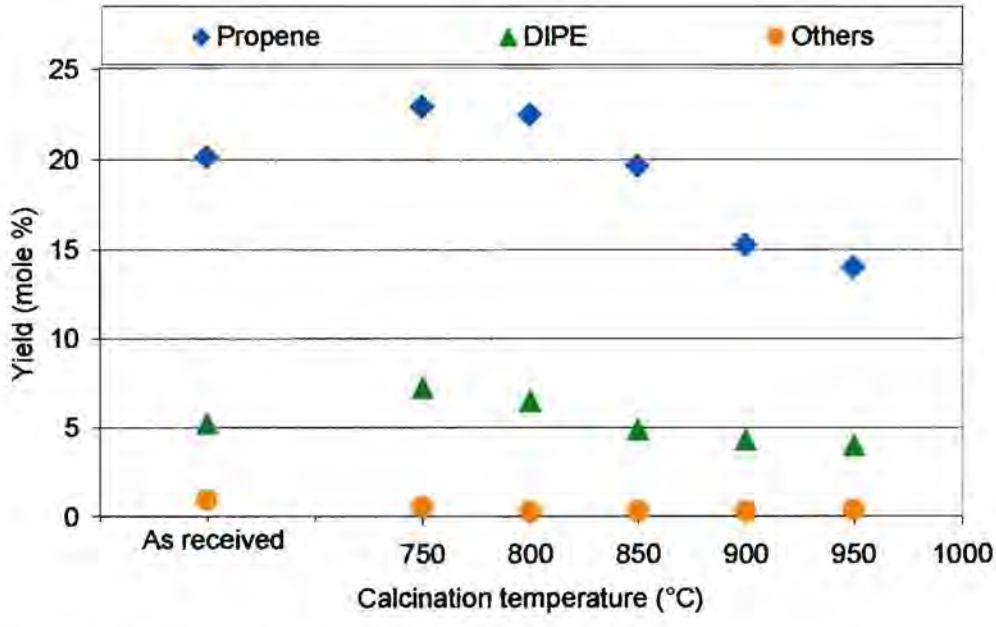

Figure 6-8a Yield of products from isopropanol conversion over Condea alumina calcined at different temperatures

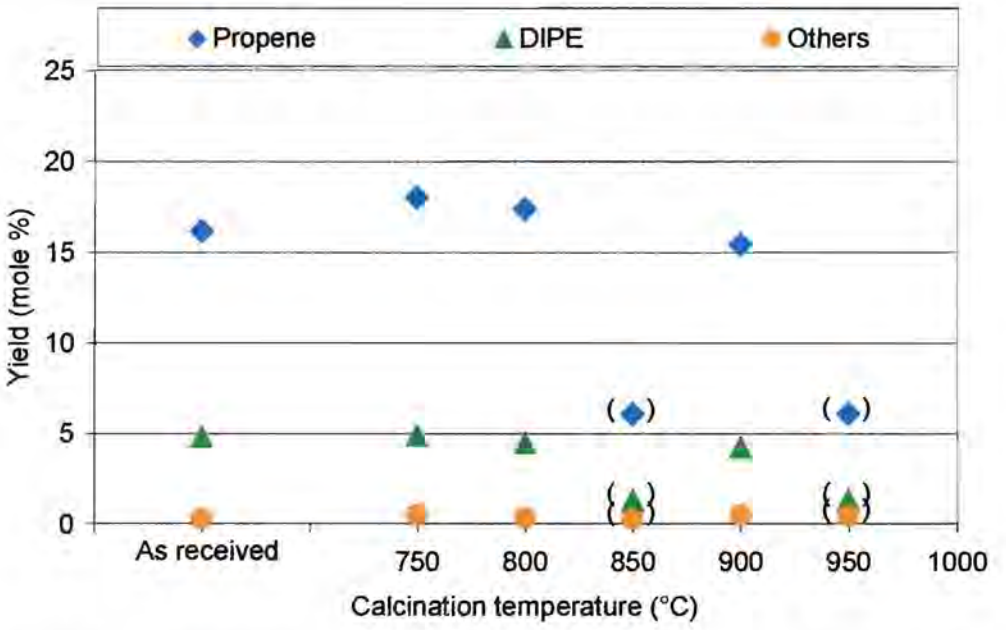

Figure 6-8b Yield of products from isopropanol conversion over Procatalyse alumina calcined at different temperatures

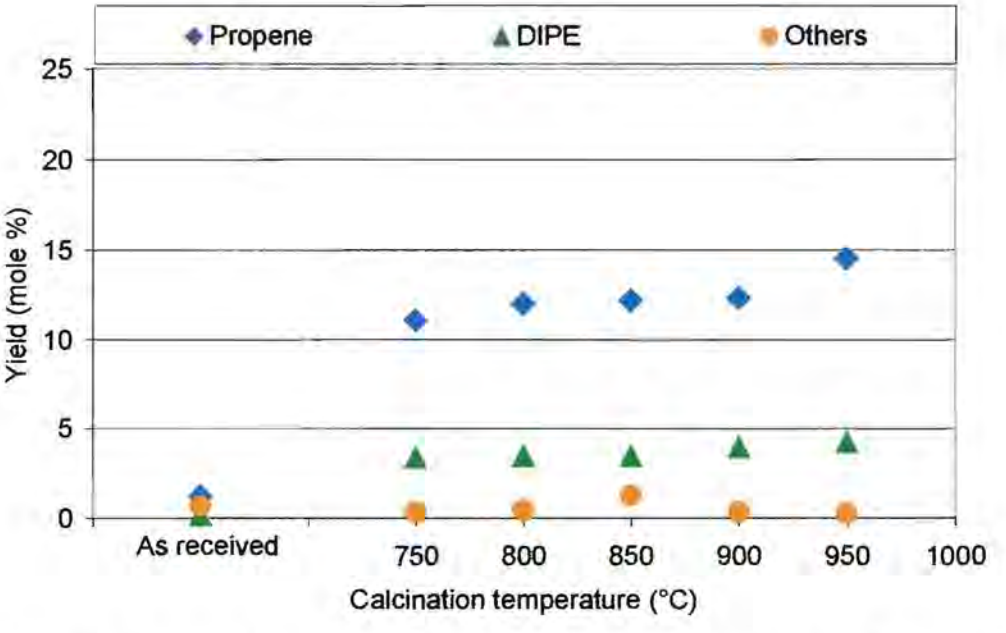

Figure 6-8c Yield of products from isopropanol conversion over La Roche sample calcined at different temperatures

In all cases the propene yield was much higher than the yield of DIPE. According to literature this would suggest the presence of a majority of medium strength acid sites (section 2.2).

6.3.3.4 SELECTIVITY

Comparison of the selectivity towards the different products obtained over the three aluminas as a function of calcination temperature is presented in figures 6-9a to d.

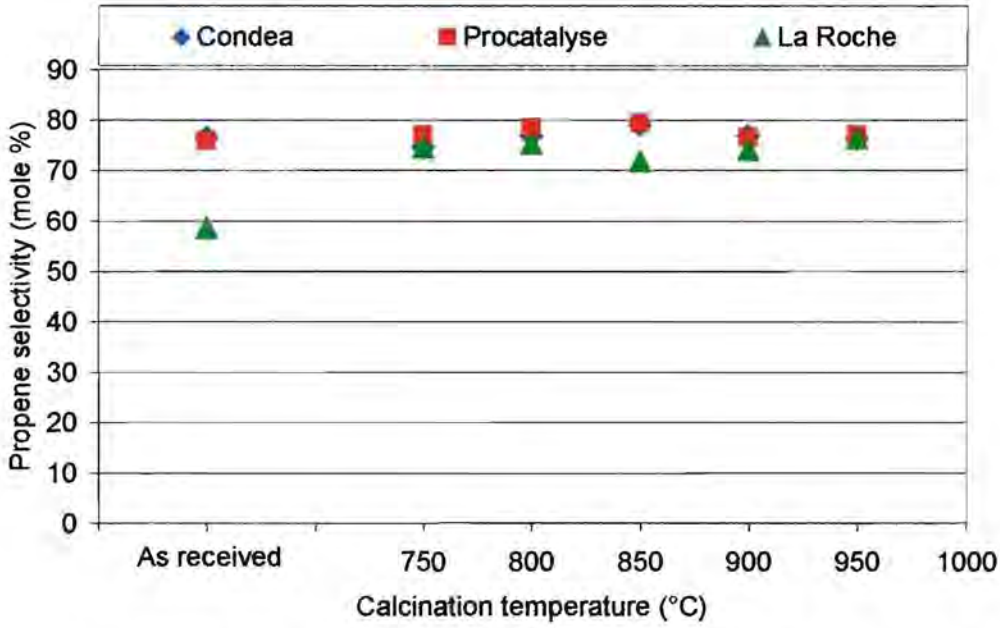

Figure 6-9a Propene selectivity as a function of calcination temperature

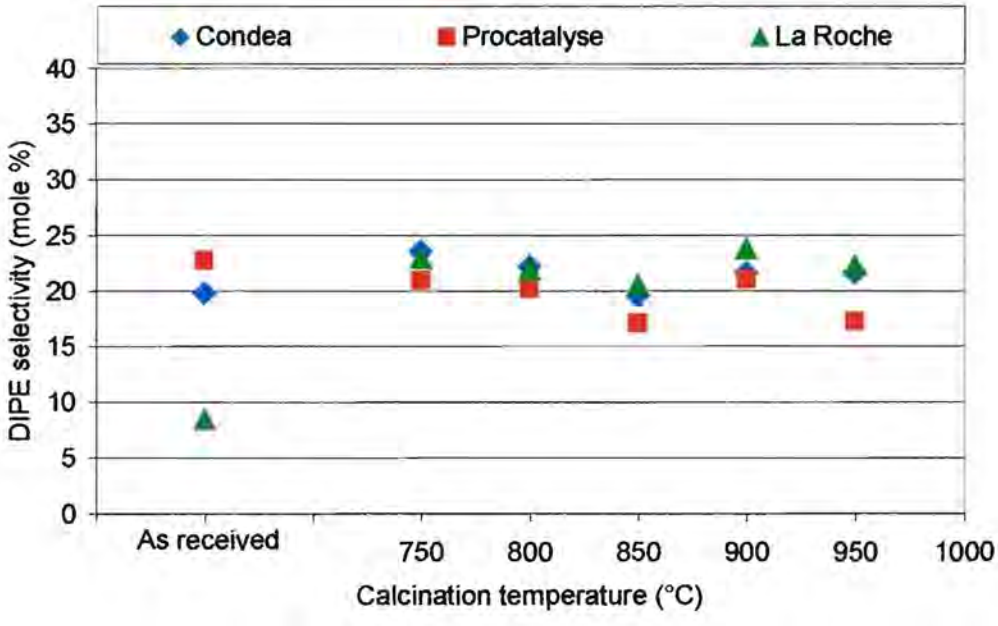

Figure 6-9b DIPE selectivity as a function of calcination temperature

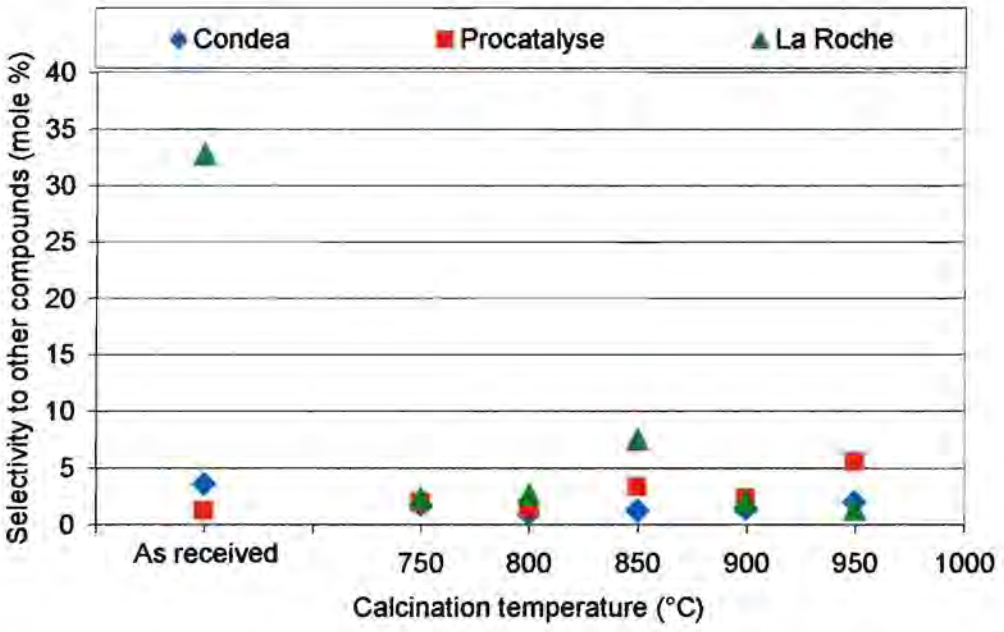

Figure 6-9c 'Other' compound selectivity as a function of calcination temperature

The lower the yield, the more the scatter. However, it is only selectivities towards 'other' compounds which scatters significantly. This is not unexpected since this product fraction is obtained with the lowest yields (see figures 5-9b, 5-10b and 5-11b).

The selectivity towards 'other' compounds for the 'as received' La Roche sample is erratic. These data result from the very low conversion (approximately 2%, figure 6-4c) so that the fraction of 'other' compounds may reflect inaccurate peak integration (noise) more than the real products.

No change in selectivity occurs upon calcination. Also, variation of the calcination temperature has no effect on the selectivity. No significant difference is observed between the selectivities of the three different variants of alumina samples.

Literature states that the different products (propene and DIPE) are preferentially formed over acid sites of different strengths. Results from this study on selectivity (constant) and conversion (variable) indicate that it is not the properties of the acid sites (strength or distribution of strength) which are

different between samples, but that it is the number of sites which differ between the alumina types.

6.4 EFFECT OF IMPURITY LEVELS IN THE ALUMINAS STUDIED

The presence of sodium is expected to possibly incorporate some basic characteristics into the alumina (section 2.2.3.2), while silica and sulphate should give rise to increased acidity and, consequently, may be expected to influence product selectivity.

No relationship, regardless of the use of analytical results or the values supplied by the manufacturers, could be discerned between the levels of the impurities reported and the catalytic behaviour of the alumina samples with respect to isopropanol conversion and selectivities toward propene and DIPE.

The effect of these impurities upon impregnation of alumina with a metal and the final catalytic activity of such a catalyst in Fischer-Tropsch synthesis can however not be predicted from the results of this study.

6.5 OTHER FINDINGS

No correlation could be found between the effect of calcination temperature and weight loss as well as the effect of calcination temperature and BET surface and related properties on the one hand and the level of conversions obtained on the other.

This is an important result, despite the fact that it is trivial since such properties did not vary at all.

CHAPTER 7: CONCLUSION AND RECOMMENDATIONS

Results initially indicated a significant amount of scatter present, but reproducibility studies verified that this was not due to the analysis procedure. It emerged that most of the scatter was introduced through considering acetone as a product, which proper analysis showed not to be the case. Acetone was neither produced nor consumed over the alumina samples tested. This can be stated at least for amounts in the percent range, which would have been discernable from the albeit variable levels of acetone already present in the feed. Possible low yields, e.g. <1.0% and corresponding trends resulting from the origin or the pretreatment of the aluminas, however, are obscured by the quite high and variable base level of acetone in the feed.

Results in this study indicated no reliable trends in respect of the isopropanol dehydrogenation pathway. Results from a different study (Erasmus, 2002), however, indicated that a lanthanum oxide catalyst produced a 40% acetone yield. Consequently, it can be concluded that the samples of this study exhibited no or only negligible basicity and that the test reaction was insensitive to any basic character at such low levels.

If this test reaction is intended to be used during further studies it is recommended that some steps should be taken to ensure proper results. Firstly, the feed used for the reaction must be absolutely free from any traces of acetone. Literature reports that some aluminas produce no acetone and some only traces, such that any basic character would be masked if acetone were already present in the feed. Steps taken to remove and keep away any oxygen from the feed storage flask were not successful and it seems that light also initiates the decomposition of isopropanol to acetone. Therefore a guard bed of some nature is recommended to remove any acetone present or formed before the reactor. It will also be important to confirm an acetone-free feed stream by performing blank runs before each experiment or by installing a reactor bypass and taking bypass samples before and after each run.

The variation of the pretreatment temperature produced trends in the activity of the alumina studied, while the selectivity remained essentially constant throughout the range. It can therefore be concluded that the changes occurring were only due to a change in the number of acid sites and not the nature of the acid sites. Moreover, performance differences between samples of different origin also appear to be restricted to differences in the number rather than the type of sites present on the samples.

No correlations were found between the catalytic activity of the aluminas studied and other physico-chemical properties investigated.

Sampling using evacuated glass ampoules produced a significant amount of other compounds present in the GC traces, which were not present when a syringe was used as sampling device. There are indications that these compounds originate from the flue gas of the flame used to seal the ampoules. This requires a refinement of this technique as it was applied during this work.

REFERENCES

Ai M and Suzuki S, Oxidation Activity and Acidity of MoO_3-P_2O_5 Catalysts, J. Catal., 30 (1973) 362-371

Augustine RL, Heterogeneous Catalysis for the Synthetic Chemist, Marcel Dekker, Inc., New York, (1996) 292-293

Benesi HA and Winquist BHC, in Advances in Catalysis, (Eds: Eley, Pines and Weisz), Academic Press, New York, 27 (1978) 123-131

Bowker M, Petts RW and Waugh KC, Temperature-programmed Desorption Studies of Alcohol Decomposition on Zinc Oxide, J. Chem. Soc., Faraday Trans. 1, 81 (1985) 3073-3080

Brinker CJ and Scherer GW, Sol-gel Science, The Physics and Chemistry of Sol-Gel Processing, Academic Press, Boston, Chapter 9, 1990

Callanan L, PhD thesis, Department of Chemical Engineering, UCT, 2000

Chadwick D and O'Malley PJR, Propan-2-ol Adsorption and Decomposition on Zinc Oxide promoted by Alkali Metal, J. Chem. Soc., Faraday Trans. 1, 83 (1987) 2227-2241

Chuang TT and Dalia Lana IG, Catalytic Activity and Selectivity of NaOH-Doped γ -Alumina, J. Chem. Soc. Faraday Trans. 1, 68 (1972) 773-784

Cortez GG, De Miguel SR, Scelza OA and Castro AA, Study of the Poisoning of γ-Al_2O_3 by Alkali Metals Addition, J. Chem. Tech. Biotechnol., 53 (1992) 177-180

Dabrowski JE, Butt JB and Bliss H, Monte Carlo Simulation of a Catalytic Surface: Activity and Selectivity of γ-Alumina for Dehydration, J. Catal., 18 (1970) 297-313

De Boer JH, Fahim RB, Linsen BG, Visseren WJ and De Vleesschauwer WFNM, Kinetics of the Dehydration of Alcohol on Alumina, J. Catal., 7 (1967) 163-172

Deo AV , Chuang TT and Dalla Lana IG, Infrared studies of the Adsorption and Surface Reactions of Some Secondary Alcohols, C3 to C5, on γ-Alumina and γ-Alumina Doped with Sodium Hydroxide, J. Phys. Chem., 75 (1971) 234-239

Deo AV and Dalla Lana IG, An Infrared study of the Adsorption and Mechanism of Surface Reactions of 1-propanol on γ-Alumina and γ-Alumina Doped with Sodium Hydroxide and Chromium Oxide, J. Phys. Chem., 73 (1969) 716-723

El Jamal MM, Forissier M and Auroux A, Nature of the β-Phase of Bismuth Molybdate, J. Chem. Soc. Faraday Trans. 1, 84 (1988) 3169

Fiedorow R and Dalla Lana IG, Interaction Between Hydroxides of Alkali Metals and Acid Centers on the Surface of Alumina, J. Phys. Chem., 84 (1980) 2779-2782

Fikis DV, Murphy WJ and Ross RA, The Formation of Propane, Propylene and Acetone from 2-Propanol over Vanadium Pentoxide and Modified Vanadium Pentoxide Catalysts, Can. J. Chem., 56 (1978) 2530-2537

Fox MA and Whitesell JK, Organic Chemistry (2nd edition), Jones and Bartlett Publishers, Boston (1997) 443-444

Griffin GL and Yates, Jr. JT, Combined Temperature-Programmed Desorption and Infrared Study on H_2 Chemisorption on ZnO, J. Catal., 73 (1982) 396-405

Harris P, University of Cape Town, South Africa, personal communications (2002)

Haupin WE, Production of Aluminium and Alumina, (Ed: Burkin), John Wiley & Sons, New York (1987) Chapter 1

Heese F, PhD thesis, Department of Chemical Engineering, UCT, 1998

Holleman AF and Wiberg E, Lehrbuch der anorganischen chemie, 57-70 issue, Walter de Gruyter & Co, Berlin (1964) 381-388

Jain JR and Pillai CN, Catalytic Dehydration of Alcohols over Alumina Mechanism of Ether Formation, J. Catal., 9, (1967) 322-330

Jiratova K and Beranek L, Properties of Modified Aluminas, Appl. Catal., 2 (1982) 125-138

Kirk-Othmer, Encyclopedia of Chemical Technology, Fourth Edition, John Wiley & Sons, New York, 2 (1992) 291-301

Knözinger H and Ratnasamy P, Surface Structure of γ- and η-Alumina, Catal. Rev. Sci. Eng., 17(1) (1978) 31-70

Knözinger H and Scheglila A, The Dehydration of Alcohols over Alumina XII Kinetic Isotope Effects in the Olefin Formation from Butanols, J. Catal., 17 (1970) 252-263

Knözinger H, Buhl H and Ress E, The Dehydration of Alcohols over Alumina VII The Dependance of Reaction Direction on the Substrate Structure, J. Catal., 12 (1968) 121-128

Koga O, Onishi T and Tamaru K, Adsorption and Decomposition of Isopropyl Alcohol over Zinc Oxide, J. Chem. Soc., Faraday Trans. 1, 76 (1980) 19-29

Lippens BC and Steggerda JJ, in Physical and Chemical Aspects of Adsorbents and Catalysts, (Ed: Linsen), Academic Press, London (1970) Chapter 4

MacIver DS, Wilmot WH and Bridges JM, Catalytic aluminas II: Catalytic Properties of Eta and Gamma Alumina, J. Catal., 3 (1964) 502-511

Mazanec TJ, On the Mechanism of Higher Alcohol Formation over Metal Oxide Catalysts, J. Catal., 98 (1986) 115-125

Moulijn JA, Van Leeuwen PWNM and Van Santen RA, Catalysis, An Integrated Approach to Homogeneous, Heterogeneous and Industrial Catalysis, Academic Press Inc., New York (1993) 314-318

Narayanan CR, Srinivasan S, Datye AK, Gorte R and Biaglow A, The Effect of Alumina Structure on Surface Sites for Alcohol Dehydration, J. Catal., 138 (1992) 659-674

Noller H and Ritter G, Temperature-programmed Desorption of Methanol, Ethanol, Propan-1-ol and Propan-2-ol on Silica-Magnesia Mixed Oxides, J. Chem. Soc., Faraday Trans. 1, 80 (1984) 275-283

Nortier P, Fourre P, Mohammed Saad AB, Saur O and Lavalley JC, Effects of Crystallinity and Morphology on the Surface Properties of Alumina, Appl. Catal., 61 (1990) 141-160

Oberlander RK, in Applied Industrial Catalysis (Ed: Leach), Academic Press inc., Orlando (1984) Chapter 4

Parry EP, An Infrared Study of Pyridine Adsorbed on Acidic Solids. Characterisation of Surface Acidity, J. Catal., 2 (1963) 371-379

Pepe F, Angeletti C and De Rossi S, Catalytic behaviour and Surface Chemistry of the ZnO/Al_2O_3 System for the Decomposition of 2-Propanol, J. Catal., 118 (1989) 1-9

Pepe F, Angeletti C, De Rossi S and Lo Jacono M, Catalytic behaviour and Surface Chemistry of Copper/Alumina Catalysts for Isopropanol Decomposition, J. Catal., 91 (1985) 69-77

Peri JB, A Model for the Surface of γ-Alumina, J. Phys. Chem., 69 (1965) 220-230

Phala N, University of Cape Town, South Africa, personal communications (2002)

Pines H and Haag WO, Alumina: Catalyst and Support. I Alumina, its Intrinsic Acidity and Catalytic Activity, J. Am. Chem. Soc., 82 (1960) 2471-2483

Pines H and Manassen J, The Mechanism of Dehydration of Alcohols over Alumina Catalysts, Adv. Catal., 16 (1966) 49-93

Poisson R, Brunelle J and Nortier P, in Catalyst Supports and Supported Catalysts, Theoretical and Applied Concepts, (Ed: Stiles), Butterworth Publishers, Boston (1987) Chapter 2

Richardson JT, Principles of Catalyst Development, (Eds: Twigg and Spencer), Plenum Press, New York (1989) Chapter 6-7

Roessner F, University of Oldenburg, Germany, personal communication with W. Böhringer (2002)

Ross RA and Bennett DER, Effect of Sodium Ion Impurities in γ-Alumina on the Catalytic, Vapour-Phase Dehydration of Ethyl Alcohol, J. Catal., 8 (1967) 289-292

Schulz H, Böhringer W, Kohl CP, Rahman NM and Will A, Entwicklung und Anwendung der Kapillar-GC-Gesamtprobentechnik für Gas/Danpf-Vielstoffgemische, DGMK Forschungsbericht 320, Hamburg (1984) 5-7

Schüth F and Unger K, in Handbook of Heterogeneous Catalysis, (Eds: Erti, Knözinger, Weitkamp), A Wiley company, 1 (1996) Chapter 2

Shi B and Davis BH, Alcohol Dehydration: Mechanism of Ether Formation Using an Alumina Catalyst, J. Catal. 157 (1995) 359-367

Stone FS, Surface Processes on Oxides and Their Significance for Heterogeneous Catalysis, J. Mol. Catal., 59 (1990) 147-163

Stull D.R., E.F.Westrum Jr. and G.C. Sinke, The Chemical Thermodynamics of Organic Compounds, John Wiley & Sons, Inc., New York, 1969

Swecker JL and Datye AK, Alcohol Dehydration over Model Nonporous Alumina Powder, J. Catal., 121 (1990) 196-201

Tanabe K, In Catalysis Science and Technology (Ed: Anderson and Boudart), Springer-Verlag, Berlin (1981) Chapter 5

Tanabe K, Solid Acids and Bases Their Catalytic Properties, Academic Press Inc., New York (1970) Chapter 4

Thomas JM and Thomas WJ, Principles and Practice of Heterogeneous Catalysis, VCH Publishers Inc., Weinheim (1997) Chapter 4

Wang JA, Bokhimi X, Novaro O, Lopez T, Tzompantzi F, Gomez R, Navarrete J Llanos ME and Lopez-Salinas E, Effects of Structural Defects and Acid-basic Properties on the Activity and Selectivity of Isopropanol Decomposition on Nanocrystallite Sol-gel Alumina Catalyst, J. Molec. Catal. A: Chem, 137 (1999) 239-252

Weissenbacher M, Leder A and Ishikawa-Yamaki M, Chemical Economics Handbook – SRI International (1998)

Weissermel K and Arpe H, Industrial Organic Chemistry, VCH Publishers Inc., New York (1997) Chapter 3

Xia WS, Wan HL and Chen Y, J. Mol. Catal. A: Chem., 138(2-3) (1999) 185-195

Youssef AM, Khalil LB and Girgis BS, Decomposition of Isopropanol on Magnesium Oxide/silica in Relation to Texture, Acidity and Chemical Composition, Appl. Catal. A: General, 81, 1-13, 1992

APPENDICES

APPENDIX A-1 CALCINATION EQUIPMENT

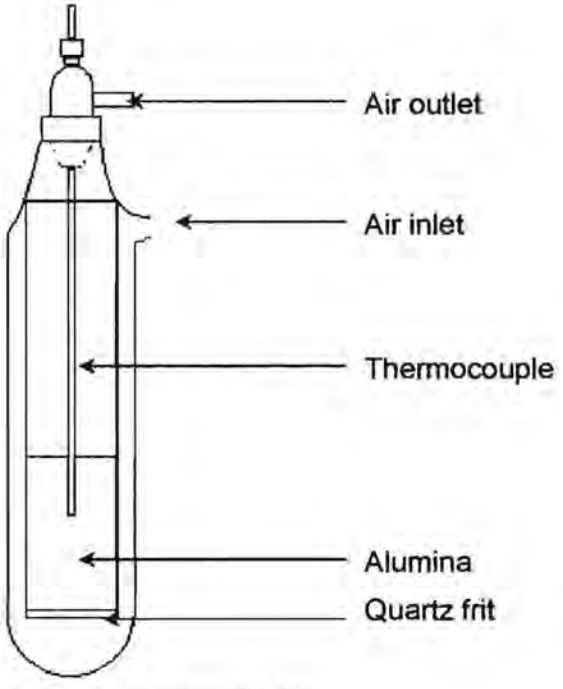

Figure A-1a Quartz calcination tube

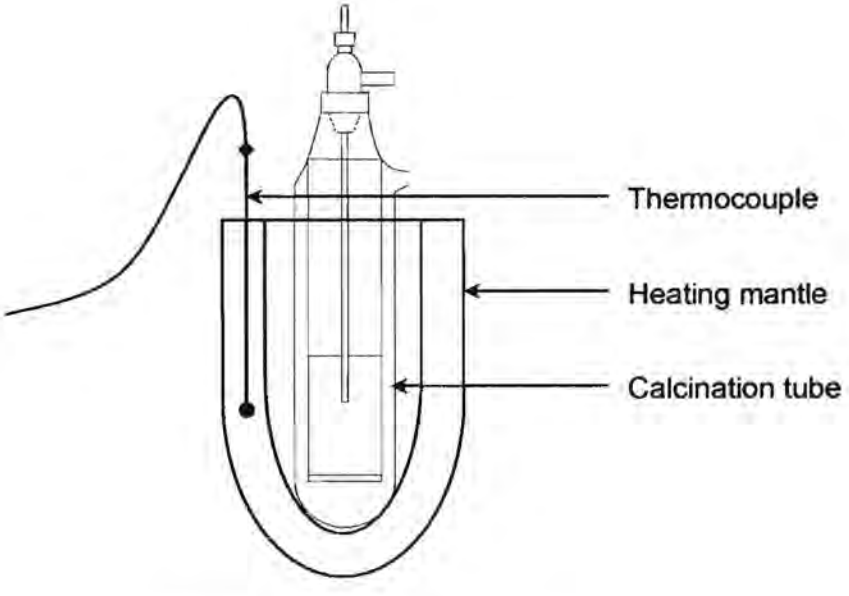

Figure A-1b Calcination oven

APPENDIX A-2 CALIBRATION OF THE FEED PUMP

The HPLC metering pump was calibrated by entering a certain setpoint, starting the pump and stopping it after a certain time. The pumping time was recorded. The mass pumped and measured by the balance was used to calculate the volume pumped per minute. This was correlated with the set point in figure A-2.

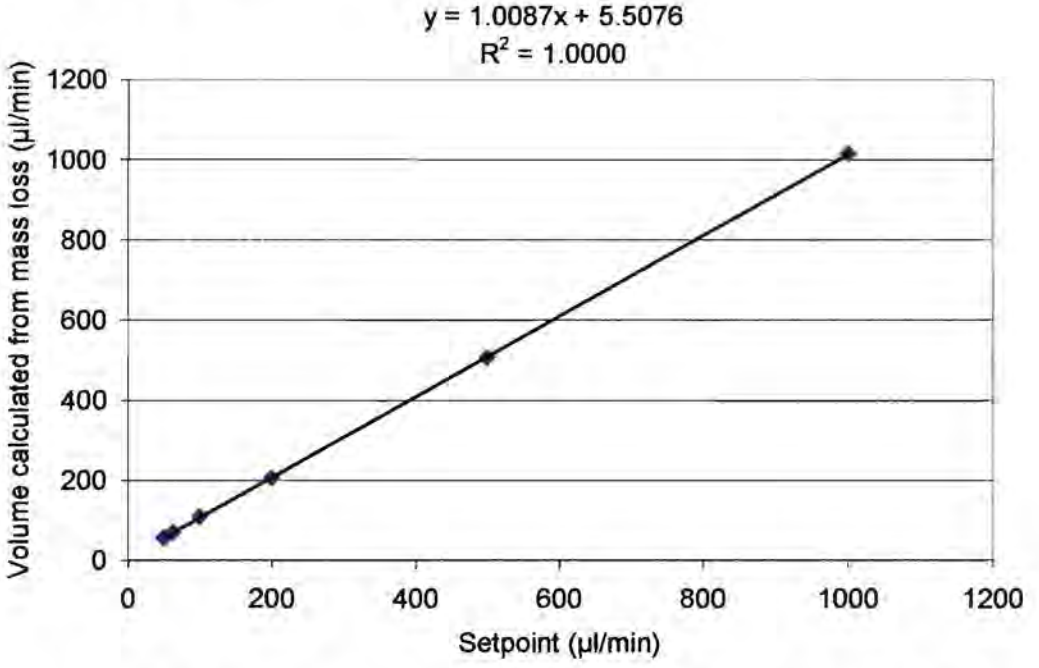

Figure A-2 Calibration data for the pump used to supply feed to the reactor

APPENDIX A-3 CALIBRATION OF GAS FLOW CONTROLLERS

The Brooks mass flow controller, regulating the carrier gas flow to the reactor was calibrated by measuring the volume of gas delivered over a certain time period at different set points with a Ritter drum-type gas meter (TG1-14571-pvc). The data are shown in figure A-3.

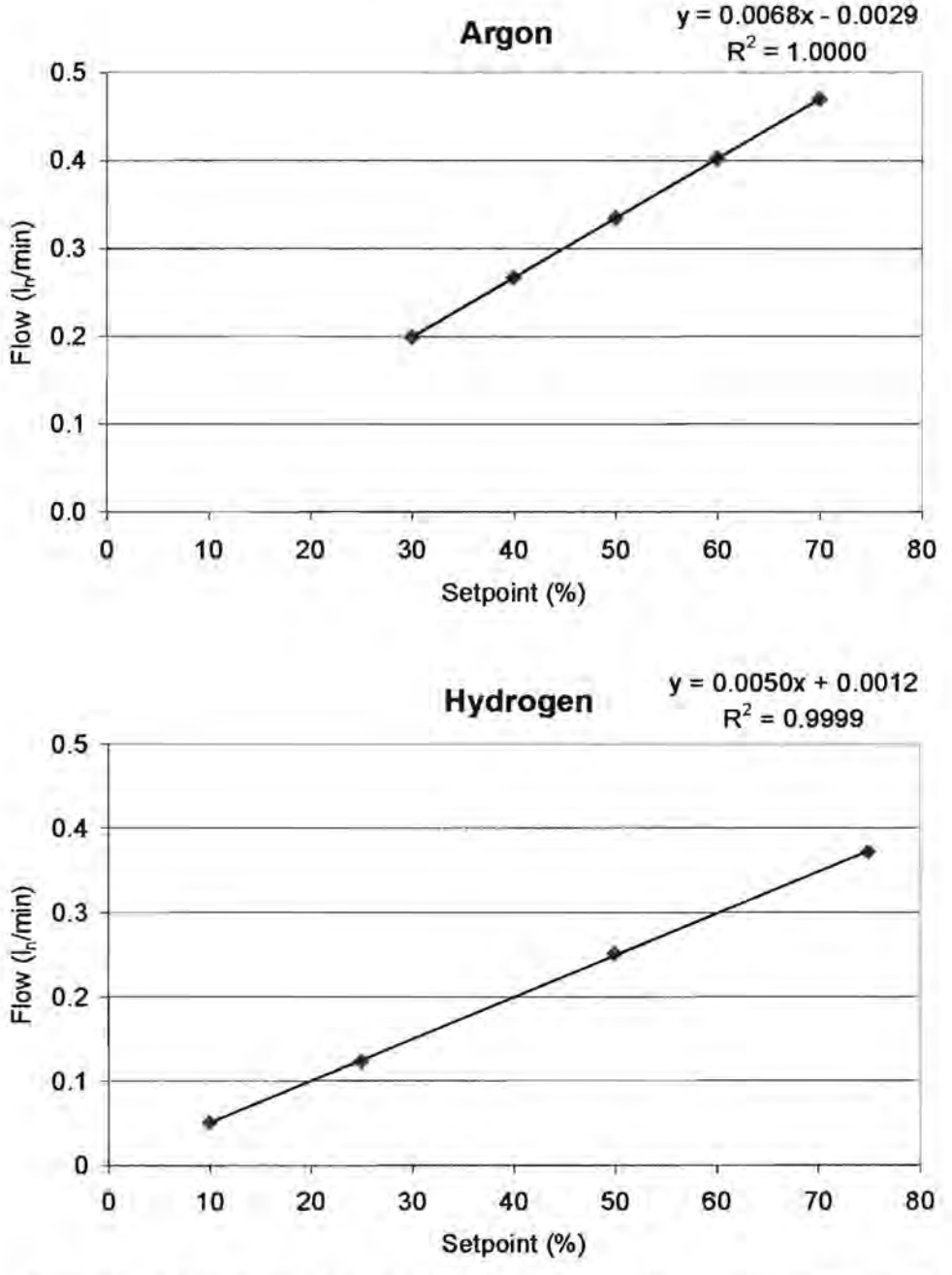

Figure A-3 Calibration data for the Brooks mass flow controllers used to supply carrier gas to the reactor

APPENDIX A-4 AMPOULE SAMPLING EQUIPMENT

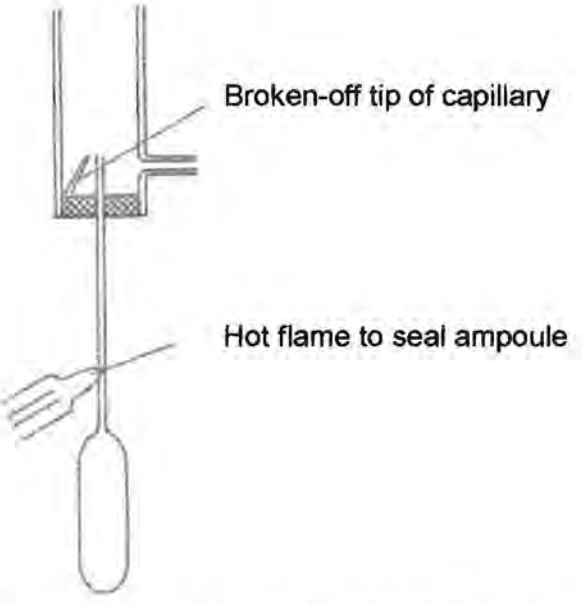

Figure A-4a Principle of the ampoule technique (Schulz et al., 1984)

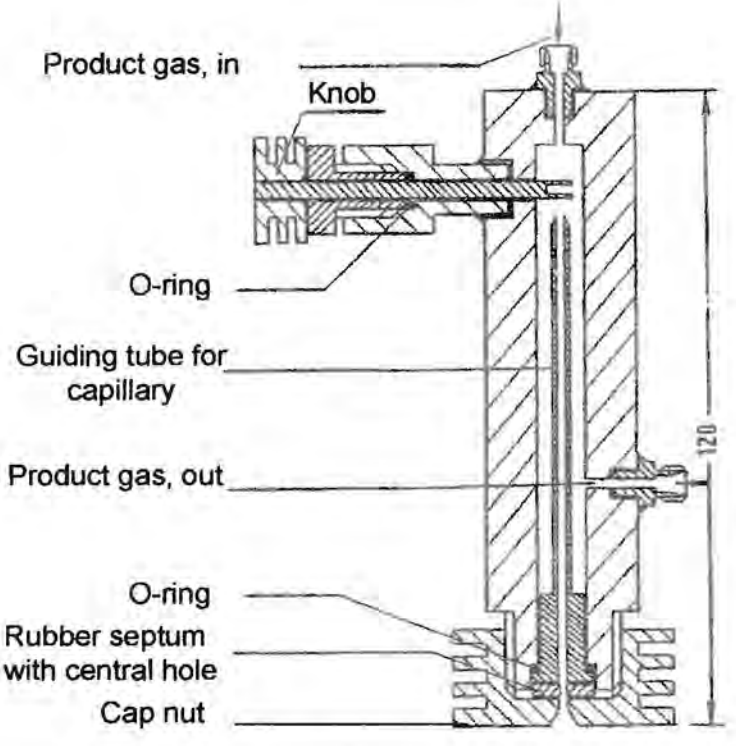

Figure A-4b Design of the ampoule sampler (Schulz et al., 1984)

Some of the sampling was performed using evacuated glass ampoules. This entails inserting the capillary end of the ampoule through the septum of an

ampoule sampler (see figure A-4a), breaking the tip of the capillary inside the sampler and sealing the capillary close to the body of the ampoule with a flame.

Figure A-4b shows the design of the ampoule sampler. After inserting the capillary, the extruding glass is heated with a burner for 10 seconds and the capillary end broken by turning the knob. Since the ampoule is under vacuum, breaking it results in a sample of the vapour surrounding the capillary end to be drawn in. The capillary is then sealed with the burner.

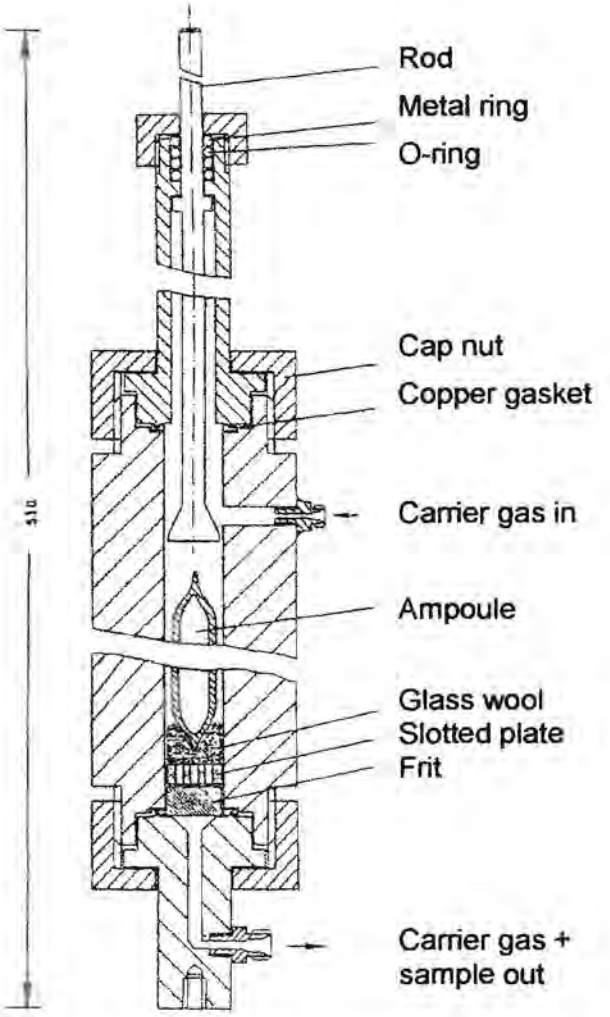

Figure A-4c Ampoule breaker (as sampler for GC analysis) (Schulz et al., 1984)

The sealed ampoules were analysed with a gas chromatograph equipped with a special ampoule breaking device (figure A-4c). The ampoule is placed in

the heated ampoule breaker and after the temperature has stabilised and possible condensates have evaporated, the rod is pushed down and breaks the ampoule. This action releases the contents into the sample holder, from where it is flushed out by the carrier gas to the GC.

APPENDIX A-5 SAMPLING SYRINGE TEMPERATURE

Some of the sampling of the gaseous reactor effluent was performed using a preheated gas syringe. Samples were taken from the ampoule sampler device (figure A-4b). The syringe had to be heated in order to avoid any condensation.

Several factors must be taken into consideration for the syringe temperature. Conversion was kept low and therefore the unconverted isopropanol was always the major compound present in the product stream. Inspection of figure A-5 reveals that at 1 bar, isopropanol will be in gaseous phase at 82.5°C. At ambient temperature the vapour pressure of isopropanol is approximately 58 mbar, which value is lower than the partial pressure of isopropanol in the effluent from the reactor.

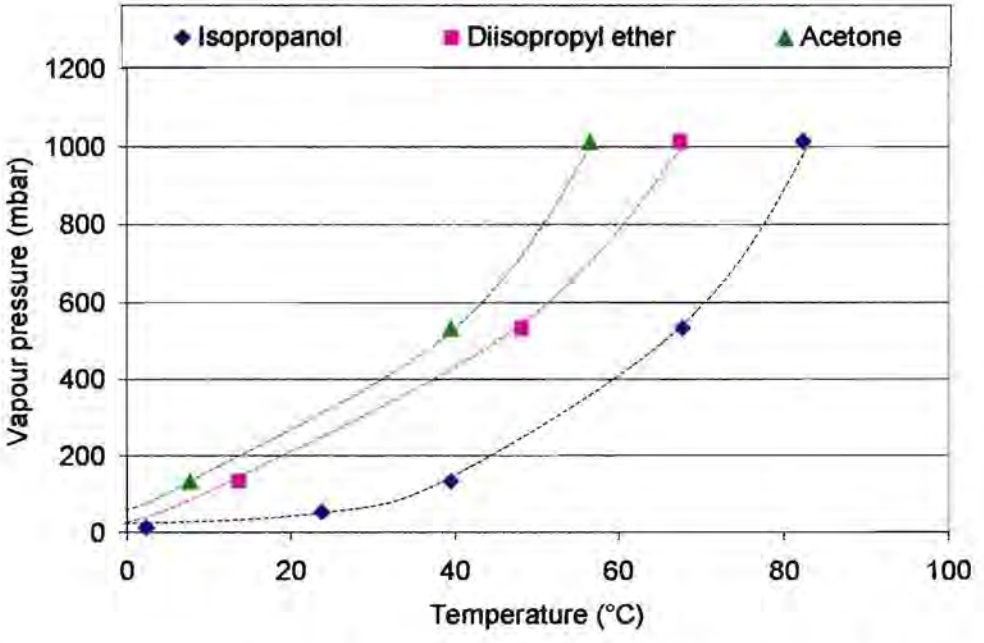

Figure A-5 Vapour pressure versus temperature (Values taken from Stull et al.,1969)

The altitude at which the experiments were conducted, Sasolburg (1494 m), must also be taken into account. Therefore the ambient pressure at which the reactions were conducted is 850 mbar.

Isopropanol was fed in a diluted state. A 1:10.3 molar ratio of isopropanol in hydrogen was used. This corresponds to 9.8 vol%, i.e. a maximum partial pressure in the reactor outlet of 84 mbar at 850 mbar ambient pressure (see figure A-5). Therefore, a minimum temperature of 34°C is required for the samples to stay in a vaporous phase. The product stream did not contain higher boiling compounds.

Keeping the syringe at a temperature of 50°C would therefore prevent any condensation processes.

APPENDIX A-6 INITIAL EXPERIMENTS CONDUCTED

Experiments were carried out under the same conditions as given in table 4-6, except that argon was used as the carrier gas, see table A-6a.

Table A-6a A list of the first set of experiments

Run numbers			Alumina	Calcination temperature (°C)
A1	A2	A17	Condea	As received
A5	A7	A43	Condea	750
A23	A24	A30	Condea	800
A13	A37	A44	Condea	850
A27	A34	A45	Condea	900
A10	A38		Condea	950
A3	A19	A21	Procatalyse	As received
A6	A9	A18	Procatalyse	750
A25	A31	A32	Procatalyse	800
A11	A39	A46	Procatalyse	850
A28	A33	A48	Procatalyse	900
A14	A40	A49	Procatalyse	950
A4	A20	A22	La Roche	As received
A8	A41	A50	La Roche	750
A26	A35	A51	La Roche	800
A12	A42	A52	La Roche	850
A29	A36	A53	La Roche	900
A15	A16	A54	La Roche	950
A57	A58		SiAl	
A60	A61	A62	Blank	

The results of the above runs indicate that some oxidation of the feed took place, as there was a steady increase in the amount of acetone found in the products as time passed (figure A-6). Blank runs performed after this period indicated that the high acetone content observed, originated from the feed.

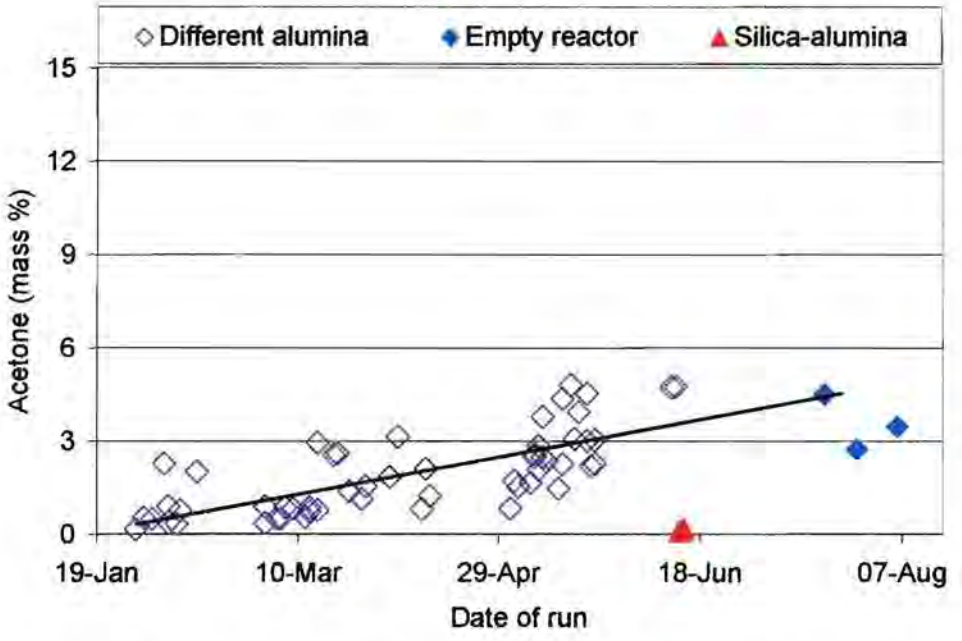

Figure A-6a Mass percentage of acetone present in the product stream versus time for initial runs

It was thought that running with hydrogen carrier gas and including a Ni catalyst in a guard reactor would convert all acetone present before the main reactor back to isopropanol. Therefore, the glass beads used in the preheater/vaporiser were replaced with an Engelhard Ni328 catalyst. A small flow of argon was introduced into the feed storage flask to eliminate any contact with air. The experiments conducted with this set-up are listed in table A-6b.

Table A-6b A list of the second set of experiments using hydrogen carrier gas and a Ni catalyst in the preheater

Run number		Alumina	Calcination temperature (°C)
B1	B20	Blank	
B19		Condea	As received
B2		Condea	750
B5		Condea	800
B8		Condea	850
B11		Condea	900
B14		Condea	950
B15		Procatalyse	As received
B17		Procatalyse	750
B3		Procatalyse	800
B6		Procatalyse	850
B9		Procatalyse	900
B12		Procatalyse	950
B13		La Roche	As received
B16		La Roche	750
B26		La Roche	800
B4		La Roche	850
B7		La Roche	900
B10		La Roche	950

Unfortunately results were made worse since the Ni catalyst produced many additional compounds. The Ni catalyst was removed from the preheater and replaced with glass beads, as before. In addition to the acetone problem, results from these runs were still quite erratic. Even without the Ni catalyst a multitude of peaks appeared in addition to what was expected. These peaks corresponded to up to 30% of the product, also showing a very large degree of scatter.

It was therefore decided to investigate what effect the sampling method had on the results. Instead of evacuated glass ampoules (for details of the method see appendix A-4) a preheated gas-tight syringe (100 μl) was used (for details see section 4.3.4.2). Using this method, the percentage of additional peaks besides those of the major products, dropped drastically to approximately 1-2%. Therefore, the final experiments (table 4-9) were carried out applying syringe sampling.

The ampoule technique is successfully applied in research facilities e.g. Sasol and the Catalysis Research Unit at UCT, and results thus far did not produce any reason for concern. It can be speculated that compounds arising from the burner flame entered the ampoule before it was sealed off. Similarly unusual results were observed when the capillary end of the ampoule was retracted from an ampoule sampler before sealing off (Böhringer, 2002).

It emerged that the outlet line (downstream of the ampoule sampler) of the rig led to a vent, resulting in a pressure below ambient. It is speculated that this vent sucked in ambient air from outside through the hole in the septum of the ampoule sampler (see bottom part of figure A-4b) in addition to the product stream.

When the ampoule has been inserted into the sampler through this hole, the rubber septum is supposed to be compressed by tightening the cap nut, which holds the septum (see bottom part of figure A-4b). Unfortunately this was not done, so that constituents of the flue gas of the flame, which was used to seal the capillary, were sucked in.

This is supported by a systematic difference between the composition of the ampoule samples and the syringe samples. It was found that the percentages of acetone and, in particular, DIPE were very similar in samples from both ampoules (figures A-6b to d) and the syringe (figures 5-7b, 5-8b and 5-9b), whereas the percentage of propene was much higher, consistently. Since the fuel for this flame was LPG (liquefied petroleum gas), which mainly consists of propane, the thermal dehydrogenation or oxi-dehydrogenation product – propene – can be expected as a major constituent of the flue gas. Significant percentages of ethene and methane were also present in these samples.

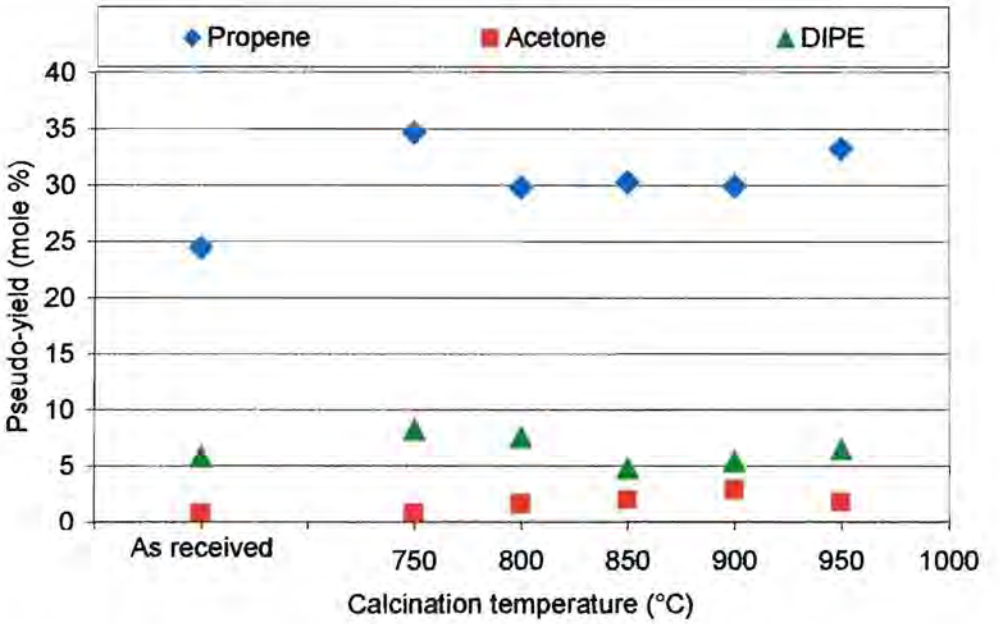

Figure A-6b Pseudo-yield over Condea alumina calcined at different temperatures ['other' peaks rejected and the average of three values reported]

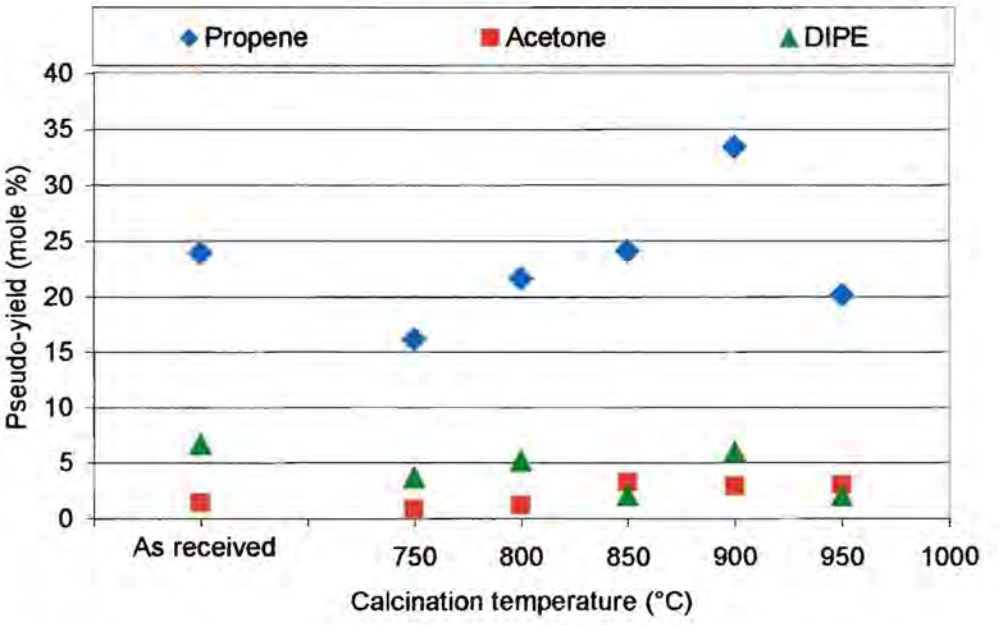

Figure A-6c Pseudo-yield over Procatalyse alumina calcined at different temperatures ['other' peaks rejected and the average of three values reported[

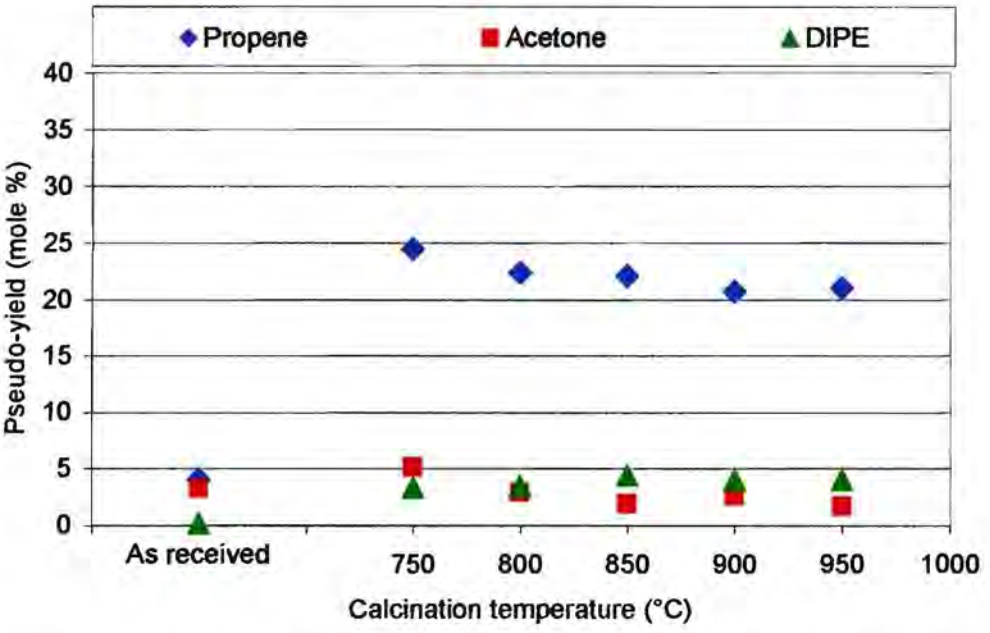

Figure A-6d Pseudo-yield over La Roche samples calcined at different temperatures ['other' peaks rejected and the average of three values reported]

APPENDIX A-7 CALCINATION DATA

Table A-7 Mass loss during calcinations

Alumina sample	Calcination temperature (°C)	Mass before (g)	Mass after (g)	Mass loss (%)	Aver-age (%)
Condea	750	48.7	48.6	0.3	
	800	48.0	48.0	0.0	
	850	40.9	40.3	1.5	0.8
	900	44.2	43.9	0.6	
	950	41.3	31.4	23.9*	
Procatalise	750	50.0	48.8	2.3	
	800	48.9	53.4	-9.2*	
	850	46.6	45.1	3.2	3.7
	900	38.7	37.2	3.7	
	950	46.1	43.5	5.6	
La Roche	750	50.2	39.8	20.7	
	800	45.1	32.7	27.5*,**	
	850	49.5	39.6	19.9	20.7
	900	46.3	36.3	21.6	

*Outliers excluded for average

**Loss due to failure of calcination equipment

APPENDIX A-8 BET DATA

Table A-8 Surface areas and pore volumes

Alumina	Calcination temperature (°C)	Surface area (m^2/g)	Pore* volume (ml/g)
Condea	As received	152	0.46
	750	148	0.46
	800	147	0.47
	850	144	0.46
	900	136	0.44
	950	144	0.47
Procatalyse	As received	145	0.46
	750	138	0.45
	800	142	0.46
	850	136	0.45
	900	131	0.45
	950	120	0.45
La Roche	As received	353	0.50
	750	217	0.57
	800	234	0.57
	850	215	0.57
	900	228	0.56
	950	206	0.62

* Determined from adsorption isotherm

The pore volumes reported are the single point adsorption total pore volumes. The difference between the adsorption and desorption pore volumes were less than 2%. No systematic errors are therefore suspected and the values show only random deviation.

APPENDIX A-9 PORE SIZE DISTRIBUTION

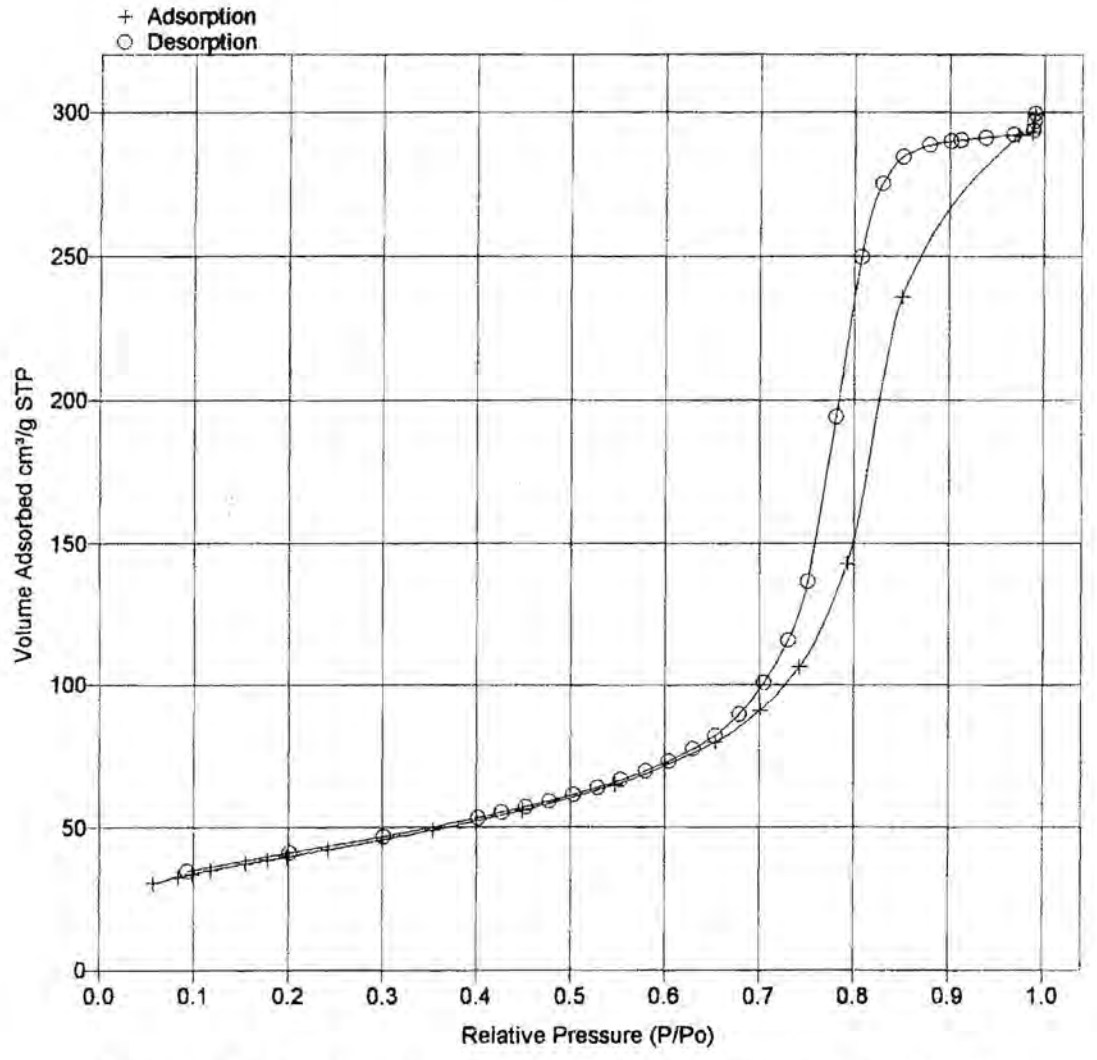

Figure A-9a Condea adsorption/desorption data (calcined at 850°C)

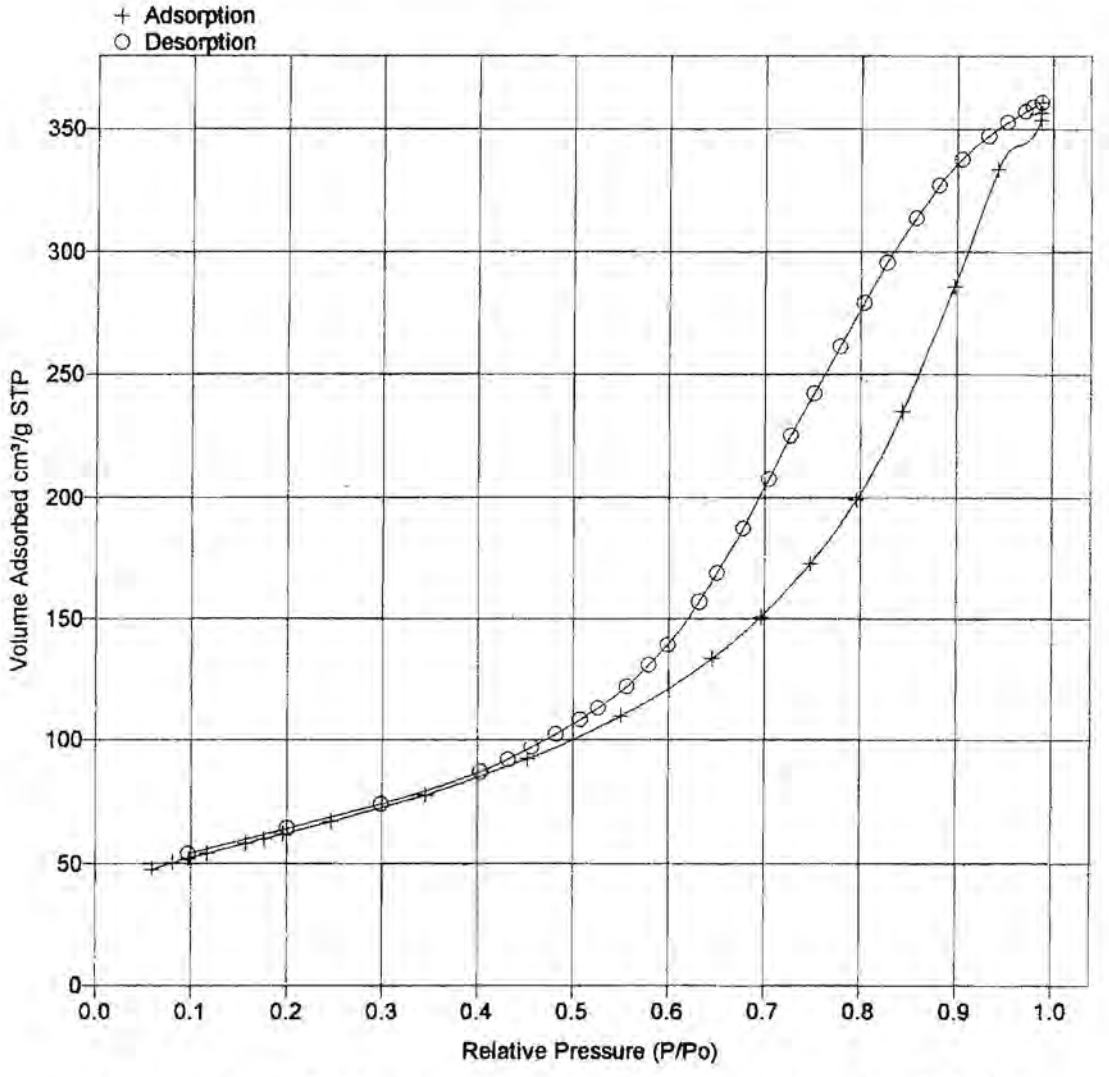

Figure A-9b La Roche adsorption/desorption data (calcined at 900°C)

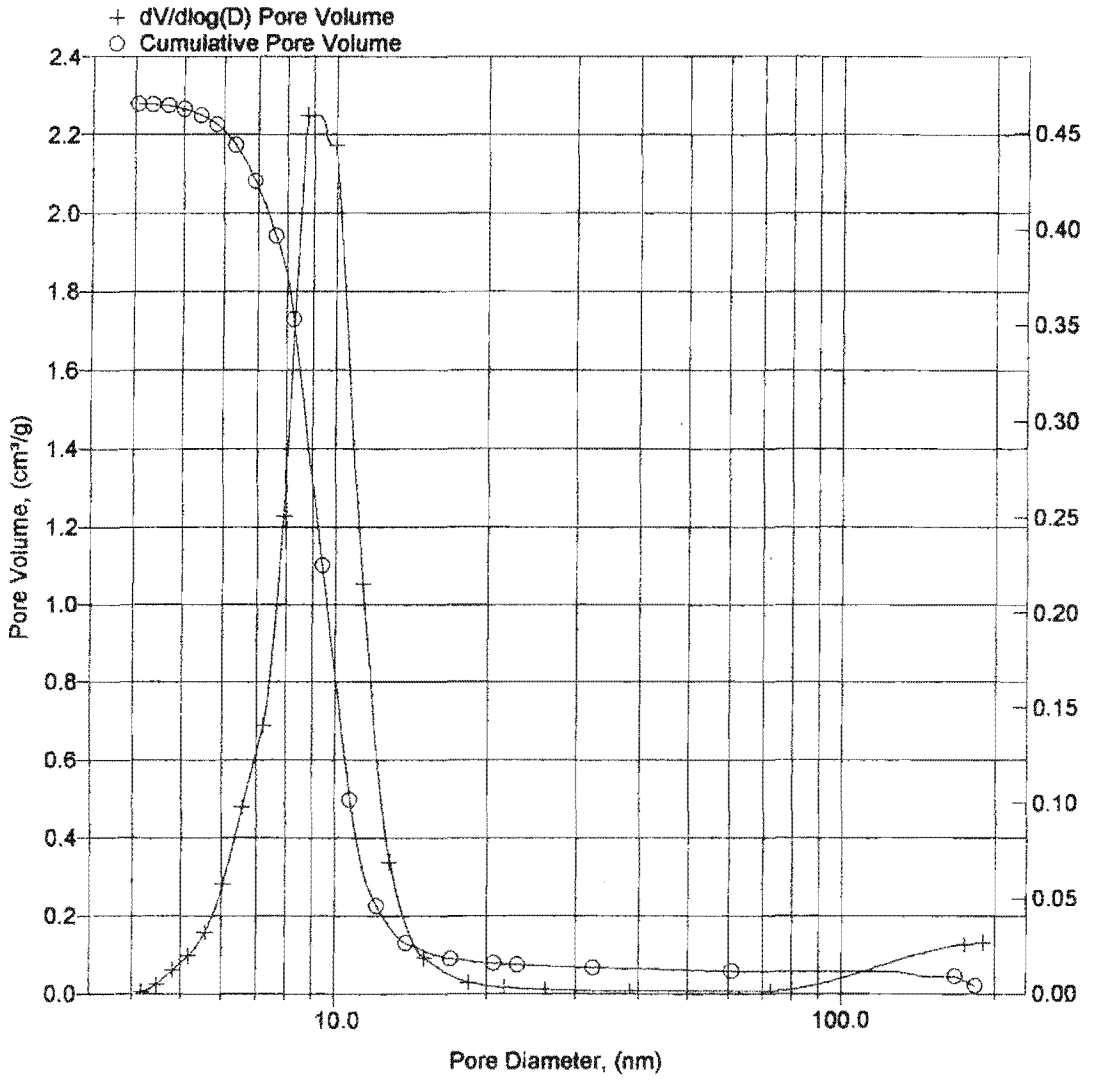

Figure A-9c Condea pore size distribution (calcined at 850°C)

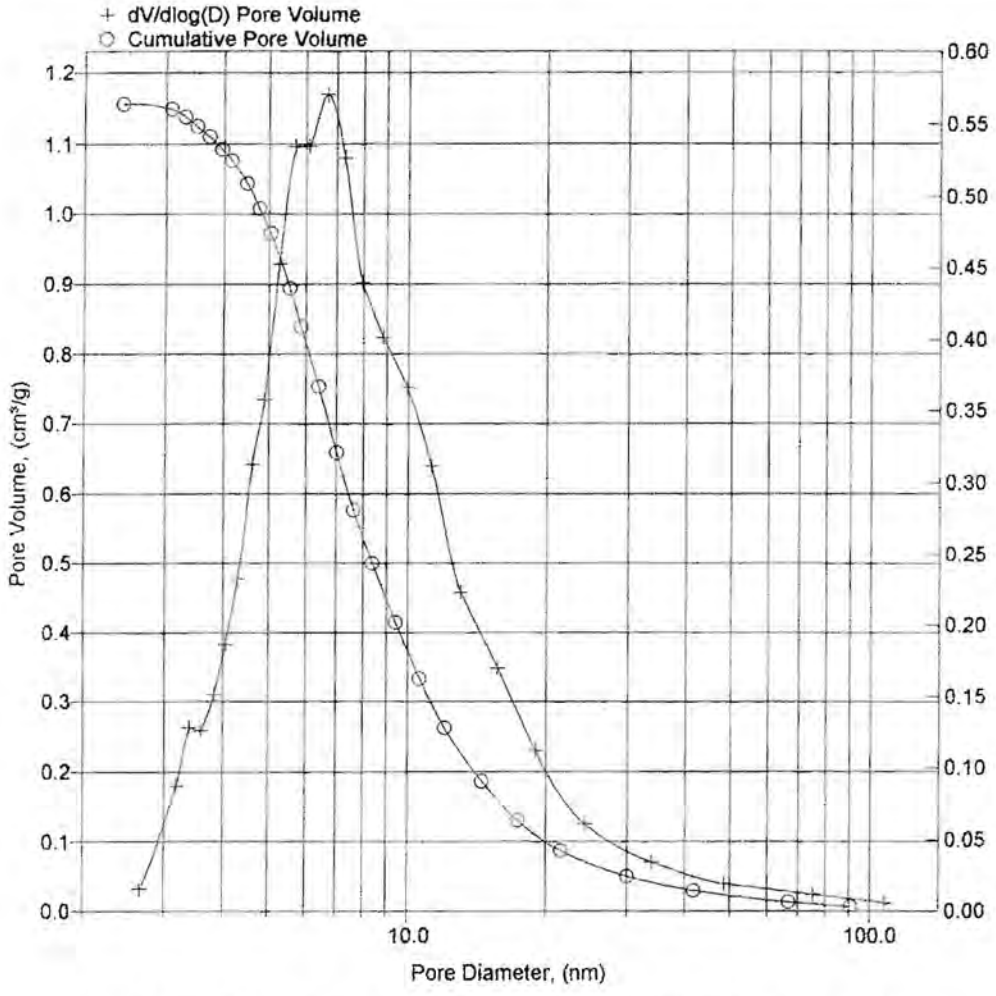

Figure A-9d La Roche pore size distribution (calcined at 900°C)

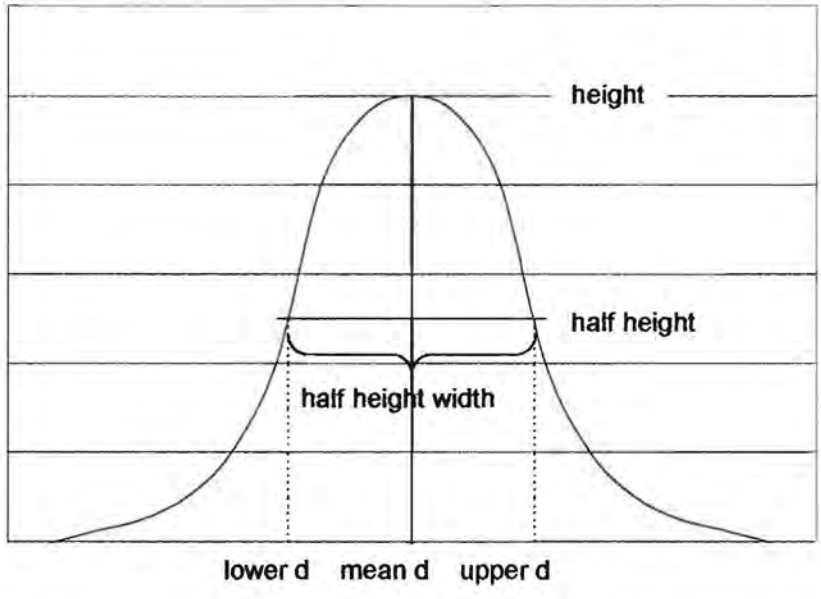

Figure A-9e Determination of half height width [the relative half height pore diameter range = (upper d – lower d) / mean d]

APPENDIX A-10 RESULTS

Run number	C0	C19	C21	C1	C38	C4	C37	C14	C26	C9	C30	C8	C31
Alumina				Condea	Condea	Condea	Condea	Condea	Condea	Condea	Condea	Condea	Condea
Calc. Temp.				Std	Std	750	750	800	800	850	850	900	900
Conversion	2.69	5.10	2.53	27.48	28.27	30.86	33.90	32.99	28.31	24.34	27.70	24.70	17.14
Selectivity													
Propene	7.43	4.87	15.74	71.68	69.90	75.03	63.58	74.09	69.35	74.63	74.27	75.32	67.34
Acetone	61.40	64.67	73.81	5.99	9.21	1.95	12.62	4.18	9.09	4.65	7.06	2.31	12.16
DIPE	0.00	0.00	0.00	18.06	18.49	21.71	21.84	20.79	20.71	19.46	17.52	21.62	18.27
Others	31.18	30.46	10.45	4.27	2.40	1.31	1.95	0.94	0.85	1.26	1.15	0.75	2.23
Total	100.00	100.00	100.00	100.00	100.00	100.00	100.00	100.00	100.00	100.00	100.00	100.00	100.00
Yield													
Propene	0.20	0.25	0.40	19.70	19.76	23.15	21.56	24.44	19.63	18.16	20.57	18.60	11.54
Acetone	1.65	3.30	1.87	1.65	2.60	0.60	4.28	1.38	2.57	1.13	1.96	0.57	2.08
DIPE	0.00	0.00	0.00	4.96	5.23	6.70	7.41	6.86	5.86	4.74	4.85	5.34	3.13
Others	0.84	1.55	0.26	1.17	0.68	0.40	0.66	0.31	0.24	0.31	0.32	0.19	0.38
Total	2.69	5.10	2.53	27.48	28.27	30.86	33.90	32.99	28.31	24.34	27.70	24.70	17.14

Run number	C3	C25	C11	C6	C33	C5	C34	C16	C24	C41	C13	C27	C10
Alumina	Condea	Condea	Procatalyse	Procatalyse	Procatalyse	Procatalyse	Procatalyse	Procatalyse	Procatalyse	Procatalyse	Procatalyse	Procatalyse	Procatalyse
Calc. Temp.	950	950	Std	750	750	800	800	850	850	850	900	900	950
Conversion	21.23	17.20	22.05	29.53	20.24	24.62	21.32	9.90	14.51	8.02	20.80	22.73	9.82
Selectivity													
Propene	73.80	70.17	72.66	73.11	67.94	76.98	72.53	69.45	60.47	63.28	69.69	69.45	69.40
Acetone	2.96	8.52	4.38	6.48	9.82	2.35	6.81	13.76	22.73	19.05	8.09	10.12	9.65
DIPE	20.85	20.02	21.76	18.35	20.75	19.09	19.48	14.53	12.26	14.15	19.68	18.58	15.89
Others	2.39	1.28	1.19	2.05	1.49	1.58	1.18	2.26	4.54	3.53	2.55	1.84	5.06
Total	100.00	100.00	100.00	100.00	100.00	100.00	100.00	100.00	100.00	100.00	100.00	100.00	100.00
Yield													
Propene	15.67	12.07	16.02	21.59	13.75	18.95	15.46	6.88	8.77	5.08	14.50	15.79	6.82
Acetone	0.63	1.47	0.97	1.91	1.99	0.58	1.45	1.36	3.30	1.53	1.68	2.30	0.95
DIPE	4.43	3.44	4.80	5.42	4.20	4.70	4.15	1.44	1.78	1.13	4.09	4.22	1.56
Others	0.51	0.22	0.26	0.61	0.30	0.39	0.25	0.22	0.66	0.28	0.53	0.42	0.50
Total	21.23	17.20	22.05	29.53	20.24	24.62	21.32	9.90	14.51	8.02	20.80	22.73	9.82

Run number	C29	C15	C12	C28	C39	C7	C32	C2	C35	C17	C23	C18	C20	C22
Alumina	Procatalyse	La Roche	La Roche	La Roche	La Roche	La Roche	La Roche	La Roche	La Roche	La Roche	La Roche	La Roche	La Roche	La Roche
Calc. Temp.	950	Std	750	750	750	800	800	850	850	900	900	950	950	950
Conversion	9.16	5.14	21.25	32.94	12.59	17.72	16.52	19.08	18.25	18.25	19.61	24.00	17.53	33.03
Selectivity														
Propene	56.43	23.06	65.65	70.48	61.61	73.19	65.52	70.13	57.98	70.39	57.12	71.75	64.38	73.35
Acetone	27.21	60.74	12.55	9.03	16.62	5.18	10.73	9.52	12.06	6.95	21.28	6.63	14.81	5.76
DIPE	12.26	3.34	19.74	18.41	19.75	20.46	19.86	17.77	18.89	21.18	19.68	20.74	19.07	18.64
Others	4.09	12.86	2.06	2.08	2.03	1.17	3.89	2.58	11.07	1.48	1.92	0.88	1.74	2.25
Total	100.00	100.00	100.00	100.00	100.00	100.00	100.00	100.00	100.00	100.00	100.00	100.00	100.00	100.00
Yield														
Propene	5.17	1.18	13.95	23.22	7.76	12.97	10.82	13.38	10.58	12.84	11.20	17.22	11.28	24.23
Acetone	2.49	3.12	2.67	2.97	2.09	0.92	1.77	1.82	2.20	1.27	4.17	1.59	2.60	1.90
DIPE	1.12	0.17	4.19	6.06	2.49	3.62	3.28	3.39	3.45	3.87	3.86	4.98	3.34	6.16
Others	0.38	0.66	0.44	0.69	0.26	0.21	0.64	0.49	2.02	0.27	0.38	0.21	0.30	0.74
Total	9.16	5.14	21.25	32.94	12.59	17.72	16.52	19.08	18.25	18.25	19.61	24.00	17.53	33.03

Note that the above results represent the pseudo-conversion, pseudo-selectivity and pseudo-yield (i.e. acetone is considered a product of the reaction).

APPENDIX A-11 REPRODUCIBILITY DURING BLANK RUN

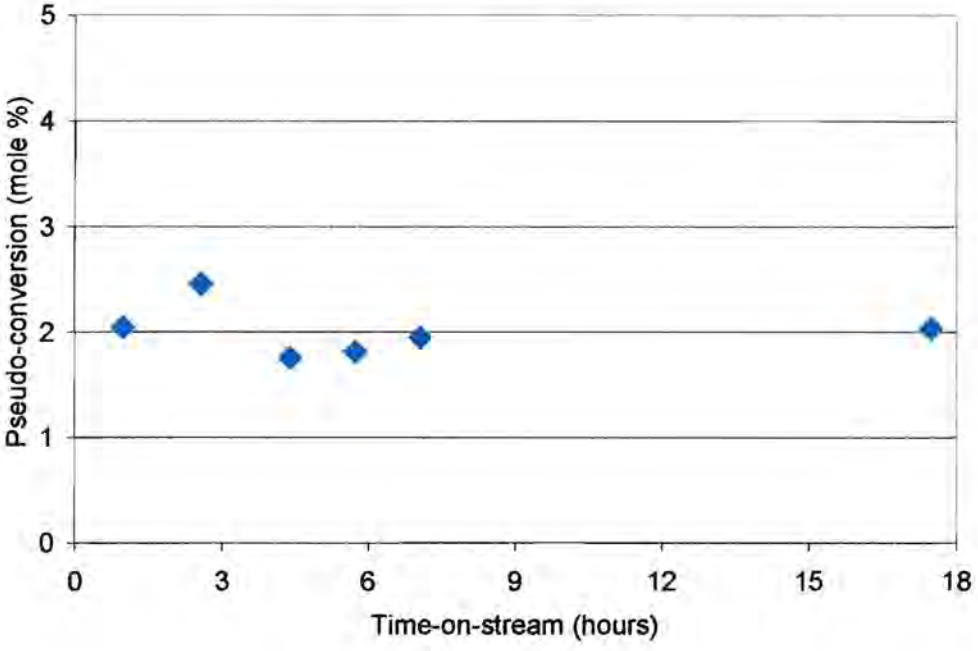

Figure A-11a Pseudo-conversion for samples taken via syringe at various times for a blank run with only carborundum loaded.

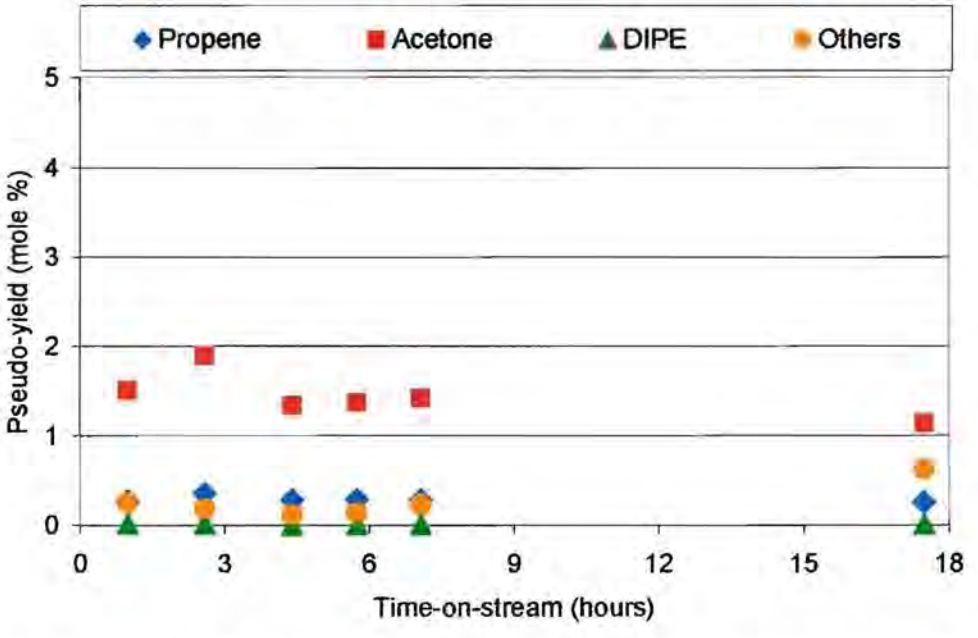

Figure A-11b Pseudo-yield for samples taken via syringe at various times for a blank run with only carborundum loaded

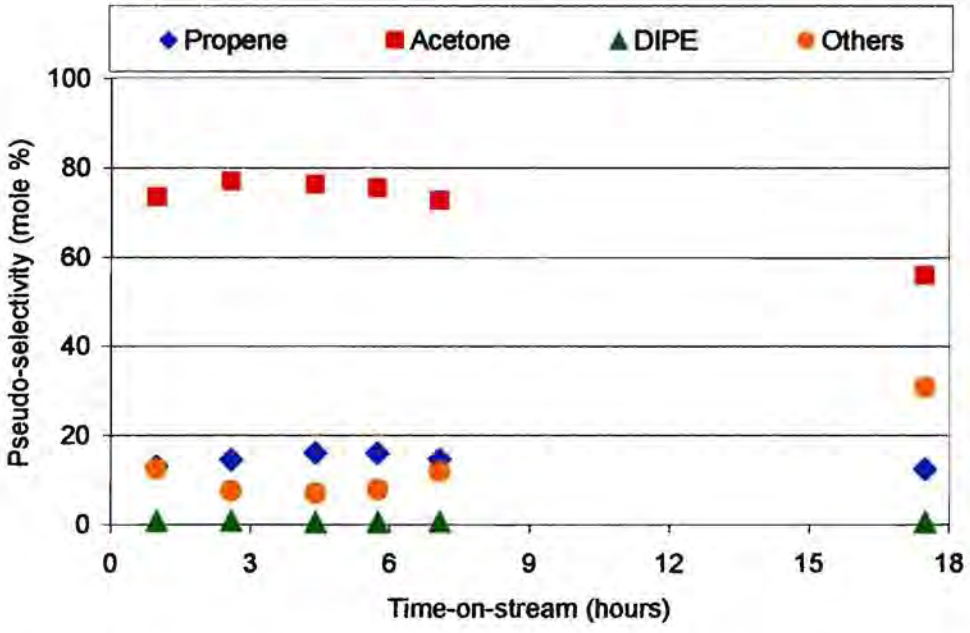

Figure A-11c Pseudo-selectivity for samples taken via syringe at various times for a blank run with only carborundum loaded

APPENDIX A-12 REPRODUCIBILITY DURING RUN OVER CATALYST

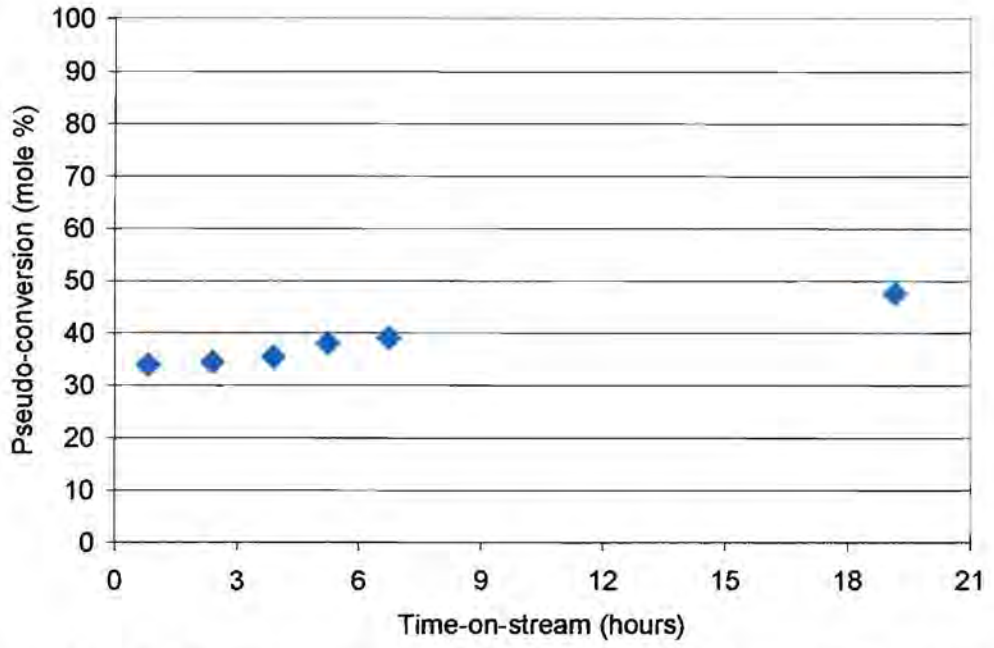

Figure A-12a Pseudo-conversionl for samples taken via syringe at various times-on-stream over Condea alumina calcined at 750°C

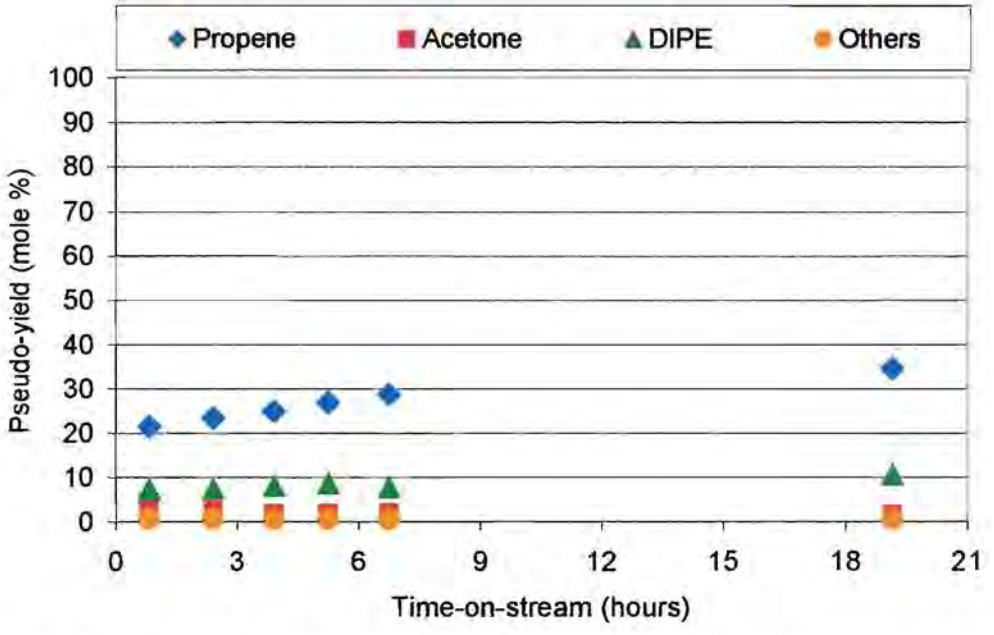

Figure A-12b Pseudo-yield for samples taken via syringe at various times-on-stream over Condea alumina calcined at 750°C

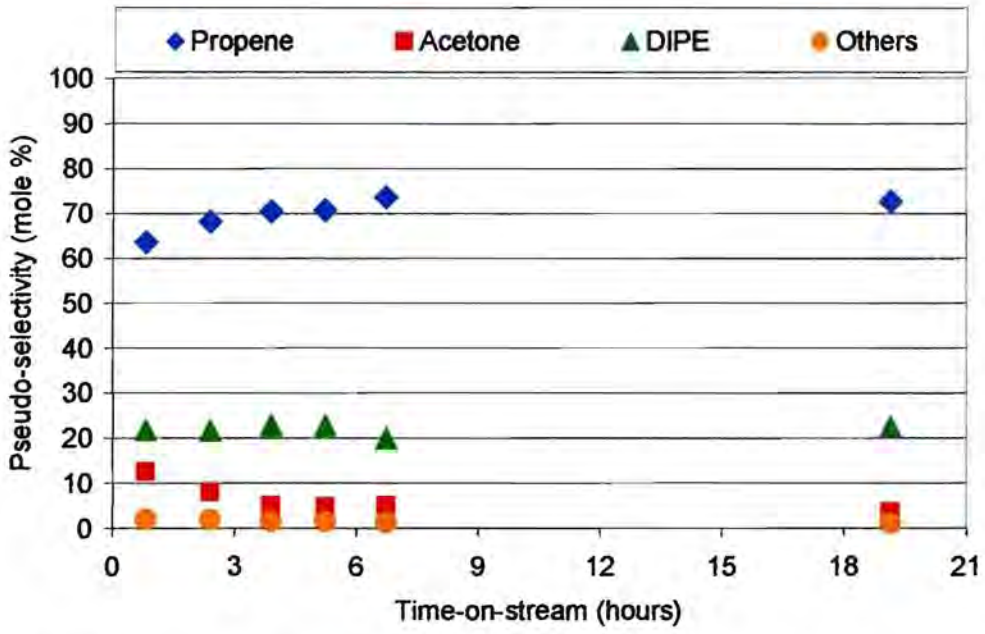

Figure A-12c Pseudo-selectivity for samples taken via syringe at various times-on-stream over Condea alumina calcined at 750°C

APPENDIX A-13 THERMODYNAMICS

The combination of possible reactions which were used for a simultaneous equilibrium calculation[1] are given in figure A-13.

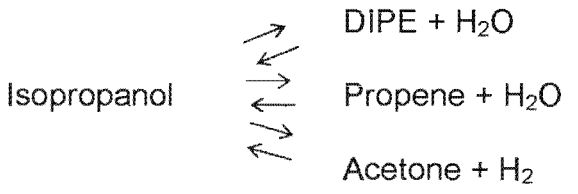

Figure A-13 Simultaneous equilibrium reactions

Results, indicating the mole fractions present at equilibrium are reported in table A-13a.

Table A-13a Equilibrium composition from isopropanol conversion at 200°C and 0.85 bar

Components	Mole fraction using inert carrier gas	Mole fraction using reactive carrier gas
Isopropanol	4.59E-05	5.58E-05
Propene	0.0736	0.0812
DIPE	1.22E-08	1.64E-08
Acetone	0.0077	8.57E-05
H_2O	0.0736	0.0812
Argon	0.8374	0.0000
Hydrogen	0.0077	0.8375

From these values, it is clear that if the reactions proceed to equilibrium, the major products will be propene and water. DIPE formation would only occur to a minor extent at equilibrium. Kinetically DIPE formation is possible, but it is of temporary nature only and will revert back to isopropanol and eventually convert to propene according to the reaction scheme (figure A-13).

[1] Performed by Noko Phala (Catalysis Research Unit, Department of Chemical Engineering, UCT) on HYSYS 1.2 HYPROTECH software

Acetone is thermodynamically stable only in the presence of argon carrier gas, but not with hydrogen.

The values from table A-13a were normalised to include only the compounds that would be recognised by gas chromotography i.e. leaving out the carrier gas and water (table A-13b). Equilibrium conversion is calculated identically to the experimental results.

Table A-13b Normalised equilibrium distribution

Mole % related to isopropanol	**With inert carrier gas**	**With hydrogen carrier gas (not inert)**
Isopropanol	0.056	0.068
Propene	90.5	99.8
Acetone	9.45	0.11
DIPE	0.00003	0.00004
Total	100.0	100.0
Equilibrium conversion	99.94	99.93

Provided H_2 carrier gas could be chemically activated over alumina under the reaction conditions applied, this would result in the removal of all acetone from the feed stream.

However, since several mole % acetone have been found in the product (figures 5-9b, 5-10b and 5-11b) when using hydrogen carrier gas, it can be concluded that hydrogen is inert with regard to acetone conversion.

Equilibrium distributions calculated for inert carrier gas, show that acetone formation is not thermodynamically limited, since percentages obtained are far lower (figures 5-13a and b).